Functional characterization of the virulence determinant ESX-1 from *Mycobacterium tuberculosis*

THÈSE N^{O} 9011 (2018)

PRÉSENTÉE LE 26 NOVEMBRE 2018

À LA FACULTÉ DES SCIENCES DE LA VIE

UNITÉ DU PROF. COLE

PROGRAMME DOCTORAL EN APPROCHES MOLÉCULAIRES DU VIVANT

ÉCOLE POLYTECHNIQUE FÉDÉRALE DE LAUSANNE

POUR L'OBTENTION DU GRADE DE DOCTEUR ÈS SCIENCES

PAR

Paloma Julia SOLER ARNEDO

acceptée sur proposition du jury:

Prof. J. Lingner, président du jury
Prof. S. Cole, directeur de thèse
Prof. R. Brosch, rapporteur
Prof. W. Bitter, rapporteur
Dr N. Dhar, rapporteur

ÉCOLE POLYTECHNIQUE
FÉDÉRALE DE LAUSANNE

Suisse
2018

To my parents

Abbreviations

ADC	Albumin/dextrose/catalase
ATP	adenosine triphosphate
BCG	Bacille de Calmette et Guérin
bp	base pair
CF	culture filtrate
CL	culture lysate
Ecc	ESX conserved component
EM	electron microscopy
ESAT-6	6 KDa early secretory antigenic target
Esp	ESX-1 secretion-associated protein
ESX-1	ESAT-6 secretion system
FBS	Fetal bovine serum
HA	hemagglutinin
HIV	human immunodeficiency virus
LB	Lysogeny broth
MIC	minimal inhibitory concentration
MS	mass spectrometry
MycP1	mycosin protease-1
OADC	oleic acid/albumin/dextrose/catalase
OD	optical density
PBS	phosphate-buffered saline
PCR	polymerase chain reaction
RD	region of difference
RNA-seq	RNA sequencing
Str	streptomycin
T7SS	Type VII secretion systems
TB	Tuberculosis
TBS	Tris-buffered saline
WGS	whole genome sequencing
WHO	world health organization
WT	wild type

Abstract

Tuberculosis (TB) is a chronic infectious disease that mainly affects the lungs and causes extensive human morbidity and mortality. It results from infection with *Mycobacterium tuberculosis*, a slow-growing intracellular pathogen that can replicate and survive inside macrophages. *M. tuberculosis* relies on the specialised ESX-1 secretion system to export virulence factors needed for intracellular spread and pathogenesis. The ESX-1 apparatus is a multi-subunit nanomachine composed of ~20 polypeptides including membrane proteins, ATPases, proteases, chaperones and substrates. Although many of the individual components of this secretion system have been characterised, the overall mechanism underlying ESX-1 secretion is still far from clear. To obtain a more comprehensive picture of the functioning of the ESX-1 apparatus, we have studied various components which were largely unexplored in *M. tuberculosis*. The structural component $EccE_1$, the ESX-1 specific protein EspL and the transcriptional regulator WhiB6 have been investigated in this thesis using an integrative approach involving genetics, biochemistry, proteomics and microscopy.

We have demonstrated that $EccE_1$ is a membrane- and cell-wall associated protein critical for secretion of ESX-1 substrates and *M. tuberculosis*-mediated cell lysis. Deletion of *eccE1* from the chromosome severely compromised secretion of EsxA, EsxB, EspA and EspC but not EspB. Localization studies using a florescent-fusion protein showed that $EccE_1$ localises to the poles of *M. tuberculosis* in the presence of an active ESX-1 system.

Our study also shows that EspL is a cytosolic protein needed for stabilising EspE, EspF and EspH, suggesting that it acts as a specific chaperone of the ESX-1 secretion system. Moreover, EspL was shown to interact with EspD and to be important for the secretion of ESX-1 substrates. Lack of EspL resulted in a growth defect *ex vivo*, loss of cytotoxicity and reduction of innate cytokine production demonstrating its critical role in *M. tuberculosis* virulence. Analysis of the transcriptional response revealed that the only gene deregulated in the absence of *espL* was *whiB6*, encoding a transcriptional factor that positively controls ESX-1 genes. To explore the role of this regulator in *M. tuberculosis* virulence, we generated a deletion mutant of *whiB6* and discovered that its loss resulted in severe reduction of cytotoxicity *ex vivo*.

Overall this investigation improves our current understanding of the ESX-1 secretion system and of the molecular basis of *M. tuberculosis* virulence. The increased knowledge of the complex interactions between the pathogen and the human host will hopefully translate into new strategies to control the spread of TB.

Keywords: tuberculosis (TB), *Mycobacterium tuberculosis*, virulence, ESX-1 secretion system, $EccE_1$, EspL and WhiB6.

Résumé

La tuberculose est une maladie pulmonaire infectieuse chronique constituant un facteur de morbidité et de mortalité majeur chez l'homme. Elle est principalement causée par un bacille à croissance lente, *Mycobacterium tuberculosis*, qui se multiplient et survie au sein des macrophages grâce à un ingénieux système de virulence appelé ESX-1. Ce système de sécrétion permet l'export des facteurs de virulence nécessaires à sa multiplication intracellulaire et sa pathogénèse. Le système ESX-1 est une nanomachine composée d'une vingtaine de polypeptides incluant des protéines membranaires, ATPases, protéases, chaperonnes et leurs substrats. Bien que plusieurs constituants de ce système aient été précédemment caractérisés, le mécanisme de sécrétion globale est loin d'être élucidé. Afin d'améliorer notre compréhension du système de sécrétion ESX-1, nous avons étudié plusieurs de ses éléments encore non décrit chez *M. tuberculois.* Ce travail de thèse vise à étudier plus particulièrement les rôles déterminant dans le processus de sécrétion des protéines $EccE_1$ et EspL situées dans l'opéron codant pour l'appareil de sécrétion ESX-1, et du régulateur WhiB6 impliqué dans la régulation des mécanismes de sécrétion, en utilisant une approche multidisciplinaire combinant la génétique, la biochimie, la protéomique et la microscopie.

Tout d'abord, nous avons démontré qu'$EccE_1$ est une protéine associée à la membrane et à la paroi bactérienne et qu'elle est essentielle pour la sécrétion des substrats du système ESX-1 ainsi qu'à la lyse des cellules de l'hôte. En étudiant les profils de sécrétion de bactéries mutantes possédant une délétion chromosomique du gène codant pour la protéine $EccE_1$, nous avons déterminé qu'$EccE_1$ est essentielle pour la sécrétion de quatre des principaux substrats d'ESX-1 (EsxA, EsxB, EspA et EspC) mais facultative pour la sécrétion du substrat EspB. Grâce à l'utilisation d'une protéine de fusion fluorescente, nous avons également pu localiser $EccE_1$ aux pôles de la bactérie et démontrer que la présence des autres gènes de l'opéron est essentielle à cette localisation spécifique.

Dans une deuxième partie, nous avons démontré qu'EspL est une protéine cytosolique essentielle pour le fonctionnement du système de sécrétion ESX-1 en jouant un rôle de chaperonne nécessaire pour la stabilité des protéines substrats EspE, EspF and EspH. De plus, nous avons également prouvé qu'EspL interagissait avec EspD, une autre protéine chaperonne stabilisant les protéines substrats EspA et EspC. L'absence d'*espL* chez *M. tuberculosis* entraine un défaut de croissance de la bactérie, une perte de la cytotoxicité et une réduction de la production de cytokines dans les cellules hôtes démontrant le rôle critique de EspL dans la virulence de *M. tuberculosis*. Pour finir, l'analyse de la réponse transcriptionnelle a rélévée que le seul gène dérégulé en l'absence de *espL* est *whiB6*, codant pour un facteur de régulation qui contrôle les gènes du système de sécrétion ESX-1. Par la suite, nous avons démontré que la délétion de WhiB6 chez *M. tuberculosis* entraine une réduction de la cytotoxicité *ex vivo*.

En général, nos investigations ont permis d'améliorer notre connaissance du système de sécrétion ESX-1 ainsi que les bases moléculaires de la virulence de *M. tuberculosis*. L'évolution et l'amélioration des connaissances

des interactions entre le pathogène et l'homme permettront de mettre en place de nouvelles stratégies pour contrôler la transmission de la tuberculose.

Mots-clés: tuberculose (TB), *Mycobacterium tuberculosis*, virulence, système de sécrétion ESX-1, $EccE_1$, EspL, WhiB6.

Contents

Chapter 1

Introduction

1.1 TUBERCULOSIS

Human tuberculosis (TB) is a bacterial infectious disease that has plagued humankind for thousands of years. Characterized by the formation of tubercles in the lungs, TB is a chronic disease that causes extensive morbidity, mortality and loss of wealth. Despite the availability of a vaccine and effective treatment, TB continues to spread in every corner of the world. Classified by the World Health Organization (WHO) as the top infectious killer worldwide, TB caused over 10.4 million new cases and 1.7 million deaths in 2017 [1].

TB is mainly a pulmonary disease but can also affect other tissues. For instance, it can develop in the central nervous system, causing meningitis, and in the bloodstream resulting in multiorgan affection. However, the lungs are the predominant site of disease manifestation [2]. TB results from infection with the bacillus *Mycobacterium tuberculosis* although other species from the *Mycobacterium tuberculosis* complex can also cause the disease [3]. It is transmitted from person to person through the airways when people suffering from pulmonary TB expel airborne droplets containing bacteria. Following initial exposure, the period required to develop symptoms can range from a few weeks to a lifetime. In about 5% to 10% of infected individuals, the disease will continue to progress soon after infection causing active TB. This rapid evolution typically occurs in infants and immunosuppressed individuals. However, in the majority of infected individuals, the immune system can arrest the progression of the disease. Nonetheless, incomplete eradication of *M. tuberculosis* can lead to the persistence of the bacilli within the human body for a lifetime causing latent TB infection (LTBI). In this case, people do not develop symptoms and cannot spread the disease but can undergo reactivation when the immune system is weakened [4].

An estimated 2 billion people have LTBI and are at risk of reactivation of the disease, creating a remarkable resource for future cases of active TB. Human immunodeficiency virus (HIV) infection accelerates reactivation in LTBI individuals and drastically increases the risk of developing active TB. HIV-coinfection represents a major driving force in the TB epidemic, especially in Africa which in 2016 accounted for 86% of deaths caused by HIV-associated TB [1]. Treatment of these patients has additional difficulties due to the adverse interaction between anti-TB and anti-retroviral drugs, making the control of the disease even more complicated. The situation in recent years was worsened mainly due to the emergence of multidrug-resistant (MDR) *M.*

tuberculosis strains, which no longer respond to frontline treatment. 4.1% of new and 19% of previously treated TB cases in the world are estimated to have MDR -TB [1].

At the present time, TB is still a global health problem far from being eradicated. The development of successful strategies to control the spread of TB will greatly depend on the proper understanding of the complex interactions between the pathogen and the human host.

1.2 A BRIEF HISTORY OF TUBERCULOSIS

Known in past times as phthisis, consumption or white plague, TB has always been a permanent challenge over the course of human history [5]. Archaeological evidence of TB and mycobacterial DNA has been found in Egyptian and South American mummies dating from 3000-5000 years BC. In Ancient Greece, TB was already known as a fatal disease. At that time, a well-documented description of the symptoms and tubercular lung lesions already existed. During the 18-19th century TB became epidemic in Europe with a mortality rate as high as 900 deaths per 100 000 inhabitants per year [5, 6]. It was not until Dr Robert Koch discovered the "*Tubercle bacillus*" as the causative agent of the disease, that the history of TB started to change. In 1882, Koch identified, isolated and cultivated the bacillus and reproduced the disease in laboratory animals [7]. In the decades following this discovery, several breakthroughs such as the development of the Bacille Calmette-Guerin (BCG) vaccine and the introduction of chemotherapy together with the improvement of living conditions, allowed to decrease TB burden during the 20th century. More recently, the HIV/ AIDS epidemic and the emergence of MDR-TB strains have worsened the situation.

1.2.1 Diagnosis

Koch's discovery resulted in the isolation of tuberculin, a glycerin extract of the bacilli. This extract was found to produce a skin reaction on infected patients and hence exploited as a diagnostic tool that became the tuberculin skin test (TST). TST was later improved by using purified protein derivative (PPD) from sterilised *M. tuberculosis* cultures [6]. Due to its low cost, TST remains widely used albeit it fails to distinguish between *M. tuberculosis*-infected individuals and the BCG vaccinated and therefore, can cause false positive results [8]. The identification of potent immunogenic secreted factors in *M. tuberculosis* resulted in the development of the interferon-gamma release assay (IGRA). This TB test is based on the *in vitro* measurement by ELISA

of interferon gamma production by T lymphocytes after stimulation with *M. tuberculosis*-specific antigens (ESAT-6 and CFP10). As these antigens are absent in BCG and most non-tuberculous mycobacteria, IGRA test can be used to differentiate between *M. tuberculosis* infection and prior BCG vaccination [8]. Since 2008, the rapid molecular Xpert MTB/RIF test allows the detection of several mycobacterial species and rifampicin-resistant bacteria in sputum using DNA analysis. It is recommended by the WHO since 2010 and represents one of the most sensitive TB tests currently available [9]. However, the most common laboratory test for diagnosing TB worldwide is sputum smear analysis, where the presence of mycobacteria in sputum samples is examined under a microscope. Overall, the most sensitive method to screen active TB and antibiotic-resistance is the culture in liquid medium. Microbiological tests are usually combined with a chest X-ray when a person is suspected to have active TB.

1.2.2 Vaccination

Based on the attenuation principle of Louis Pasteur, Albert Calmette and Camille Guerin developed, at the beginning of the 20th century, the first vaccine against TB named BCG. They sub-cultured the virulent bovine strain *Mycobacterium bovis* during eleven years in a glycerin-bile-potato mixture. During the course of the passages, *M. bovis* lost its virulence as demonstrated when injected into cattle and other animals [10]. Since 1921, when it was shown to be harmless and protective in humans, BCG has been extensively used as a live attenuated strain. Over 90 years, more than 4 billion individuals have been vaccinated with BCG. Unfortunately, its efficiency remains controversial. Whereas some studies reported a high protection rate for tuberculosis meningitis in children, others have claimed an inconsistent efficacy against pulmonary disease, particularly in adolescents and young adults [10, 11]. Additionally, BCG is contraindicated in HIV-infected adults as it can disseminate in immunocompromised individuals.

Today, BCG is the only available vaccine against TB, but a range of new TB vaccine candidates have been developed, of which several have reached the clinical trial pipeline. One promising case is the H1/IC31 vaccine. This subunit vaccine is composed of two immunodominant and specific antigens of *M. tuberculosis*

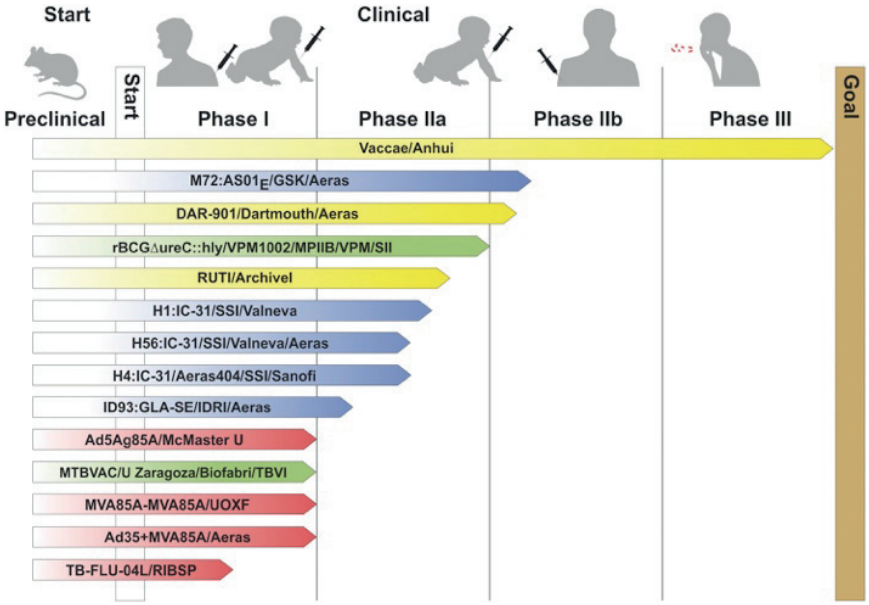

Figure 1. TB vaccines in clinical trials. Taken from [14]. TB vaccine candidates are classified into therapeutics vaccines (Ruti and Vaccae) and preventive vaccines (the rest indicated in the figure). Preventive vaccines come in three generic types: viable whole-cell vaccines such as MTBVAC (deletion of *phoP* and *fadD26)*, inactivated whole-cell vaccines such as SRL172 (derived from a non-tuberculous Mycobacterium) and subunit vaccines (compose of one or more antigens combined with adjuvants). Examples of antigens used in subunit vaccines: ESAT-6, Ag85B, Ag85A and PPE family members. (Abbreviations: GSK, Glaxo Smith Kline; MPIIB, Max Planck Institute for Infection Biology; VPM, Vakzine Projekt Management; SII, Serum Institute India; SSI, Statens Serum Institute; McMaster U, McMaster University; TBVI, Tuberculosis Vaccine Initiative; UOXF, University of Oxford; RIBSP, Research Institute for Biological Safety Problems)[14].

expressed as a fusion protein: Ag85B (antigen 85b)-ESAT-6 (early secreted antigenic target of 6 kDa, or EsxA). To increase protectivity and boost the BCG primed-individuals, H1 is formulated with the adjuvant IC3 [12, 13]. Introducing immunodominant antigens has also been chosen in many other vaccine candidates as it was found to enhance protection [14].

1.2.3 Antibiotic treatment

Three decades after the development of the BCG vaccine, a significant breakthrough in controlling TB came with the introduction of chemotherapy. Streptomycin, isolated in 1944 by Waksman and colleagues, was the first antibiotic and bactericidal agent effective against *M. tuberculosis*. Initially, streptomycin caused a dramatic reduction in mortality, but it was soon realised that administration of this drug alone resulted in the appearance of drug resistance [15]. Although disappointing, this outcome demonstrated that TB is not easily

Table. Classification of anti-TB drugs divided into WHO groups A-D for drug resistant tuberculosis and first-line oral drugs

Standard first-line therapy	**Second-line drugs**			**Third-line drugs**	
	Fluoroquinolones (group A)	Injectable agents (group B)	Others (group C)	Add-on agents (group D)	
Isoniazid	levofloxacin	kanamycin	D-cycloserine	Clofazimine	Delamanid
rifampicin	moxifloxacin	amikacin	ethionamide	imipenem/cilastin	Bedaquiline
ethambutol	gatifloxacin	capreomycin	prothionamide	High-dose isoniazid	Linezolid
pyrazinamide		(streptomycin)	terizodone	meropenem	
			p-Aminosalicylic acid	amoxicillin/clavulanate	
				clarithromycin	

curable by monotherapy. In the following years, several other anti-TB drugs were discovered which paved the way for combination therapy. The current tuberculosis treatment was introduced 40 years ago and consists of a combination therapy involving isoniazid, rifampicin, pyrazinamide and ethambutol. The treatment requires a minimum of 6 months which is divided into two phases: 2 months of the four drugs together followed by 4 months of isoniazid and rifampicin. This regimen is effective against drug sensitive *M. tuberculosis* and achieves up to 95% cure rate when administered through directly observed therapy (DOT) and follow-up support [16]. Most anti-TB medicines have been used for decades, and resistance to them is widespread. Treatment of MDR-TB consists of second-line drugs commonly administered for 18 months or longer. The regimen is less efficacious, more expensive and more toxic. Ideally, *in vitro* drug-susceptibility testing (DST) of each patient's isolate should be used to design the appropriate treatment [16].

Many research efforts are currently focused on increasing the repertory of TB drugs to find more efficient and shorter chemotherapy. Development of anti-virulence drugs is a new strategy that is being explored in *M. tuberculosis*. This approach proposes an alternative way to treat TB where, rather than kill bacteria, the pathogen's ability to cause disease is reduced by blocking the secretion of virulence proteins [17]. This strategy has several advantages such as the potential harmless impact on the normal microflora and the prevention of resistance development. As compounds that block virulence do not affect essential functions, it is thought that they do not exert an intense selective pressure for resistance [18]. Thus far, two classes of molecules that inhibit the secretion of the major *M. tuberculosis* virulence factor EsxA have been identified [19]. Although they have a different mode of action, both molecules were effective in protecting host cells from *M. tuberculosis* damage [19]. A better understanding of the *M. tuberculosis* virulence mechanism is critical to enhancing the development of more anti-virulence drugs.

1.3 MYCOBACTERIA

TB in humans and animals is caused by a group of bacteria collectively known as the *Mycobacterium tuberculosis* Complex (MTBC). These bacteria are highly related species belonging to the order Actinomycetales and genus *Mycobacterium*. MTBC comprises the obligate human pathogens *M. tuberculosis* and *M. africanum* as well as several other species mainly affecting wild and domestic mammals such as *M. bovis* (cattle), *M. microti* (voles)*, M. pinnipedii* (seals) *and M. caprae* (ovine) [3]. Other major mycobacterial pathogens are *M. leprae*, the causative agent of leprosy, and *M. ulcerans*, the agent of Buruli ulcer [2].

1.3.1 Cell wall

Mycobacteria are rod-shaped prokaryotes with a highly GC-rich genome and a complex cell envelope, which is characterised by the presence of long fatty acids called mycolic acids. The envelope of mycobacteria consists of a regular phospholipid bilayer plasma membrane, a unique lipid-rich cell wall and an outer capsule [2]. Because of the high lipid content, mycobacteria are identified using acid-fast staining (Ziehl-Neelsen stain) and not with the commonly used Gram-staining. The particular cell wall of mycobacteria is composed of a large core complex where mycolic acids are covalently linked to the peptidoglycan-arabinogalactan matrix. Additionally, mycolic acids also associate with a diverse set of free lipids, forming a hydrophobic layer of extremely low fluidity called the mycomembrane. Surrounding the cell wall, there is a thick capsular layer composed of polysaccharides, proteins and glycolipids. This organisation contributes to the exceptional thickness of the mycobacterial cell envelope and the formation of a double protective barrier that confers impenetrability to polar molecules and certain host defences [20, 21].

Additionally, all members of the MTBC are also characterised by a slow growth rate with a replication time close to 24h. The robust cell envelope, the slow growth rate and the ability to persist in a latent state are fundamental characteristics underlying the chronic nature of TB infection [22].

1.3.2 Intracellular life cycle

M. tuberculosis is an intracellular human pathogen with limited ability to survive outside the human body, and therefore, it needs to infect human cells to survive and replicate [23]. To initiate the infection in a new host, *M. tuberculosis* must penetrate into the lung alveoli where it is quickly surrounded and phagocytosed by

alveolar macrophages [24]. Macrophages play an important role in controlling bacterial infection as they are at the crossroads between the innate and the adaptative immune response. To kill bacteria and control infection, macrophages use a set of mechanisms including digestion processes. Thus, after phagocytosis by macrophages, bacteria-containing phagosomes interact with endosomes and lysosomes, which ultimately leads to the destruction of the invading microorganism. *M. tuberculosis*, however, has the ability to circumvent macrophage killing and replicate inside these immune cells. To avoid intracellular destruction, *M. tuberculosis* interferes with the normal maturation process of the phagosome by blocking phagosome-lysosome fusion and thereby avoiding the catalytic environment of this intracellular compartment [25]. This blockage is then followed by the escape of the pathogen from the phagosomal compartment, an event required for infection progression [26]. To this end, *M. tuberculosis* prevents phagosome acidification and induces phagosomal membrane rupture which results in the release of bacteria into the cytosol [26–28]. Escape from the phagosome and the presence of bacterial-derived molecules in the cytosol activate innate immune sensors such as cGAS and the NLRP3 inflammasome [29–31]. Consequently, a complex immune response is triggered leading to the recruitment of immune cells to the site of the infection and eventually to the formation of a compact aggregate of cells creating the granuloma. Most of the times, the immune response fails to eliminate the bacilli. It has been suggested that *M. tuberculosis* can exploit the cellular recruitment to proliferate and disseminate [32]. Alternatively, when contained within the walled-off granuloma, *M. tuberculosis* can enter the so-called dormant (latent) state and remain quiescent within the infected tissue [33].

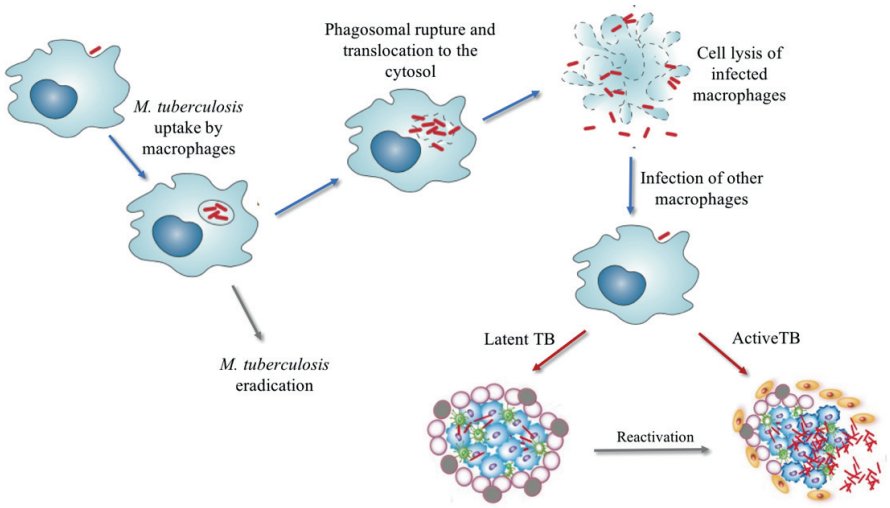

Figure 2. Intracellular cycle of *M. tuberculosis*. Adapted from [106, 107]. Bacteria are first phagocytosed by alveolar macrophages and subsequently enclosed in a phagosomal compartment. Then, pathogenic mycobacteria can block the phagosome-lysosome fusion, disrupt the membrane and translocate to the cytosol where it can induce a necrotic cell death of infected macrophages. Afterwards, *M. tuberculosis* can infect other surrounding cells and spread intracellularly. Depending on the immune system of the host, the infection can progress causing active TB or be arrested leading to latent TB.

1.4 SECRETION SYSTEMS IN BACTERIA

Bacteria rely on sophisticated nanomachineries to transport proteins across the cell envelope. Many exported proteins have essential functions that require an extracytoplasmic location and, therefore, their export pathway is critical for bacterial physiology. The general secretory (Sec) pathway is a highly conserved and essential system present in all bacteria and used as the primary route for exporting proteins. It has a channel in the cytoplasmic membrane through which unfolded proteins, containing an N-terminal signal peptide, are transported using ATP hydrolysis [34]. The twin-arginine translocation (Tat) export machinery is another essential pathway, but in contrast to the general Sec, it secretes prefolded proteins, and it is not present in all bacteria. Proteins directed to the Tat pathway have an N-terminal signal peptide with a pair of arginine residues [34].

Additionally, pathogenic bacteria also possess specialised secretion systems dedicated to the export of effectors that interact with the host. In this context, substrates can be displayed on the bacterial cell surface, secreted into the extracellular environment or injected directly into a host cell. Released macromolecules through these

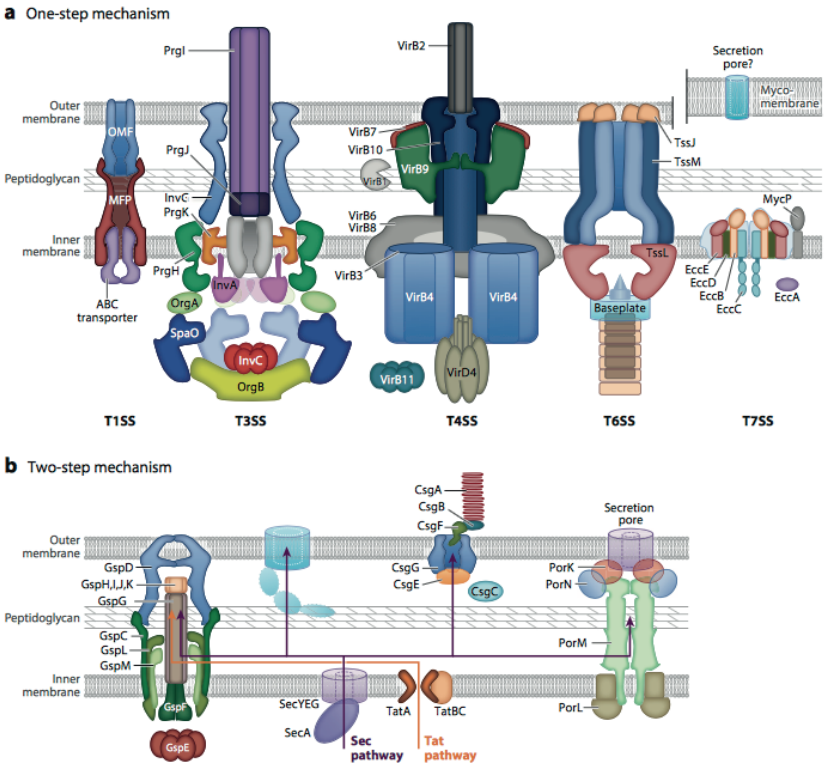

Figure 3. Secretion systems in didermal bacteria. Taken from [35]. Substrates secreted by a one-step mechanism are directly translocated from the cytoplasm into the extracellular environment or into target cells. Five kind of secretion system has been described to use one-step secretion: type I secretion systems (T1SSs), T3SSs, T4SSs, T6SSs and T7SSs (ESX-5 shown). T7SSs are mainly found in mycobacteria, Gram positive bacteria with a mycomembrane which is indicated separately in this figure. Secretion by a two-step mechanism occurs when substrates are first translocated across the plasma membrane thought the Sec/Tat systems and subsequently into the extracellular milieu. Secretion system using this mechanism are: T2SS, T5SS, T8SS and T9SS.

systems include proteins, DNA and small molecules. Historically, secretion systems have been extensively studied in Gram-negative bacteria which has led to the identification of several specialised systems designated type I-IX (T1SS-T9SS) [35, 36]. Exceptionally, the T7SS, which was first discovered in the pathogen *M. tuberculosis,* is only present in Gram-positive bacteria [21]. These machineries can be divided into two categories; those spanning both the inner membrane (IM) and the outer membrane (OM), and those that span the OM only. Secretion across the cell envelope can occur either by a one-step or a two-step mechanism. In the case of single-step secretion, substrates can be directly translocated from the cytoplasm into the extracellular environment or into target cells. This is typically observed in export systems that span both the inner and outer membranes (T1SS, T3SS, T4SS, T6SS). When substrates are secreted by two-step process,

they are first translocated through the cytoplasmic membrane by the Sec/Tat systems and subsequently secreted into the extracellular milieu (T2SS, T5SS, T8SS, T9SS) [35, 36].

Although these specialised secretion systems are distinct in structure and function, they all require the presence of a membrane channel, and all use ATP as the primary source of energy to drive the active transport of effectors.

1.4.1 ESX systems in mycobacteria

In *M. tuberculosis* there are two essential protein export systems that are responsible for the majority of protein export: the Sec and the Tat pathway. In addition, *M. tuberculosis* also possesses five specialised secretion systems dedicated to the export of a more limited set of proteins: the ESX systems. The ESX systems are named after the first known identified effector, the 6kDa early secretory antigenic target (ESAT-6; also known as EsxA) of *M. tuberculosis*. More recently, ESX systems have also been referred to as Type VII secretion systems following the nomenclature of Gram-negative bacteria to emphasise their presence in a diderm cell envelope [21]. Although the ESX systems were first discovered in *M. tuberculosis,* they also exist across pathogenic and non-pathogenic mycobacteria, as well as in other genera of the phylum Actinobacteria [37]. Their broad presence suggests diversified functions and probably a long evolutionary process that involved gene duplication, gene diversification and horizontal gene transfer between chromosomes and plasmids [37–39]. In mycobacteria, the ESX systems are multi-protein complexes that transport selected substrates through the complex cell envelope [21]. The five ESX systems present in *M. tuberculosis* are sub-categorised into ESX-1 to ESX-5. Although they vary in function and the number of genes, they share common characteristics such as the presence of a tandem pair of WXG proteins, an ATPase with a FTSK-SpoIIIE motif and several proteins with predicted transmembrane domains [39].

ESX-1, which was the first Type VII system identified, is required for the full virulence of *M. tuberculosis* [40]. Apart from protein secretion, the ESX-1 system is also involved in DNA transfer through conjugation in the non-pathogenic *M. smegmatis* [41]. ESX-5 has also been linked to virulence as the well as cell envelope integrity and uptake of nutrients. ESX-5 is the most-recently evolved cluster and is restricted to slow growing mycobacterial species. It is dedicated to the export of a large number of PE and PPE proteins, some of which are immunogenic and important for virulence [42–44]. The ESX-3 system is involved in physiologic processes

and -particularly- in iron and zinc homeostasis. It is conserved among different mycobacterial species and its expression is regulated by the availability of iron and zinc [45]. In contrast to ESX-1, ESX-3 and ESX-5, the function of ESX-2 and ESX-4 is unknown. So far, genome mutagenesis showed that ESX-2 and ESX-4 are not required for *in vitro* growth or virulence [46, 47]. Of the five ESX systems, the *esx-4* locus has the smallest number of genes and it is thought to encode the simplest and most ancient ESX system [37, 48].

1.4.2 The ESX-1 secretion system

Among all ESX secretion systems, ESX-1 is the most well studied apparatus due to its essential role in the virulence mechanism of *M. tuberculosis*. The ESX-1 apparatus is encoded by a multigene cluster that includes two WXG secreted effectors (EsxA and EsxB), genes encoding ESX-conserved components (Ecc), ESX secretion-associated proteins (Esp) as well as PE and PPE locus-specific proteins and a subtilisin-like protease (MycP). Apart from genes localized in the *esx*-1 cluster, additional genes situated elsewhere on the chromosome are required for the function of ESX systems. For instance, the *espACD* operon that encodes three proteins (EspA, EspC, and EspD) is required for proper ESX-1 activity [49, 50]. The importance of the ESX-1 system for virulence was first shown by comparative genomic studies between the attenuated live vaccine *M. bovis* BCG strain and the virulent H37Rv *M. tuberculosis* strain. These studies revealed a deletion of ≈ 9.5 kb within the *esx-1* locus spanning from *rv3871* to *rv3879*. This deleted region is named region of difference 1 (RD1) and it contains 9 genes including *esxA* [51]. Reintroduction of the RD1 region into a BCG strain showed increased virulence in immunodeficient mice[40]. Consistent with this, deletion of the RD1 region from *M. tuberculosis* attenuated mycobacterial growth *ex vivo* and *in vivo,* demonstrating the crucial role of RD1 genes and of the ESX-1 secretion system in *M. tuberculosis* pathogenesis [52, 53, 54].

Studies on the intracellular cycle of *M. tuberculosis* demonstrated the critical role of the ESX-1 apparatus during macrophage infection. To circumvent macrophage defences, *M. tuberculosis* induces phagosomal rupture and translocates to the cytosol where it can trigger a necrotic cell death in infected macrophages. However, this effect is not observed in non-pathogenic mycobacterial species or attenuated *M. tuberculosis* strains as

A

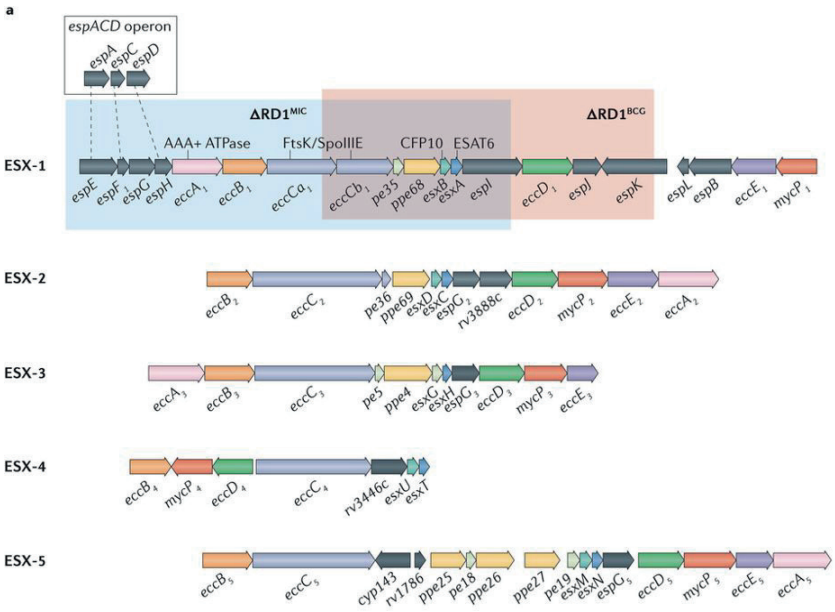

B

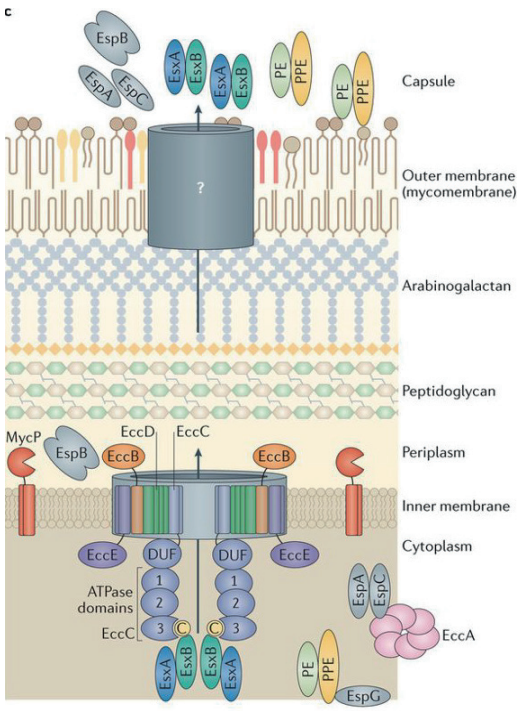

Figure 4. Genetic organisation and model of ESX systems. Taken from [31]. A. The five *esx* loci are characterised by the presence of two *esx* genes that encode secreted effectors, several *ecc* genes that encode for ESX-conserved components and various locus-specific genes. The spontaneous deletion in the *esx-1* region present in the *M. bovis* BCG strain and *M. microti* are indicated with red and blue shading. These deletions are thought to be associated with its attenuated phenotype. **B**. Model of the ESX secretion systems. The membrane proteins EccB, EccC, EccD, EccE and MycP form the core structure in the inner membrane. EccC has ATPase domains in the cytoplasm involved in substrate recognition and energy production for active secretion. EccA and EspG interact with substrates and could potentially execute a chaperone-like activity. Substrates are usually secreted as heterodimers (PE/PPE, EsxA/EsxB, EspA/EspC) and some of them are co-dependent for secretion (EsxA/EsxB and EspA/EspC). How proteins are transported across the mycomembrane is still unclear.

they remain enclosed within the phagosome [55, 56]. Furthermore, complementation of the attenuated strains *M. tuberculosis* ΔRD1 or BCG with the ESX-1 secretion system restores the ability to cause phagosomal rupture, suggesting that this effect depends on ESX-1 [55, 56]. Hence, the ability to translocate to the cytosol, which depends on the ESX-1 secretion system, has been linked to *M. tuberculosis* cytotoxicity and virulence.

1.4.2.1 ESX-1 substrates

The first ESX-1 substrates to be identified were the immunodominant protein antigens, EsxA and EsxB (otherwise known as CFP10 (culture filtrate protein of 10KDa)). Both proteins are encoded within the RD1 region and their deletion results in similar attenuated phenotypes as a mutant strain deficient for RD1 (ΔRD1) [53, 57]. EsxA induces a potent and highly specific T-cell response in humans and multiple laboratory animal species [58–60].

EsxA and EsxB are small secreted proteins with an approximate size of ~100 aa characterised by the lack of a classical signal sequence and the presence of a conserved Trp-x-Gly (WxG) motif which contributes to the formation of a helix-turn-helix structure [61, 62]. They form a 1:1 complex *in vitro* and are co-secreted in mycobacteria; therefore they are thought to be exported as a heterodimer by the ESX-1 apparatus [49, 63, 64]. The C-terminal domain of EsxA was shown to be essential for biological functions whereas the C-terminus of EsxB, which contains a secretion motif (Trp-XXX-Asp/Glu), was reported to be critical for secretion of both proteins [65, 66]. The EsxA/B complex can dissociate in acidic pH conditions, which is an important factor inside phagosomes [63, 67]. In such conditions, EsxA and EsxB were showed to interact with biologically relevant liposomal preparations suggesting that a similar scenario can occur during host cell infection [67]. Several lines of evidence indicate that EsxA can lyse membranes and act as a cytolysin [53, 67, 68], therefore, EsxA seems to be the principal candidate for mediating phagosomal escape. Recently, the lytic activity of EsxA has been linked to the presence of extractable lipids phthiocerol dimycocerosates (DIM) and membrane fluidity. Thus, the presence of DIM was reported to rigidify fluid membranes and decrease the lytic efficiency of EsxA [28]. Others, however, have disputed the lytic activity of EsxA and suggested that the ESX-1-mediated membrane lysis is contact-dependent and involves gross disruptions [69].

Aside from the main *esx-1* locus, the *espACD* cluster, which is located more than 260 kb upstream of the *esx-1* locus, is also involved in ESX-1 function. This operon is present in slow-growing and pathogenic

mycobacterial species such as *M. tuberculosis*, *M. leprae* and *M. marinum* but absent in non-pathogenic species such as *M. smegmatis*. Although its origin is still unclear, it has been hypothesised that the *espACD* operon was acquired by horizontal gene transfer events that might have contributed to pathogenesis [31]. Interestingly, it has a paralogous cluster at the 5' extremity of the *esx-1* locus of *M. tuberculosis* comprising *espEFH*. The *espACD* operon encodes three proteins, EspA, EspC and EspD. Importantly, EspA and EspC are co-secreted with EsxA and EsxB through the ESX-1 apparatus. Thus, disruption of *espA* or *espC* results in abolition of EsxA/B secretion and attenuation [49, 50]. EspD, by contrast, is not co-secreted or secreted via ESX-1 although its expression but not secretion is required for EsxA and EsxB translocation. Additionally, EspD is also needed for stabilizing EspA and EspC levels by an unknown mechanism [70]. The role played by these three ESX-1 substrates in the virulence mechanism of *M. tuberculosis* is still under investigations. Besides its implication in EsxA and EsxB secretion, EspC has recently been proposed to act as a needle protein, as it polymerises upon secretion and forms filaments on the surface of *M. tuberculosis* [71].

Another Esp protein and ESX-1 substrate is EspB. This protein contains PE (Pro-Glu) and PPE (Pro-ProGlu) domains with helical structure [72]. EspB is expressed as a full-length substrate, but during the secretion process, it is cleaved at the C-terminus by the membrane protease $MycP_1$ [73]. In contrast to the full length EspB, the processed form of the protein generated during secretion forms oligomers [72]. Secretion of EspB was shown to be dependent on EsxA and EsxB expression but independent of EspACD expression [74]. These finding demonstrated that EspB could be secreted even though EspA, EspC, EsxA and EsxB are not [74, 75]. Although EspB is not co-secreted with EsxA and EsxB, the C-terminus of EspB was shown to be essential for secretion of these two Esx substrates as it interacts with and stabilizes EsxA levels [76]. Additionally, EspB was reported to bind phospholipids and mediate an EsxA-independent virulence response [74].

1.4.2.2 Structural components

The five conserved elements $EccB_1$, $EccCa_1$, $EccCb_1$, $EccD_1$ and $EccE_1$, are putative membrane proteins and predicted to be core components of the ESX-1 machinery. Homologues of these proteins that are encoded by

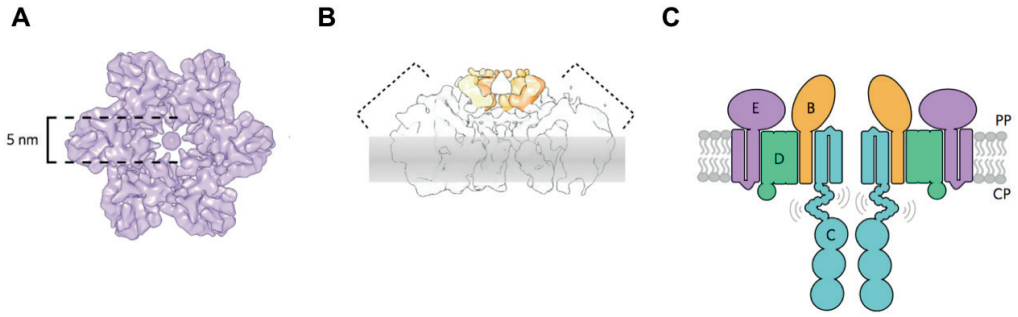

Figure 5. **Reconstruction of the ESX-5 membrane complex. Adapted from** [**79**]**.** The architecture of the ESX-5 membrane complex from *Mycobacterium xenopi* determined at 13 Å resolution by electron microscopy showed that $EccB_5$, $EccC_5$, $EccD_5$ and $EccE_5$ assemble with equimolar stoichiometry into a complex with six-fold symmetry [79]. **A.** Top view of the three-dimensional reconstruction showing a central channel with a diameter of ~5nm. **B**. A side-view cross-section presenting the complex embedded in the inner membrane (shadowed grey) and the density of the periplasmic region. The brackets indicate the predicted position of $EccE_5$. **C**. Model of the ESX membrane complex: EccB (B), EccC (C), EccD (D), EccE (E). Periplasmic (PP) and cytoplasmic (CP).

the *esx-5* locus were shown to form a membrane complex of ~1500 kDa in *Mycobacterium bovis*, *Mycobacterium marinum* and *Mycobacterium xenopi* [77–79]. New insight into the structure of the membrane complex indicated that the four components $Ecc(BCDE)_5$ are present in equimolar amounts and assemble into a hexameric arrangement around a central pore. This membrane complex seems to be embedded exclusively in the inner membrane [79]. Considering the conserved nature of the Ecc elements, the presumed structure of the ESX-1 membrane complex might resemble that shown for ESX-5. Although the atomic structure of the ESX-1 complex has not been resolved yet, studying the individual elements has provided significant insights into the working mechanism of the machinery.

EccB1

$EccB_1$ is an essential component for ESX-1 secretion that is localised in both the membrane and the cell wall in *M. tuberculosis* [80–82]. It contains an N-terminal transmembrane domain and a large C-terminal region in the periplasmic space with a hydrophobic core and an elongated shape that shares structural similarities to a known peptidoglycan binding protein [82]. These characteristics suggest a role in anchoring the ESX-1 system within the periplasmic space [83]. Additionally, $EccB_1$ was reported to have an ATPase activity and to probably form hexamers, indicating that it could serve as a transport channel in the periplasmic space and use ATP hydrolysis for substrate translocation [82]. However, there is still no

experimental evidence showing that ATP hydrolysis by this component is related to substrate secretion. Furthermore, the structure of $EccB_1$ seems too short to span both the plasma membrane and the mycomembrane [82]. If this protein acts as a channel, it may require other components to translocate substrates across the cell envelope.

$EccC_1$

$EccC_1$ is a member of the FtsK/SpoIIIE-like ATPase family encoded by two operonic genes: *$eccCa_1$* and *$eccCb_1$*. Both components interact to form a functional unit with two N-terminal transmembrane domains and three ATP-binding sites. Deletion of either *$eccCa_1$* or *$eccCb_1$* resulted in disruption of ESX-1-related secretion and significant attenuation of *M. tuberculosis in vivo*. Further studies have shown that hydrolysis of ATP by $EccCa_1$ and the interaction between $EccCb_1$ and EsxB are critical for ESX-1-related secretion. Therefore, $EccC_1$ is likely involved in substrate recognition and may supply energy for protein translocation [84–86].

$EccD_1$

The gene that codes for the conserved component $EccD_1$ is located within the RD1 region. Several studies have shown that it is required for ESX-1-dependent secretion and virulence [40, 81, 86]. $EccD_1$ has an N-terminal cytoplasmic domain followed by 11 predicted transmembrane helices, and it has been proposed to form a cytoplasmic membrane channel. The cytoplasmic region can dimerise creating a negatively charged surface, which indicates that it may associate with positively charged elements [83]. Therefore, $EccD_1$ may not only form the pore in the cytoplasmic membrane but may also play a role in recruiting other components.

$EccE_1$

The functions of EccE components within the secretion apparatus are less clear. $EccE_1$ is predicted to have two N-terminal transmembrane domains and a large C-terminal region in the periplasm, but its biochemical characteristics and structure remain unknown. The work of Beckham and colleagues on the structure of the ESX-5 membrane complex demonstrated that $EccE_5$ localises at the perimeter of the membrane complex and is important for its formation and stability. Additionally, they suggested that the bulk of the protein is in the periplasm in agreement with previous bioinformatic predictions.

Interestingly, EccE is the only membrane component that is not present in ESX-4, the most ancestral of the ESX systems [37]. This absence may indicate that EccE appeared later in evolution or that it is dispensable to form a basic membrane complex. Exceptionally, the *esx4* locus of *Mycobacterium abscessus,* a rapidly growing mycobacterium and an opportunistic human pathogen, includes the EccE component. In contrast to *M. tuberculosis*, *M. abscessus* has a functional ESX-4 system that is required for intracellular survival [87]. This data may indicate that the membrane component EccE could be required to assemble a functional ESX system. Indeed, the homologue of $EccE_1$ in *M. smegmatis* is required for EsxA and EsxB secretion [80] however, further information about this component in other mycobacterial species are missing.

$MycP_1$

Another conserved component of the ESX-1 apparatus is $MycP_1$, a subtilisin-like protease. MycP1 has a C-terminal transmembrane domain to anchor the protein in the membrane and direct the protease domain to the periplasm [88]. The only known substrate of $MycP_1$ is EspB, which is cleaved at the carboxy terminus region after translocation through the inner membrane. Beside its role in substrate processing, $MycP_1$ plays a second role by stabilising the ESX-1 membrane complex [78]. In contrast to other membrane and conserved components, $MycP_1$ is not part of the core membrane complex although it can loosely associate with it [78]. As deletion of the *$mycP_1$* gene resulted in disruption of ESX-1-protein secretion, the interaction between $MycP_1$ and the membrane complex is probably crucial for the integrity and functioning of the machinery [73]. Despite the critical role of $MycP_1$ in the secretion process, its protease activity was shown to be dispensable for secretion [73, 78]. These observations suggest that processing EspB is not essential for ESX-1 secretion and may serve as a regulatory mechanism.

1.4.2.3 Localisation

Elucidating the structure of the ESX-1 apparatus as well as its localization will probably provide us with a more comprehensive understanding of its function. Thus far, two studies have addressed the fundamental question of ESX localization. The first one used *M. marinum* KasB-deficient bacteria, which have a permeable cell wall, to detect an ESX-1 core component ($EccCa_1$) and a substrate (EspE) by immunofluorescence. Both proteins were found at the poles of *M. marinum,* although the core component was preferentially found in the new pole with active peptidoglycan synthesis. Importantly, the polar localization was also confirmed during

host cell infection [89]. In line with this finding, a second study found fluorescently tagged proteins required for ESX-1 activity ($EccCb_1$ and EspE) at one of the poles of *M. smegmatis*. However, when the *esx-1* locus was deleted, the tagged $EccCb_1$ protein did not localise to the cell pole anymore, suggesting the need for other ESX-1 proteins for polar assembly [90]. Overall, these studies indicate a polar localisation of ESX-1 components in two species related to *M. tuberculosis*.

1.4.2.4 ESX-1 regulation

The ESX-1 system is active in *in vitro* grown cultures, and it is upregulated when mycobacteria infect macrophages [91]. This process is regulated by multiple transcriptional regulators such as the two-component systems (TCS) PhoPR and MprAB, the nucleoid-associated protein EspR and the redox sensor WhiB6. Interestingly, most of the transcriptional effects on ESX-1 converge at the distal *espACD* operon.

PhoPR and MprAB respond to environmental signals via sensor kinases (PhoR and MprB) to activate their cognate effector proteins which are transcriptional regulatory factors (PhoP and MprA). MprAB is activated by cell envelope stress and directly regulates the *espACD* operon [92, 93]. Inhibition of MprB activity was shown to negatively impact ESX-1 secretion and protect host-cells from *M. tuberculosis*-mediated lysis [19]. Consistent with this, deletion of *mprAB* in *M. tuberculosis* resulted in aberrant ESX-1 activity [92]. In the case of PhoPR, its activation is induced by acidic pH [94], a condition that occurs in maturing phagosomes. Mutations in *phoP* lead to attenuation *in vivo* in a mouse infection model [95]. Likewise, the point mutation in the DNA binding site of PhoP, which is naturally present in the *M. tuberculosis* H37Ra strain, is responsible for the reduced virulence displayed by this strain [96, 97]. PhoP positively regulates many genes within the *esx-1* locus and also the transcriptional regulator EspR, which in turn binds to several sites upstream of the *espACD* locus to promote its expression [98, 99]. EspR, the ESX-1 secreted protein regulator, was first suggested to be an ESX-1 substrate but it was later demonstrated to act as a general nucleoid-associated protein that localises to the cytoplasm [100]. It regulates the expression of a wide range of virulence-associated factors, and its deletion leads to reduced virulence in macrophages [100, 101]. Another gene that is part of the PhoP regulon is *whiB6*, whose product positively regulates the expression of ESX-1 substrates such as *esxA*, *espA* or *espE*. PhoP binds to the promoter region of *whiB6* to, generally, promote its expression. Thus, upregulation of *whiB6* was shown to correlate with increased ESX-1 secretion [102]. Overall, ESX-1 secretion seems to be tightly modulated by multiple layers of regulatory mechanisms.

1.5 THESIS RATIONAL AND OUTLINE

Since the publication of the genome sequence of *M. tuberculosis* H37Rv in 1998 [39], considerable research effort has focused on the identification of factors that contribute to the virulence of this pathogen. In this context, mycobacterial genetics and functional genomics have been instrumental in improving our understanding of host-pathogen interactions.

A key finding from the research on mycobacterial pathogenesis and *M. bovis* BCG attenuation was the identification of the ESX-1 secretion system [40, 51, 53]. This specialised apparatus is dedicated to the secretion of virulence factors required for intracellular spread and disease progression and represents a potential target for novel anti-TB drug discovery [17]. Although the molecular mechanism underlying the ESX-1 secretion process is not fully understood, studying individual components has provided valuable insights. Genetic approaches and structure-based functional studies have contributed significantly to our knowledge about the composition and dynamics of the ESX-1 secretion system. However, we are still far from a complete understanding of each of the elements included in the machinery. The objective of the present work is to characterise and provide new insights into the functional role of various ESX-1 components in *M. tuberculosis*. To this aim, an integrated approach involving genetics, biochemistry, proteomics and microscopy was used.

Of the five proteins predicted to form the ESX-1 membrane complex ($EccB_1$, $EccCa_1$, $EccCb_1$, $EccD_1$ and $EccE_1$), $EccE_1$ is the least investigated especially in *M. tuberculosis* where no experimental work has been reported yet. To improve our knowledge about the membrane apparatus of the ESX-1 secretion system, in **Chapter 2** we characterised the $EccE_1$ component of *M. tuberculosis*. For this purpose, we first explored the impact of $EccE_1$ on the ESX-1-related activity as well as its localisation in subcellular fractions. As $EccE_1$ was found to be a membrane- and cell wall-associated protein critical for ESX-1 function, we tagged $EccE_1$ with a fluorescent protein to reveal its localisation and, eventually, that of ESX-1. Our data demonstrate that, in the presence of a functional ESX-1 system, $EccE_1$ consistently localises to the poles of *M. tuberculosis* and suggest that the ESX-1 secretion system is located at the polar regions.

The membrane machinery of ESX-1 is dedicated to the transport of a specific subset of substrates. How these substrates are specifically recognised and targeted to the ESX-1 apparatus is not fully understood. Although

the general motif YxxxD/E is crucial for the secretion, this motif does not determine system specificity [66]. In recent years, it has become clear that dedicated chaperones play a crucial role in the secretion of substrates by preventing self-aggregation but also by specifically directing substrates to their respective systems [103]. ESX-1 proteins such as $EspG_1$ and EspD were suggested to act as chaperones of ESX-1 substrates [66, 70, 103]. In addition, EspD was shown to share structural similarity to YbaB, a DNA-binding protein widely-distributed in bacteria [104]. Interestingly, EspL, an ESX-1 specific protein with an unknown function, also has structural similarity to YbaB, suggesting that it can function as a DNA-binding protein or as a chaperone [105]. This background knowledge provided a new research direction which led us to investigate the functional role of EspL in *M. tuberculosis*. **Chapter 3** describes how we identified EspL as a critical component for ESX-1 activity and also for the stability of the additional ESX-1 members EspE, EspF and EspH. Furthermore, EspL was also found to impact the expression of the transcriptional regulator *whiB6.* This observation prompted us to study this transcriptional activator of ESX-1 genes and demonstrate its essential role in *M. tuberculosis*-mediated cytotoxicity as described in **Chapter 4**. **Chapter 5** combines these results in a general conclusion and presents future perspectives for this work.

By studying these ESX-1 components, we contributed to delineating a more comprehensive picture about the functioning of the ESX-1 apparatus. Understanding how this secretion system works will help us to characterise the molecular basis of *M. tuberculosis* virulence and obtain deeper knowledge about the complex interaction between this pathogen and the human host. This will possibly translate into new preventive and pharmacological strategies to fight TB.

1.6 BIBLIOGRAPHY

1. Global Tuberculosis Report 2017. http://apps.who.int/medicinedocs/en/d/Js23360en/. Accessed 28 Aug 2018.

2. Bloom BR, editor. Tuberculosis. American Society of Microbiology; 1994. doi:10.1128/9781555818357.

3. Gagneux S, editor. Strain Variation in the Mycobacterium tuberculosis Complex: Its Role in Biology, Epidemiology and Control. Cham: Springer International Publishing; 2017. doi:10.1007/978-3-319-64371-7.

4. Koul A, Arnoult E, Lounis N, Guillemont J, Andries K. The challenge of new drug discovery for tuberculosis. Nature. 2011;469:483–90. doi:10.1038/nature09657.

5. Barberis I, Bragazzi NL, Galluzzo L, Martini M. The history of tuberculosis: from the first historical records to the isolation of Koch's bacillus. J Prev Med Hyg. 2017;58:E9–12.

6. Daniel TM. The history of tuberculosis. Respir Med. 2006;100:1862–70. doi:10.1016/j.rmed.2006.08.006.

7. Gradmann C. Robert Koch and the pressures of scientific research: tuberculosis and tuberculin. Med Hist. 2001;45:1–32.

8. Doan TN, Eisen DP, Rose MT, Slack A, Stearnes G, McBryde ES. Interferon-gamma release assay for the diagnosis of latent tuberculosis infection: A latent-class analysis. PLoS One. 2017;12:e0188631. doi:10.1371/journal.pone.0188631.

9. Piatek AS, Van Cleeff M, Alexander H, Coggin WL, Rehr M, Van Kampen S, et al. GeneXpert for TB diagnosis: planned and purposeful implementation. Glob Health Sci Pract. 2013;1:18–23. doi:10.9745/GHSP-D-12-00004.

10. Luca S, Mihaescu T. History of BCG vaccine. Maedica (Buchar). 2013;8:53–8.

11. McShane H, Jacobs WR, Fine PE, Reed SG, McMurray DN, Behr M, et al. BCG: Myths, realities, and the need for alternative vaccine strategies. Tuberculosis (Edinb). 2012;92:283–8. doi:10.1016/j.tube.2011.12.003.

12. van Dissel JT, Soonawala D, Joosten SA, Prins C, Arend SM, Bang P, et al. Ag85B-ESAT-6 adjuvanted with IC31® promotes strong and long-lived Mycobacterium tuberculosis specific T cell responses in volunteers with previous BCG vaccination or tuberculosis infection. Vaccine. 2011;29:2100–9. doi:10.1016/j.vaccine.2010.12.135.

13. Reither K, Katsoulis L, Beattie T, Gardiner N, Lenz N, Said K, et al. Safety and immunogenicity of H1/IC31®, an adjuvanted TB subunit vaccine, in HIV-infected adults with CD4+ lymphocyte counts greater than 350 cells/mm3: a phase II, multi-centre, double-blind, randomized, placebo-controlled trial. PLoS One. 2014;9:e114602. doi:10.1371/journal.pone.0114602.

14. Kaufmann SHE, Weiner J, von Reyn CF. Novel approaches to tuberculosis vaccine development. Int J Infect Dis. 2017;56:263–7. doi:10.1016/j.ijid.2016.10.018.

15. Murray JF, Schraufnagel DE, Hopewell PC. Treatment of tuberculosis. A historical perspective. Annals of the American Thoracic Society. 2015;12:1749–59. doi:10.1513/AnnalsATS.201509-632PS.

16. Zumla A, Nahid P, Cole ST. Advances in the development of new tuberculosis drugs and treatment regimens. Nat Rev Drug Discov. 2013;12:388–404. doi:10.1038/nrd4001.

17. Chen JM, Pojer F, Blasco B, Cole ST. Towards anti-virulence drugs targeting ESX-1 mediated pathogenesis of Mycobacterium tuberculosis. Drug Discovery Today: Disease Mechanisms. 2010;7:e25–31. doi:10.1016/j.ddmec.2010.09.002.

18. Bitter W, Kuijl C. Targeting bacterial virulence: the coming out of type VII secretion inhibitors. Cell Host Microbe. 2014;16:430–2. doi:10.1016/j.chom.2014.09.010.

19. Rybniker J, Chen JM, Sala C, Hartkoorn RC, Vocat A, Benjak A, et al. Anticytolytic screen identifies inhibitors of mycobacterial virulence protein secretion. Cell Host Microbe. 2014;16:538–48. doi:10.1016/j.chom.2014.09.008.

20. Brennan PJ, Nikaido H. The envelope of mycobacteria. Annu Rev Biochem. 1995;64:29–63. doi:10.1146/annurev.bi.64.070195.000333.

21. Abdallah AM, Gey van Pittius NC, Champion PAD, Cox J, Luirink J, Vandenbroucke-Grauls CMJE, et al. Type VII secretion--mycobacteria show the way. Nat Rev Microbiol. 2007;5:883–91. doi:10.1038/nrmicro1773.

22. Cole ST. Comparative and functional genomics of the Mycobacterium tuberculosis complex. Microbiology (Reading, Engl). 2002;148 Pt 10:2919–28. doi:10.1099/00221287-148-10-2919.

23. Glickman MS, Jacobs WR. Microbial pathogenesis of Mycobacterium tuberculosis: dawn of a discipline. Cell. 2001;104:477–85. doi:10.1016/S0092-8674(01)00236-7.

24. Knechel NA. Tuberculosis: pathophysiology, clinical features, and diagnosis. Crit Care Nurse. 2009;29:34–43; quiz 44. doi:10.4037/ccn2009968.

25. Rohde K, Yates RM, Purdy GE, Russell DG. Mycobacterium tuberculosis and the environment within the phagosome. Immunol Rev. 2007;219:37–54. doi:10.1111/j.1600-065X.2007.00547.x.

26. van der Wel N, Hava D, Houben D, Fluitsma D, van Zon M, Pierson J, et al. M. tuberculosis and M. leprae translocate

from the phagolysosome to the cytosol in myeloid cells. Cell. 2007;129:1287–98. doi:10.1016/j.cell.2007.05.059.

27. Simeone R, Sayes F, Song O, Gröschel MI, Brodin P, Brosch R, et al. Cytosolic access of Mycobacterium tuberculosis: critical impact of phagosomal acidification control and demonstration of occurrence in vivo. PLoS Pathog. 2015;11:e1004650. doi:10.1371/journal.ppat.1004650.

28. Augenstreich J, Arbues A, Simeone R, Haanappel E, Wegener A, Sayes F, et al. ESX-1 and phthiocerol dimycocerosates of Mycobacterium tuberculosis act in concert to cause phagosomal rupture and host cell apoptosis. Cell Microbiol. 2017;19. doi:10.1111/cmi.12726.

29. Wassermann R, Gulen MF, Sala C, Perin SG, Lou Y, Rybniker J, et al. Mycobacterium tuberculosis Differentially Activates cGAS- and Inflammasome-Dependent Intracellular Immune Responses through ESX-1. Cell Host Microbe. 2015;17:799–810. doi:10.1016/j.chom.2015.05.003.

30. Mishra BB, Moura-Alves P, Sonawane A, Hacohen N, Griffiths G, Moita LF, et al. Mycobacterium tuberculosis protein ESAT-6 is a potent activator of the NLRP3/ASC inflammasome. Cell Microbiol. 2010;12:1046–63. doi:10.1111/j.1462-5822.2010.01450.x.

31. Gröschel MI, Sayes F, Simeone R, Majlessi L, Brosch R. ESX secretion systems: mycobacterial evolution to counter host immunity. Nat Rev Microbiol. 2016;14:677–91. doi:10.1038/nrmicro.2016.131.

32. Ramakrishnan L. Revisiting the role of the granuloma in tuberculosis. Nat Rev Immunol. 2012;12:352–66. doi:10.1038/nri3211.

33. Guirado E, Schlesinger LS. Modeling the Mycobacterium tuberculosis Granuloma - the Critical Battlefield in Host Immunity and Disease. Front Immunol. 2013;4:98. doi:10.3389/fimmu.2013.00098.

34. Green ER, Mecsas J. Bacterial secretion systems: an overview. Microbiol Spectr. 2016;4. doi:10.1128/microbiolspec.VMBF-0012-2015.

35. Rapisarda C, Tassinari M, Gubellini F, Fronzes R. Using Cryo-EM to Investigate Bacterial Secretion Systems. Annu Rev Microbiol. 2018. doi:10.1146/annurev-micro-090817-062702.

36. Costa TRD, Felisberto-Rodrigues C, Meir A, Prevost MS, Redzej A, Trokter M, et al. Secretion systems in Gram-negative bacteria: structural and mechanistic insights. Nat Rev Microbiol. 2015;13:343–59. doi:10.1038/nrmicro3456.

37. Gey Van Pittius NC, Gamieldien J, Hide W, Brown GD, Siezen RJ, Beyers AD. The ESAT-6 gene cluster of Mycobacterium tuberculosis and other high G+C Gram-positive bacteria. Genome Biol. 2001;2:RESEARCH0044.

38. Dumas E, Christina Boritsch E, Vandenbogaert M, Rodríguez de la Vega RC, Thiberge J-M, Caro V, et al. Mycobacterial Pan-Genome Analysis Suggests Important Role of Plasmids in the Radiation of Type VII Secretion Systems. Genome Biol Evol. 2016;8:387–402. doi:10.1093/gbe/evw001.

39. Cole ST, Brosch R, Parkhill J, Garnier T, Churcher C, Harris D, et al. Deciphering the biology of Mycobacterium tuberculosis from the complete genome sequence. Nature. 1998;393:537–44. doi:10.1038/31159.

40. Pym AS, Brodin P, Brosch R, Huerre M, Cole ST. Loss of RD1 contributed to the attenuation of the live tuberculosis vaccines Mycobacterium bovis BCG and Mycobacterium microti. Mol Microbiol. 2002;46:709–17. doi:10.1046/j.1365-2958.2002.03237.x.

41. Coros A, Callahan B, Battaglioli E, Derbyshire KM. The specialized secretory apparatus ESX-1 is essential for DNA transfer in Mycobacterium smegmatis. Mol Microbiol. 2008;69:794–808. doi:10.1111/j.1365-2958.2008.06299.x.

42. Bottai D, Di Luca M, Majlessi L, Frigui W, Simeone R, Sayes F, et al. Disruption of the ESX-5 system of Mycobacterium tuberculosis causes loss of PPE protein secretion, reduction of cell wall integrity and strong attenuation. Mol Microbiol. 2012;83:1195–209. doi:10.1111/j.1365-2958.2012.08001.x.

43. Ates LS, Ummels R, Commandeur S, van de Weerd R, Sparrius M, Weerdenburg E, et al. Essential Role of the ESX-5 Secretion System in Outer Membrane Permeability of Pathogenic Mycobacteria. PLoS Genet. 2015;11:e1005190. doi:10.1371/journal.pgen.1005190.

44. Sayes F, Sun L, Di Luca M, Simeone R, Degaiffier N, Fiette L, et al. Strong immunogenicity and cross-reactivity of Mycobacterium tuberculosis ESX-5 type VII secretion: encoded PE-PPE proteins predicts vaccine potential. Cell Host Microbe. 2012;11:352–63. doi:10.1016/j.chom.2012.03.003.

45. Serafini A, Pisu D, Palù G, Rodriguez GM, Manganelli R. The ESX-3 secretion system is necessary for iron and zinc homeostasis in Mycobacterium tuberculosis. PLoS One. 2013;8:e78351. doi:10.1371/journal.pone.0078351.

46. Sassetti CM, Boyd DH, Rubin EJ. Genes required for mycobacterial growth defined by high density mutagenesis. Mol Microbiol. 2003;48:77–84. doi:10.1046/j.1365-2958.2003.03425.x.

47. Sassetti CM, Rubin EJ. Genetic requirements for mycobacterial survival during infection. Proc Natl Acad Sci USA. 2003;100:12989–94. doi:10.1073/pnas.2134250100.

48. Bitter W, Houben ENG, Bottai D, Brodin P, Brown EJ, Cox JS, et al. Systematic genetic nomenclature for type VII secretion systems. PLoS Pathog. 2009;5:e1000507. doi:10.1371/journal.ppat.1000507.

49. Fortune SM, Jaeger A, Sarracino DA, Chase MR, Sassetti CM, Sherman DR, et al. Mutually dependent secretion of proteins required for mycobacterial virulence. Proc Natl Acad Sci USA. 2005;102:10676–81. doi:10.1073/pnas.0504922102.

50. MacGurn JA, Raghavan S, Stanley SA, Cox JS. A non-RD1 gene cluster is required for Snm secretion in Mycobacterium tuberculosis. Mol Microbiol. 2005;57:1653–63. doi:10.1111/j.1365-2958.2005.04800.x.

51. Mahairas GG, Sabo PJ, Hickey MJ, Singh DC, Stover CK. Molecular analysis of genetic differences between Mycobacterium bovis BCG and virulent M. bovis. J Bacteriol. 1996;178:1274–82.

52. Lewis KN, Liao R, Guinn KM, Hickey MJ, Smith S, Behr MA, et al. Deletion of RD1 from Mycobacterium tuberculosis mimics bacille Calmette-Guérin attenuation. J Infect Dis. 2003;187:117–23. doi:10.1086/345862.

53. Hsu T, Hingley-Wilson SM, Chen B, Chen M, Dai AZ, Morin PM, et al. The primary mechanism of attenuation of bacillus Calmette-Guerin is a loss of secreted lytic function required for invasion of lung interstitial tissue. Proc Natl Acad Sci USA. 2003;100:12420–5. doi:10.1073/pnas.1635213100.

54. Guinn KM, Hickey MJ, Mathur SK, Zakel KL, Grotzke JE, Lewinsohn DM, et al. Individual RD1-region genes are required for export of ESAT-6/CFP-10 and for virulence of Mycobacterium tuberculosis. Mol Microbiol. 2004;51:359–70. doi:10.1046/j.1365-2958.2003.03844.x.

55. Simeone R, Bobard A, Lippmann J, Bitter W, Majlessi L, Brosch R, et al. Phagosomal rupture by Mycobacterium tuberculosis results in toxicity and host cell death. PLoS Pathog. 2012;8:e1002507. doi:10.1371/journal.ppat.1002507.

56. Houben D, Demangel C, van Ingen J, Perez J, Baldeón L, Abdallah AM, et al. ESX-1-mediated translocation to the cytosol controls virulence of mycobacteria. Cell Microbiol. 2012;14:1287–98. doi:10.1111/j.1462-5822.2012.01799.x.

57. Wards BJ, de Lisle GW, Collins DM. An esat6 knockout mutant of Mycobacterium bovis produced by homologous recombination will contribute to the development of a live tuberculosis vaccine. Tuber Lung Dis. 2000;80:185–9. doi:10.1054/tuld.2000.0244.

58. Elhay MJ, Oettinger T, Andersen P. Delayed-type hypersensitivity responses to ESAT-6 and MPT64 from Mycobacterium tuberculosis in the guinea pig. Infect Immun. 1998;66:3454–6.

59. Ravn P, Demissie A, Eguale T, Wondwosson H, Lein D, Amoudy HA, et al. Human T cell responses to the ESAT-6 antigen from Mycobacterium tuberculosis. J Infect Dis. 1999;179:637–45. doi:10.1086/314640.

60. Brandt L, Oettinger T, Holm A, Andersen AB, Andersen P. Key epitopes on the ESAT-6 antigen recognized in mice during the recall of protective immunity to Mycobacterium tuberculosis. J Immunol. 1996;157:3527–33.

61. Poulsen C, Panjikar S, Holton SJ, Wilmanns M, Song Y-H. WXG100 protein superfamily consists of three subfamilies and exhibits an α-helical C-terminal conserved residue pattern. PLoS One. 2014;9:e89313. doi:10.1371/journal.pone.0089313.

62. Pallen MJ. The ESAT-6/WXG100 superfamily -- and a new Gram-positive secretion system? Trends Microbiol. 2002;10:209–12. doi:10.1016/S0966-842X(02)02345-4.

63. Renshaw PS, Panagiotidou P, Whelan A, Gordon SV, Hewinson RG, Williamson RA, et al. Conclusive evidence that the major T-cell antigens of the Mycobacterium tuberculosis complex ESAT-6 and CFP-10 form a tight, 1:1 complex and characterization of the structural properties of ESAT-6, CFP-10, and the ESAT-6*CFP-10 complex. Implications for pathogenesis and virulence. J Biol Chem. 2002;277:21598–603. doi:10.1074/jbc.M201625200.

64. Renshaw PS, Lightbody KL, Veverka V, Muskett FW, Kelly G, Frenkiel TA, et al. Structure and function of the complex formed by the tuberculosis virulence factors CFP-10 and ESAT-6. EMBO J. 2005;24:2491–8. doi:10.1038/sj.emboj.7600732.

65. Brodin P, de Jonge MI, Majlessi L, Leclerc C, Nilges M, Cole ST, et al. Functional analysis of early secreted antigenic target-6, the dominant T-cell antigen of Mycobacterium tuberculosis, reveals key residues involved in secretion, complex formation, virulence, and immunogenicity. J Biol Chem. 2005;280:33953–9. doi:10.1074/jbc.M503515200.

66. Daleke MH, Ummels R, Bawono P, Heringa J, Vandenbroucke-Grauls CMJE, Luirink J, et al. General secretion signal for the mycobacterial type VII secretion pathway. Proc Natl Acad Sci USA. 2012;109:11342–7. doi:10.1073/pnas.1119453109.

67. de Jonge MI, Pehau-Arnaudet G, Fretz MM, Romain F, Bottai D, Brodin P, et al. ESAT-6 from Mycobacterium tuberculosis dissociates from its putative chaperone CFP-10 under acidic conditions and exhibits membrane-lysing activity. J Bacteriol. 2007;189:6028–34. doi:10.1128/JB.00469-07.

68. Ma Y, Keil V, Sun J. Characterization of Mycobacterium tuberculosis EsxA membrane insertion: roles of N- and C-terminal flexible arms and central helix-turn-helix motif. J Biol Chem. 2015;290:7314–22. doi:10.1074/jbc.M114.622076.

69. Conrad WH, Osman MM, Shanahan JK, Chu F, Takaki KK, Cameron J, et al. Mycobacterial ESX-1 secretion system mediates host cell lysis through bacterium contact-dependent gross membrane disruptions. Proc Natl Acad Sci USA. 2017;114:1371–6. doi:10.1073/pnas.1620133114.

70. Chen JM, Boy-Röttger S, Dhar N, Sweeney N, Buxton RS, Pojer F, et al. EspD is critical for the virulence-mediating ESX-1 secretion system in Mycobacterium tuberculosis. J Bacteriol. 2012;194:884–93. doi:10.1128/JB.06417-11.

71. Lou Y, Rybniker J, Sala C, Cole ST. EspC forms a filamentous structure in the cell envelope of Mycobacterium tuberculosis and impacts ESX-1 secretion. Mol Microbiol. 2017;103:26–38. doi:10.1111/mmi.13575.

72. Korotkova N, Piton J, Wagner JM, Boy-Röttger S, Japaridze A, Evans TJ, et al. Structure of EspB, a secreted substrate of the ESX-1 secretion system of Mycobacterium tuberculosis. J Struct Biol. 2015;191:236–44. doi:10.1016/j.jsb.2015.06.003.

73. Ohol YM, Goetz DH, Chan K, Shiloh MU, Craik CS, Cox JS. Mycobacterium tuberculosis MycP1 protease plays a dual role in regulation of ESX-1 secretion and virulence. Cell Host Microbe. 2010;7:210–20. doi:10.1016/j.chom.2010.02.006.

74. Chen JM, Zhang M, Rybniker J, Boy-Röttger S, Dhar N, Pojer F, et al. Mycobacterium tuberculosis EspB binds phospholipids and mediates EsxA-independent virulence. Mol Microbiol. 2013;89:1154–66. doi:10.1111/mmi.12336.

75. Champion PAD, Champion MM, Manzanillo P, Cox JS. ESX-1 secreted virulence factors are recognized by multiple cytosolic AAA ATPases in pathogenic mycobacteria. Mol Microbiol. 2009;73:950–62. doi:10.1111/j.1365-2958.2009.06821.x.

76. Xu J, Laine O, Masciocchi M, Manoranjan J, Smith J, Du SJ, et al. A unique Mycobacterium ESX-1 protein co-secretes with CFP-10/ESAT-6 and is necessary for inhibiting phagosome maturation. Mol Microbiol. 2007;66:787–800. doi:10.1111/j.1365-2958.2007.05959.x.

77. Houben ENG, Bestebroer J, Ummels R, Wilson L, Piersma SR, Jiménez CR, et al. Composition of the type VII secretion system membrane complex. Mol Microbiol. 2012;86:472–84. doi:10.1111/j.1365-2958.2012.08206.x.

78. van Winden VJC, Ummels R, Piersma SR, Jiménez CR, Korotkov KV, Bitter W, et al. Mycosins Are Required for the Stabilization of the ESX-1 and ESX-5 Type VII Secretion Membrane Complexes. MBio. 2016;7. doi:10.1128/mBio.01471-16.

79. Beckham KSH, Ciccarelli L, Bunduc CM, Mertens HDT, Ummels R, Lugmayr W, et al. Structure of the mycobacterial ESX-5 type VII secretion system membrane complex by single-particle analysis. Nat Microbiol. 2017;2:17047. doi:10.1038/nmicrobiol.2017.47.

80. Converse SE, Cox JS. A protein secretion pathway critical for Mycobacterium tuberculosis virulence is conserved and functional in Mycobacterium smegmatis. J Bacteriol. 2005;187:1238–45. doi:10.1128/JB.187.4.1238-1245.2005.

81. Brodin P, Majlessi L, Marsollier L, de Jonge MI, Bottai D, Demangel C, et al. Dissection of ESAT-6 system 1 of

Mycobacterium tuberculosis and impact on immunogenicity and virulence. Infect Immun. 2006;74:88–98. doi:10.1128/IAI.74.1.88-98.2006.

82. Zhang X-L, Li D-F, Fleming J, Wang L-W, Zhou Y, Wang D-C, et al. Core component EccB1 of the Mycobacterium tuberculosis type VII secretion system is a periplasmic ATPase. FASEB J. 2015;29:4804–14. doi:10.1096/fj.15-270843.

83. Wagner JM, Chan S, Evans TJ, Kahng S, Kim J, Arbing MA, et al. Structures of EccB1 and EccD1 from the core complex of the mycobacterial ESX-1 type VII secretion system. BMC Struct Biol. 2016;16:5. doi:10.1186/s12900-016-0056-6.

84. Ramsdell TL, Huppert LA, Sysoeva TA, Fortune SM, Burton BM. Linked domain architectures allow for specialization of function in the FtsK/SpoIIIE ATPases of ESX secretion systems. J Mol Biol. 2015;427:1119–32. doi:10.1016/j.jmb.2014.06.013.

85. Champion PAD, Stanley SA, Champion MM, Brown EJ, Cox JS. C-terminal signal sequence promotes virulence factor secretion in Mycobacterium tuberculosis. Science. 2006;313:1632–6. doi:10.1126/science.1131167.

86. Stanley SA, Raghavan S, Hwang WW, Cox JS. Acute infection and macrophage subversion by Mycobacterium tuberculosis require a specialized secretion system. Proc Natl Acad Sci USA. 2003;100:13001–6. doi:10.1073/pnas.2235593100.

87. Laencina L, Dubois V, Le Moigne V, Viljoen A, Majlessi L, Pritchard J, et al. Identification of genes required for Mycobacterium abscessus growth in vivo with a prominent role of the ESX-4 locus. Proc Natl Acad Sci USA. 2018;115:E1002–11. doi:10.1073/pnas.1713195115.

88. Solomonson M, Huesgen PF, Wasney GA, Watanabe N, Gruninger RJ, Prehna G, et al. Structure of the mycosin-1 protease from the mycobacterial ESX-1 protein type VII secretion system. J Biol Chem. 2013;288:17782–90. doi:10.1074/jbc.M113.462036.

89. Carlsson F, Joshi SA, Rangell L, Brown EJ. Polar localization of virulence-related Esx-1 secretion in mycobacteria. PLoS Pathog. 2009;5:e1000285. doi:10.1371/journal.ppat.1000285.

90. Wirth SE, Krywy JA, Aldridge BB, Fortune SM, Fernandez-Suarez M, Gray TA, et al. Polar assembly and scaffolding proteins of the virulence-associated ESX-1 secretory apparatus in mycobacteria. Mol Microbiol. 2012;83:654–64. doi:10.1111/j.1365-2958.2011.07958.x.

91. Ates LS, Houben ENG, Bitter W. Type VII secretion: A highly versatile secretion system. Microbiol Spectr. 2016;4. doi:10.1128/microbiolspec.VMBF-0011-2015.

92. Pang X, Samten B, Cao G, Wang X, Tvinnereim AR, Chen X-L, et al. MprAB regulates the espA operon in Mycobacterium tuberculosis and modulates ESX-1 function and host cytokine response. J Bacteriol. 2013;195:66–75. doi:10.1128/JB.01067-12.

93. He H, Hovey R, Kane J, Singh V, Zahrt TC. MprAB is a stress-responsive two-component system that directly regulates expression of sigma factors SigB and SigE in Mycobacterium tuberculosis. J Bacteriol. 2006;188:2134–43. doi:10.1128/JB.188.6.2134-2143.2006.

94. Abramovitch RB, Rohde KH, Hsu F-F, Russell DG. aprABC: a Mycobacterium tuberculosis complex-specific locus that modulates pH-driven adaptation to the macrophage phagosome. Mol Microbiol. 2011;80:678–94. doi:10.1111/j.1365-2958.2011.07601.x.

95. Pérez E, Samper S, Bordas Y, Guilhot C, Gicquel B, Martín C. An essential role for phoP in Mycobacterium tuberculosis virulence. Mol Microbiol. 2001;41:179–87.

96. Lee JS, Krause R, Schreiber J, Mollenkopf H-J, Kowall J, Stein R, et al. Mutation in the transcriptional regulator PhoP contributes to avirulence of Mycobacterium tuberculosis H37Ra strain. Cell Host Microbe. 2008;3:97–103. doi:10.1016/j.chom.2008.01.002.

97. Gonzalo-Asensio J, Soto CY, Arbués A, Sancho J, del Carmen Menéndez M, García MJ, et al. The Mycobacterium tuberculosis phoPR operon is positively autoregulated in the virulent strain H37Rv. J Bacteriol. 2008;190:7068–78. doi:10.1128/JB.00712-08.

98. Solans L, Gonzalo-Asensio J, Sala C, Benjak A, Uplekar S, Rougemont J, et al. The PhoP-dependent ncRNA Mcr7 modulates the TAT secretion system in Mycobacterium tuberculosis. PLoS Pathog. 2014;10:e1004183.

doi:10.1371/journal.ppat.1004183.

99. Blasco B, Japaridze A, Stenta M, Wicky BIM, Dietler G, Dal Peraro M, et al. Functional dissection of intersubunit interactions in the EspR virulence regulator of Mycobacterium tuberculosis. J Bacteriol. 2014;196:1889–900. doi:10.1128/JB.00039-14.

100. Blasco B, Chen JM, Hartkoorn R, Sala C, Uplekar S, Rougemont J, et al. Virulence regulator EspR of Mycobacterium tuberculosis is a nucleoid-associated protein. PLoS Pathog. 2012;8:e1002621. doi:10.1371/journal.ppat.1002621.

101. Raghavan S, Manzanillo P, Chan K, Dovey C, Cox JS. Secreted transcription factor controls Mycobacterium tuberculosis virulence. Nature. 2008;454:717–21. doi:10.1038/nature07219.

102. Solans L, Aguiló N, Samper S, Pawlik A, Frigui W, Martín C, et al. A specific polymorphism in Mycobacterium tuberculosis H37Rv causes differential ESAT-6 expression and identifies WhiB6 as a novel ESX-1 component. Infect Immun. 2014;82:3446–56. doi:10.1128/IAI.01824-14.

103. Phan TH, Ummels R, Bitter W, Houben ENG. Identification of a substrate domain that determines system specificity in mycobacterial type VII secretion systems. Sci Rep. 2017;7:42704. doi:10.1038/srep42704.

104. Phan TH, Houben ENG. Bacterial secretion chaperones; the mycobacterial type VII case. FEMS Microbiol Lett. 2018. doi:10.1093/femsle/fny197.

105. Tian S, Chen H, Sun T, Wang H, Zhang X, Liu Y, et al. Expression, purification and characterization of Esx-1 secretion-associated protein EspL from Mycobacterium tuberculosis. Protein Expr Purif. 2016;128:42–51. doi:10.1016/j.pep.2016.08.001.

106. Behar SM, Divangahi M, Remold HG. Evasion of innate immunity by Mycobacterium tuberculosis: is death an exit strategy? Nat Rev Microbiol. 2010;8:668–74. doi:10.1038/nrmicro2387.

107. Yuk J-M, Jo E-K. Host immune responses to mycobacterial antigens and their implications for the development of a vaccine to control tuberculosis. Clin Exp Vaccine Res. 2014;3:155–67. doi:10.7774/cevr.2014.3.2.155.

Chapter 2

EccE$_1$ assembles at the poles of *Mycobacterium tuberculosis* and is critical for ESX-1 function

Paloma Soler-Arnedo[1], Ming Zhang[1,2], Claudia Sala[1], Jérémie Piton[1], Stewart T. Cole[1,3*]

[1] Global Health Institute, Ecole Polytechnique Fédérale de Lausanne, Switzerland.

[2] Current address: Walter and Eliza Hall Institute of Medical Research, Parkville Victoria, Australia.

[3] Current address: Institut Pasteur, Paris, France.

Manuscript in preparation (2018)

2.1 ABSTRACT

Mycobacterium tuberculosis is a slow-growing intracellular bacterium with the ability to induce host cell death and persist indefinitely in the human body. This pathogen uses the specialised ESX-1 secretion system to secrete virulence factors and potent immunogenic effectors required for disease progression. ESX-1 is a multi-subunit apparatus with a membrane complex that is predicted to form a pore in the cytoplasmic membrane. In *M. tuberculosis* this complex is made of five membrane proteins: $EccB_1$, $EccCa_1$, $EccCb_1$, $EccD_1$, $EccE_1$. In this study, we have characterised the membrane component $EccE_1$, and we found that deletion of *eccE1* leads to disruption of ESX-1 secretion and attenuation of *M. tuberculosis ex vivo*. Surprisingly, secretion of EspB was not affected by loss of $EccE_1$. Furthermore, $EccE_1$ was found to be a membrane- and cell-wall associated protein that needs the presence of other ESX-1 components to assemble into a stable complex at the poles of *M. tuberculosis*. Overall, this study provides new insights into the role of $EccE_1$ and its localisation in *M. tuberculosis*.

2.2 INTRODUCTION

Mycobacterium tuberculosis is a slow-growing intracellular pathogen with the ability to infect and survive inside macrophages, the front line of the immune response. Virulence and host-pathogen interaction are mediated by protein secretion in the tubercle bacilli [1]. In addition to the general Sec secretory pathway and the twin-arginine transporter (TAT) system, *M. tuberculosis* also encodes five specialised Type VII secretion systems (T7SS) which are sub-categorised into ESX-1 to ESX-5 [2]. The T7SS is a multi-subunit apparatus dedicated to the transport of selected proteins across the diderm cell envelope. ESX systems share a similar structure and secrete related proteins but for different functions [3, 4]. ESX-1 is involved in virulence factor secretion and pathogenesis. ESX-3 is critical for bacterial survival due to its function in iron and zinc homeostasis. ESX-5 secretes the majority of the PE and PPE proteins, which play an important role in cell wall stability and virulence [5]. To date, the functions of the ESX-2 and ESX-4 systems in *M. tuberculosis* are unclear.

ESX-1 was identified as essential to induce phagosomal rupture thereby allowing translocation to the cytosol where bacteria can induce host cell death and subsequently spread to neighbouring cells [6–9]. Deletion or inactivation of ESX-1 does not affect growth *in vitro* but causes attenuation of virulence in infection models [10, 11]. Indeed, loss of eight genes (RD1) from the *esx-1* locus is the primary attenuating deletion of the live tuberculosis vaccine, *Mycobacterium bovis* BCG [12].

The locus coding for the ESX-1 secretion system spans 20 genes and codes for secreted factors and structural components. Additionally, the distal *espACD* operon encoding three proteins (EspA, EspC and EspD) is also required for proper ESX-1 activity [13, 14].

The main ESX-1 substrates, EsxA and EsxB, are two major virulence factors and amongst the most potent T-cell antigens of *M. tuberculosis* [4, 15, 16]. Aside from these two substrates, other proteins are also secreted through the ESX-1 machinery such as EspB, EspA and EspC. Importantly, EsxA/EsxB and EspA/EspC, but not EspB, are co-dependent for secretion [13, 17, 18]. Depletion of any of these proteins leads to severe attenuation in cellular and animal models of infection [11, 12, 18–21].

ESX-1 has a set of conserved components with homologues in all mycobacterial ESX systems. Thus far, all the conserved components are required for the ESX secretion process in at least one mycobacterial species [10, 11, 22–28]. The five conserved elements $EccB_1$, $EccCa_1$, $EccCb_1$, $EccD_1$ and $EccE_1$, are putative membrane proteins and are considered core components of the ESX-1 machinery. Homologues of these proteins encoded by the *esx-5* locus form the membrane complex of the ESX-5 secretion system in *Mycobacterium bovis*, *Mycobacterium marinum* and *Mycobacterium xenopi* [24, 26, 29]. New insights into the structure of the membrane complex indicated that the four components $Ecc(BCDE)_5$ are present in equimolar amounts and assemble into an hexameric arrangement around a central pore [29]. Considering the conserved nature of the Ecc elements, the presumed structure of the ESX-1 membrane complex might resemble that of ESX-5.

Another conserved component of the ESX-1 apparatus is $MycP_1$, a membrane protein which is not part of the core membrane complex but loosely associated with it [26]. $MycP_1$ is a subtilisin-like serine protease that cleaves EspB in the periplasmic space [22, 26]. Beside its role in substrate processing, $MycP_1$ plays a second role in the secretion process by stabilising the ESX-1 membrane complex [26]. In the *esx-1* locus of *M. tuberculosis, mycP1* is situated upstream of *eccE1* and the two genes are co-transcribed [30, 31]. $EccE_1$ is the conserved element that has been the least explored, especially in *M. tuberculosis* where no experimental work on this component has been reported yet. In *M. smegmatis,* the homologue of $EccE_1$ is required for EsxA and EsxB secretion. Previous work on the composition and structure of the ESX-5 membrane complex demonstrated that $EccE_5$ is located at the perimeter of the membrane complex and is important for its formation and stability [24, 29]. Interestingly, EccE is missing in the ESX-4 apparatus of *M. tuberculosis* which is the most ancestral system. This absence may indicate that EccE appeared later in evolution or that it is dispensable to form a basic membrane complex. Indeed, a membrane subcomplex without $EccE_5$ can be constituted in *M. xenopi*. This ESX-5 subcomplex is less abundant, smaller but with similar hexameric assembly as the complete membrane complex [29]. Exceptionally, the *esx-4* locus of *Mycobacterium abscessus,* a rapidly growing mycobacterium and an opportunistic human pathogen, includes the EccE component. In addition, *M. abscessus* lacks the ESX-1 secretion system and needs the ESX-4 apparatus for intracellular survival [32].

Although the molecular mechanisms underlying the ESX secretion process are not fully understood, studying individual components has provided important insights. Localizing the active ESX systems can also offer valuable information about the mechanism of secretion. ESX-1-related proteins have been visualised at the cell poles of *M. marinum* and *M. smegmatis* [33, 34]. Nonetheless, information about the localisation of the entire ESX-1 system in *M. tuberculosis* is missing. Considering that Ecc are conserved and core membrane components, $EccE_1$ appears as an interesting candidate to localise the active ESX-1 system in *M. tuberculosis.* Moreover, its likely peripheral localisation at the membrane complex is an interesting feature when considering the addition of a tag.

In this study, we explored the role of $EccE_1$ in *M. tuberculosis* virulence. We showed that $EccE_1$ is required for ESX-1-related secretion and *ex vivo* virulence. Moreover, we investigated the localisation of the protein and incorporation into a functional ESX-1 system. Our findings suggest that $EccE_1$ is a membrane- and a cell wall-associated protein that requires other ESX-1 components to form a stable complex at the poles of *M. tuberculosis*.

2.3 RESULTS

Mutant construction

To assess the role of $EccE_1$ in the ESX-1-related function, we first constructed an *eccE1* deletion mutant in *M. tuberculosis*. As *eccE1* is in the same transcriptional unit as *mycP1* [30, 31], we initially deleted the entire *mycP1-eccE1* region from the chromosome by allelic exchange. Whole genome sequencing confirmed the complete deletion of the *mycP1-eccE1* coding sequences (CDS) and the absence of other mutations in the genome. The resulting *mycP1-eccE1* double mutant was then partially or fully complemented with an integrative plasmid encoding either the single genes *mycP1* or *eccE1*, or the entire *mycP1-eccE1* locus under the control of the PTR promoter. As a result, we obtained four strains: a double mutant Δ*mycP1-eccE1*, a fully complemented strain Δ*mycP1-eccE1*/*mycP1-eccE1* and two partially complemented strains Δ*mycP1-eccE1*/*mycP1* and Δ*mycP1-eccE1*/*eccE1* which correspond to the single mutants Δ*eccE1* and Δ*mycP1* respectively.

The four strains were subsequently analysed by RNA sequencing and the transcriptional profile compared to that of the H37Rv wild type (WT) strain. As anticipated, no de-regulated genes were found except for the deleted genes, suggesting that the excision of *eccE1*-*mycP*1 and their complementation *in trans* did not impact the transcription of other genes. In the complemented derivatives, the expression levels of *mycP1* and *eccE1* were very similar to those measured in the WT strain (Table S1).

The ability of the defective strains to grow in synthetic media was explored. The Δ*eccE1* mutant, as well as the Δ*mycP*1 and the Δ*mycP*1-*eccE1,* exhibited growth kinetics similar to that of the WT strain (Figure S1). These results indicate that *eccE1* and *mycP*1 are not required for *in vitro* growth of *M. tuberculosis*.

$EccE_1$ and $MycP_1$ are not involved in susceptibility to drugs targeting the cell envelope

Previous studies on the ESX-5 system demonstrated that disruption of this apparatus in *M. tuberculosis* reduces cell wall integrity [23]. Consequently, the susceptibility to various antibiotics targeting several steps in the cell wall biosynthetic pathway highly increased [23]. To test whether its paralogue, the ESX-1 system, is also involved in maintaining the stability of the cell envelope, the drug susceptibility of the mutants to various cell wall targeting antibiotics was evaluated using the resazurin-based microdilution assay (REMA) [35]. The Δ*eccE1* mutant and the WT strain were characterised by similar minimal inhibitory concentrations (MIC) to all antibiotics tested. The same phenotype was observed for the Δ*mycP*1 and the Δ*mycP*1-*eccE1* mutants (Table S2). We concluded that the absence of either *eccE*1 or *mycP*1 did not impact the susceptibility to β-lactams (penicillins and cephalosporins) or to glycopeptides (vancomycin). These results suggest that loss of the ESX-1 system does not affect the integrity of the cell envelope in *M. tuberculosis*.

$EccE_1$ and $MycP_1$ are required for *M. tuberculosis*-mediated cell death

EccE was identified as a peripheral component of the ESX membrane complex, but further information about its role in *M. tuberculosis* is missing. To investigate the implication of $EccE_1$ in ESX-1-mediated function, we exploited the ability of *M. tuberculosis* to induce host cell death, which is linked to ESX-1-related secretion [6, 8]. To this aim, THP-1 human macrophages were infected with the *mycP1* and *eccE1* mutants as well as with the WT strain and the survival of macrophages was monitored. In the presence of WT *M. tuberculosis*, the survival of macrophages significantly decreased compared to the non-infected control. In contrast, when

macrophages were infected with strains lacking either *eccE1* and/or *mycP1*, the macrophages survived to levels similar to the non-infected control. Importantly, the complemented mutant restored the WT phenotype (Figure 1A). This result indicates that *M. tuberculosis* needs both $EccE_1$ and $MycP_1$ for cytotoxicity and that the absence of either of these ESX-1 components leads to complete attenuation of *M. tuberculosis ex vivo*.

To validate the attenuated phenotype displayed in the absence of *eccE1* and/or *mycP1*, we evaluated the levels of intracellular bacteria at 4h, 24h and 72h post-infection by colony forming units (CFU) enumeration. At 4h after infection, the bacterial burden was similar for the WT and the mutants, indicating that all strains were phagocytosed with similar efficiency (Figure 1B). Once inside the host cell, the Δ*eccE1*, Δ*mycP*$_1$ and the Δ*mycP*$_1$-*eccE1* mutants showed similar and stable CFU numbers over the course of the infection, whereas the WT and the complemented mutant exhibited a reduced number of bacteria at 72h post-infection compared to previous time points (Figure 1B). The decrease in intracellular bacteria confirmed the ability of the WT strain and of the complemented mutant to induce macrophage lysis. Overall, these results demonstrated that *M. tuberculosis* does not require $EccE_1$ or $MycP_1$ to infect or survive inside macrophages, but it needs both components to induce host cell death.

$EccE_1$ and $MycP_1$ are essential for ESX-1-protein-secretion

To determine if $EccE_1$ and $MycP_1$ are crucial to the function of the ESX-1 machinery, we checked whether the deletion of *eccE1* and/or *mycP1* impacts ESX-protein secretion. To this end, cell lysates and culture filtrates of WT and mutant bacteria were prepared and analysed by immunoblotting. The presence of Ag85B, an ESX-1 independent secreted protein, and the absence of the cytosolic GroEL2 protein from culture filtrates served as controls. As expected, EsxA and EsxB were present in the secreted fraction of the WT *M. tuberculosis* strain. However, EsxA and EsxB were not detected in the culture filtrates of the strains lacking *eccE1* and/or *mycP1* although both substrates were present in the cell lysates. Furthermore, secretion of EsxA and EsxB was restored in the fully complemented strain Δ*mycP*$_1$-*eccE1*/*mycP*$_1$-*eccE1* (Figure 2A). These data indicate that the presence of both $MycP_1$ and $EccE_1$ is required for secretion of the two main ESX-1 substrates. In contrast, EspB, another known ESX-1 substrate, was found in the cell lysates and culture filtrates of the WT, mutant and complemented strains (Figure 2A), suggesting that secretion of EspB is independent of $EccE_1$ or $MycP_1$. Overall, we can conclude that the expression of EsxA, EsxB and EspB is not affected by the absence of $EccE_1$ or $MycP_1$.

However, both ESX-1 membrane proteins are essential for EsxA and EsxB secretion but dispensable for the release of EspB into the culture filtrate.

To obtain deeper knowledge into the impact of $EccE_1$ and of $MycP_1$ on *M. tuberculosis* secretion and to identify potential $EccE_1$-dependent substrates, the whole secretome of the mutants was analysed and compared to that of the WT strain. Bacteria were grown in the same conditions as previously described for immunoblotting and the secreted fraction analysed by mass spectrometry. We found that EsxA, EsxB, EspA and EspC were the only proteins significantly deregulated in the culture filtrates (Figure 2B). Moreover, in the WT strain, EsxA was in the top ten most abundant proteins. On the other hand, the secretion of this protein decreased by 5-fold on average when $EccE_1$ and $MycP_1$ were missing (Figure 2C). The same trend was observed for EsxB, EspA and EspC whose secretion was also highly decreased (fold change between 3.6-7.8) in the deletion mutants compared to the WT strain (Figure 2C). It was noteworthy that the levels of the rest of ESX-1-related proteins, including EspB, was not different in the absence or presence of $EccE_1$ and $MycP_1$. Proteins secreted through other secretion systems, such as Ag85B, were secreted at similar levels in the WT and in the mutants (Figure 2C). Taken together, the secretome analysis demonstrated that only the secretion of EsxA, EsxB, EspA and EspC is dependent on $EccE_1$ and $MycP_1$. This analysis also confirmed the previous results obtained by immunoblotting.

$EccE_1$ is a membrane and cell wall-associated protein

As antibodies against $EccE_1$ of *M. tuberculosis* were not available, an HA tag, which has been successfully exploited in the past to study ESX-1-related proteins [36], was inserted in the C-terminal part of $EccE_1$ by genetic engineering. For this propose, the double mutant Δ*mycP*$_1$-*eccE*$_1$ was complemented with an integrative plasmid carrying *mycP*$_1$ and *eccE*$_1$-*HA* (Δ*mycP*$_1$-*eccE*$_1$/*mycP*$_1$-*eccE*$_1$*HA*). Both genes were present in single copy and expressed under the control of the same promoter, PTR. To make sure that the presence of the tag did not interfere with the activity of $EccE_1$, the ability of the HA-tagged mutant to induce cell lysis was tested. The THP-1 *ex vivo* model of infection confirmed that the $EccE_1$-HA expressing mutant was as cytolytic as the WT strain, thereby implying the presence of a functional ESX-1 system and so, a functional $EccE_1$ protein (Figure 3B).

$EccE_1$ is predicted to be a membrane protein in *M. tuberculosis*. To support this prediction, subcellular fractionation followed by immunoblotting was performed using the mutant carrying *eccE1-HA*. Bacterial extracts were separated into cytosolic, membrane, cell wall, capsular and secreted fractions. Several controls were employed to validate the procedure. RpoB, an RNA polymerase subunit, was found mainly in the cytosol and partly in the membrane. Rv3852, a membrane protein, was only present in the membrane fraction as previously described [37]. EsxB, a substrate of the ESX-1 system, was detected in the cytosol and slightly in the capsule although it was mainly found in the culture filtrate. Importantly, EsxB was not detected in the membrane and the cell wall. Interestingly, EspB, another ESX-1 substrate, was detected everywhere but mainly in the cytosol and secreted fractions. Finally, $EccE_1$ was identified in the membrane and cell wall but not in other compartments of *M. tuberculosis* (Figure 3A).

$EccE_1$ assembles with other ESX-1 proteins at the poles of *M. tuberculosis*

Fluorescent-fusion proteins have been successfully employed to study ESX-1-related proteins in *M. smegmatis* [34]. Overexpression of reporter proteins is usually required for visualisation, however, production of a large amount of proteins can eventually lead to artificial phenotypes or artefacts. To avoid this potential problem, we constructed a fluorescent-fusion protein of $EccE_1$ with mNeon, a 27 kDa monomeric fluorescent protein reported to be three to five times brighter than GFP and export-competent [38–40]. To generate the $EccE_1$-mNeon expressing strain, the same strategy used for generating the Δ*eccE1/eccE1-HA* was followed. The complemented derivative (Δ$mycP_1$-*eccE1*/$mycP_1$-$eccE_1$mNeon) has a single copy of $mycP_1$ and $eccE_1$-mNeon genes under the control of the PTR promoter, which provides expression of $EccE_1$-mNeon close to physiological conditions. To check whether fusion to mNeon impacted $EccE_1$ function, the cytotoxic phenotype of the mutant was analysed using THP-1 macrophages. The $EccE_1$-mNeon expressing mutant induced cell death similarly to the WT strain (Figure 4B), suggesting that this mutant can form a functional ESX-1 secretion system. Since the WT copy of $EccE_1$ is not present in the mutant and this protein is required for ESX-1 function in *M. tuberculosis*, all active ESX-1 apparatuses in the fluorescent mutant should contain $EccE_1$-mNeon proteins.

To gain more insights into the localisation of $EccE_1$ and of the ESX-1 system in *M. tuberculosis*, the fluorescent mutant Δ$mycP_1$-*eccE1*/$mycP_1$-$eccE_1$mNeon was used to image live bacteria. The double mutant Δ$mycP_1$-*eccE1*

expressing mNeon alone (Δ*mycP*$_1$-*eccE*$_1$/mNeon) and the H37Rv ΔΔRD$_1$ mutant (lacking most of the *esx-1* locus) expressing EccE$_1$-mNeon (ΔΔRD$_1$/*mycP*$_1$-*eccE*$_1$mNeon) were used as controls. We observed bi-polar foci in 100% of Δ*mycP*$_1$-*eccE*$_1$/*mycP*$_1$-*eccE*$_1$mNeon cells (Figure S2). However, cells expressing mNeon alone did not display polar localisation but a diffuse signal all over the bacterium (Figure 4A). Moreover, the ΔΔRD$_1$ expressing EccE$_1$-mNeon did not show the same bi-polar fluorescent pattern but a more diffuse signal (Figure 4A). These results indicate that EccE$_1$ localises to the poles of *M. tuberculosis* and needs others ESX-1-associated proteins to form a stable complex at the poles of the bacilli. Altogether, we can conclude that the bi-polar localisation may not only correspond to the EccE$_1$ protein but also to the functional and assembled ESX-1 apparatus.

2.4 DISCUSSION

Our current knowledge of the ESX secretion systems comes mainly from research on ESX-1 and ESX-5. In this context, the role of the membrane protein EccE$_1$ in the secretion process has been so far poorly understood. In the present study, we constructed and utilised genetic tools to gain insights into the functional role of EccE$_1$ in the virulence mechanism of *M. tuberculosis*.

EccE$_5$ was recently described as a peripheral component of the membrane complex important for stabilising the machinery [29]. Here, we demonstrated that the absence of EccE$_1$ did not affect *M. tuberculosis* growth in culture medium indicating that this protein is not essential for bacterial survival (Fig. S1). Additionally, EccE$_1$ was proved to be essential for macrophage lysis, a function required for *M. tuberculosis* pathogenesis (Fig. 1). In line with these observations, previous work reported the inability of the ΔRD1 mutant and other ESX-1 mutants to mediate host cell death and induce full virulence [10, 11, 41]. To the best of our knowledge, this is the first time that disruption of the core component EccE$_1$ in *M. tuberculosis* has been proved to lead to complete attenuation *ex vivo*.

Analysis of ESX-1-secreted proteins offers a solid explanation for this phenotype. Thus, secretion of EsxA, EsxB, EspA and EspC, which is essential to promote virulence [13, 14, 27], was found to be strongly dependent on EccE$_1$. This analysis confirmed the critical role of this peripheral membrane protein in the ESX-1 secretion process and consequently in the virulence response of *M. tuberculosis*. Interestingly, EsxA, EsxB, EspA and

EspC are known to be co-dependent for secretion, meaning that the absence of one of them completely abolishes secretion of the others [13, 14]. Due to this interdependence, we cannot exclude that $EccE_1$ is only directly implicated in the secretion of an individual substrate, and consequently, indirectly impacts the secretion of other dependent proteins. Similar phenotypes were also observed in the Δ*mycP1* mutant, confirming that $MycP_1$ presence is essential for EsxA/B secretion and virulence in *M. tuberculosis* as previously reported [22]. Surprisingly, secretion of EspB was not affected by the absence of $EccE_1$ and/or $MycP_1$ suggesting that secretion of this protein is independent of a fully assembled ESX-1 system. It is tempting to hypothesise that EspB might be secreted by a minimal core component before the addition of peripheral proteins such as $MycP_1$ and $EccE_1$. Alternatively, an ESX-1-independent secretion mechanism may be involved, as postulated for EspD [21]. In contrast with our findings, EspB secretion was previously reported to require the presence of $MycP_1$ in both *M. tuberculosis* and *M. marinum* [22, 26]. Interestingly, the ESX-2 secretion system is absent in *M. marinum* and it may be non-functional in the *M. tuberculosis* Erdman strain as various ESX-2 conserved components are mutated. In the present study, the secretion of EspB was analysed in the *M. tuberculosis* H37Rv strain whereas in previous studies an Erdman background was used [22]. The differences in the ESX-2 secretion system may explain the discrepancy of EspB secretion. Thus, EspB might be translocated through both the ESX-1 and the ESX-2 secretion systems. However, in the absence of a functional ESX-2, EspB secretion may depend exclusively on the ESX-1 apparatus.

We confirmed that $EccE_1$ is a membrane-anchored protein (Fig. 3). Two potential transmembrane regions in the N-terminal part of the protein were identified by the THMM prediction server [42]. However, this region is the tip of the iceberg and the C-terminal part of the protein, corresponding to 90% of the protein, is predicted to be hydrophilic. The large amount of $EccE_1$ found in the cell wall fraction during our cell fractionation experiment strongly suggests that the C-terminus of $EccE_1$ localises in the cell wall. Furthermore, this part of the protein is probably malleable and not buried in the complex as the HA and mNeon tags did not interfere with $EccE_1$ function. Hence, we hypothesise that $EccE_1$ is a cell wall-associated protein maintained in the membrane via a transmembrane anchor. This is consistent with the structure of the ESX-5 membrane complex where the soluble domain of $EccE_5$ was predicted to be located in the periplasmic space [29].

$EccE_5$ is one of the peripheral proteins of the ESX-5 complex, and consequently, it may be one of the last proteins of the core component to associate [24, 29]. Considering the critical role of $EccE_1$ in the secretion of EsxA and EsxB in *M. tuberculosis* (Fig. 2) and its homology with $EccE_5$, we think that $EccE_1$ could be a good reporter of a fully assembled and functional ESX-1 secretion system. Two previous studies demonstrated the presence of ESX-1 core components at a single cell pole in *M. marinum* and *M. smegmatis* using immunofluorescence and microscopy analysis of single cells overexpressing fluorescent fusion proteins [33, 34]. In this study, we localised the fully assembled ESX-1 machinery to both poles of *M. tuberculosis* using non-overexpressed fluorescent $EccE_1$ fusion protein. The fluorescent bipolar foci pattern coming from $EccE_1$-mNeon was observed in the presence of a functional ESX-1 apparatus, whereas, in the absence of a complete *esx-1* locus, the $EccE_1$-mNeon signal at the membrane was more diffuse. These observations suggest that the polar localisation of $EccE_1$ in *M. tuberculosis* also corresponds to the fully assembled ESX-1 system. In contrast to *M. smegmatis* and *M. marinum,* where ESX-1 was preferentially found at a single cell pole, in *M. tuberculosis* 100% of cells displayed bipolar localisation.

Interestingly, many proteins involved in peptidoglycan, arabinogalactan and mycolic acid biosynthesis also localise to polar regions in *M. tuberculosis* [43, 44]. Previous studies hypothesised that ESX-1 might function in the generation or modification of the mycobacterial cell wall [34]. However, we demonstrated that disruption of the core components *eccE1* and *mycP1* and therefore, disruption of the ESX-1 apparatus, did not impact cell wall permeability as evidenced by unaltered susceptibility to antibiotics (Table S2).

Overall, this work has provided new understanding of the ESX-1 system in *M. tuberculosis* and demonstrated that the core component $EccE_1$ is essential for secretion of virulence factors and induction of host cell lysis. Moreover, this is the first time that a functional ESX-1 apparatus was localised in *M. tuberculosis* which could be extremely useful for future research aimed to visualise the nanomachine *in situ*. Investigating how proteins are directed to the poles and elucidating the mechanism governing ESX-1 assembly and localisation will provide us with important insights to understand this complex virulence determinant.

2.5 MATERIALS AND METHODS

Bacterial culture conditions

M. tuberculosis was routinely grown in 7H9 broth (supplemented with 0.2% glycerol, 10% ADC, 0.05% Tween-80) or on 7H10 agar (supplemented with 0.5% glycerol and 10% OADC). *Escherichia coli* TOP10 or chemically-competent *E. coli* DH5α cells were used for cloning and plasmid propagation and were grown on LB broth or agar.

Mutant construction

Deletion of the *mycP1-eccE1* region was accomplished in the H37Rv strain by two-step homologous recombination using the pJG1100-derived vector [45]. To construct the required plasmid, two fragments of about 900 bp corresponding to the upstream and downstream regions of *mycP1-eccE1*, were amplified with oligonucleotides MZ-198-F and MZ-199-R and inserted in the pJG1110 vector. After transformation of *M. tuberculosis* H37Rv with the pJG1100-derived vector, the first recombination event was selected on Middlebrook 7H10 medium containing hygromycin (50 μg/ml) and kanamycin (20 μg/ml). Positive colonies were identified by PCR and subjected to a second round of selection on 7H10 medium supplemented with 2.5% sucrose. The absence of *mycP1-eccE1* in the resulting clones was scored by PCR and further confirmed by Southern blotting.

DNA extraction and whole-genome sequencing

The *M. tuberculosis* Δ*mycP1-eccE1* mutant was grown in 10 mL 7H9 broth to OD_{600} 0.8. Bacteria were harvested by centrifugation and DNA was extracted using the QIAmp UCP pathogen kit (Qiagen) as described previously [46]. DNA was quantified using the Qubit dsDNA HS Assay Kit and the Qubit 2.0 Fluorometer (Thermo Fisher Sc.). Ilumina libraries were prepared using the Kapa Hyper prep kit as described [46]. Briefly, 1μg of extracted DNA was sonicated to obtain 400 bp long fragments with the S220 Covaris (Covaris) using the manufacturer's protocol and purified using 1.8X AMPure beads (ThermoFisher Sc.) and eluted in 50 μL of Tris-HCl 10mM. Sequencing libraries were synthesised with the Kapa Hyper prep kit (Kapa Biosystems) according to the manufacturer's instructions and an adapter stock of 15 μM of

PentAdaptersTM (PentaBase) was used to barcode the library. After the final amplification step, libraries were quantified using Qubit dsDNA BR Assay Kit (Thermo Fisher Sc) and the fragment size was assessed on a Fragment Analyzer (Advanced Analytical Technologies). Finally, libraries were multiplexed and sequenced as 100 base-long single-end reads on an Illumina HiSeq 2500 instrument. Reads were adapter- and quality-trimmed with Trimmomatic v0.33 [47] and mapped onto the *M. tuberculosis* H37Rv reference genome (RefSeq NC_000962.3) using Bowtie2 v2.2.5 [48].

Complemented derivative constructions

The integrative pGA44 vector [49] was used to construct all complemented derivates. All plasmids used in this study are listed in Table S3. Briefly, the genes of interest were PCR amplified from *M. tuberculosis* H37Rv genomic DNA using appropriate oligonucleotides (Table S4). Then, the PCR fragments were cloned in-frame under the PTR promoter into the AvrII and PacI sites. All plasmids were checked by Sanger sequencing and were further transformed into competent *M. tuberculosis ΔmycP1-eccE1* cells together with pGA80 [49] which provided the integrase. Transformants were selected on 7H10 agar containing streptomycin (20 μg/ml). Note that pPS12 was also transformed in the *M. tuberculosis* ΔΔRD1 mutant. All complemented derivatives used in this study are listed in Table S5.

RNA-seq

M. tuberculosis strains were grown in 25 ml of Sauton's medium without detergent to OD_{600} ~ 0.5. Then, cultures were harvested by centrifugation and the resulting pellets resuspended in 1 mL TRIzol Reagent (ThermoFisher) and stored at -80°C until further processing. Bacteria were disrupted by bead-beating and total RNA was isolated as previously described [50]. Two independent cultures for each strain were used for this experiment. Total RNA concentration was measured using the Qubit RNA HS Assay Kit Libraries of ribosomal-depleted RNA were prepared with 300 ng of fragmented RNA by the Lausanne Genomic Technologies Facility, using the Ribo-zero rRNA removal kit for Gram positive bacteria and the Truseq Stranded mRNA Library Prep kit reagents (Illumina). Libraries were multiplexed and sequenced on Illuma HiSeq 2500 as single-end 100 nt-long reads and data were processed using the Illumina Pipeline Software version 1.84. Reads were adapter- and quality-trimmed with Trimmomatic v0.33 [47] and mapped onto the *M.*

tuberculosis H37Rv reference genome (RefSeq NC_000962.3) using Bowtie2 v2.2.5 [48]. Counting reads over features was done with featureCounts from the Subread package v1.4.6 [51] and DESeq2 [52] was used to infer differentially expressed genes.

In vitro growth curves

All strains were diluted to an initial OD_{600} of 0.05 in Middlebrook 7H9 medium, and the OD_{600} recorded at different time points over a period of 7 days. Data from three independent experiments were used for growth representation.

Antibiotic susceptibility

To evaluate the susceptibility of bacteria to antibiotics, the MIC values were determined by using the resazurin-based microdilution assay (REMA) as previously described [35]. *M. tuberculosis* strains were grown in 7H9 broth to mid-logarithmic phase (optical density at 600 nm [OD_{600}] of ~0.6) and diluted to an OD_{600} of 0.0001. Then, 3×10^3 cells/well (100 μl/well) were pipetted into a 96-well plate. Antibiotics (amoxicillin, ampicillin, cefadroxil, cefdinir, vancomycin and rifampin) were added to the first column, and subsequently, 2-fold serial dilutions were made. Bacteria were incubated in the presence of antibiotics for 6 days at 37°C and afterwards, 10 μl (1/10 of the total volume) of 0.025% (wt/vol) resazurin were added to each well. The fluorescence intensity was read after 16-24 h of incubation at 37°C by using an Infinite F200 Tecan plate reader. MIC values were determined by nonlinear fitting of the data to the Gompertz equation [53] using GraphPad Prism.

Macrophage survival

Human monocytic THP-1 cells were grown in RPMI medium supplemented with 10% FBS. Monocytes were prepared at a concentration of $2x10^6$ cell/ml and differentiated into macrophages using phorbol-12-myristate-13-acetate (PMA) at a final concentration of 4 nM. Subsequently, 10^5 cell/well (50 μl/well) were pipetted into a 96 well-plate before the plate was sealed with a gas-permeable film and incubated at 37°C with 5% CO_2 for 18h. Medium containing PMA was removed and replaced with 50 μl of new RPMI medium. Bacteria were grown to OD_{600} 0.4-0.8, washed, resuspended in 7H9 broth to an OD_{600} of 1 (3×10^8 bacteria/ml) and diluted in RPMI medium at a concentration of 10^7 bacteria/ml. THP-1 cells were then infected at a multiplicity of

infection (MOI) of 5 (50 µl/well of 10^7 bacteria/ml in RPMI) and incubated for three days at 37°C with 5% CO_2. Afterwards, 5 µl (1:20) of PrestoBlue cell viability reagent (Life Technologies) was added to each well, the plate incubated for 30 min at 37°C and the fluorescence measured using a Tecan M200 instrument (excitation/emission wavelength of 560/590 nm). Fluorescence (560/590) unit of three biological replicates (for each strain tested) was analysed in GraphPad Prism (version 5) and significant difference between the conditions was determined using the Student t-test.

Intracellular bacteria

THP-1 macrophages were infected with *M. tuberculosis* strains at MOI of 5 as described above. Four hours post-infection, extracellular bacteria were removed by washing with warm RPMI medium. Infected macrophages were further incubated at 37°C with 5% CO_2 in the presence of RPMI. At 4, 24 and 72h post-infection, cells were washed twice with warm PBS to remove extracellular bacteria and lysed with 0.1% TritonX-100 in PBS. Lysates were diluted, plated on 7H10 medium and the plates were incubated for three weeks before the CFU were determined. Results from three independent replicates are represented.

Protein preparation for secretion analysis

Bacteria were first grown in 7H9 broth to mid-logarithmic phase (OD_{600} ~ 0.6). Then, bacteria were cultured in 30 ml of Sauton's liquid medium supplemented with 0.05% Tween80 at a starting OD_{600} of 0.1. Cells were grown to OD_{600} of 0.6, centrifuged, resuspended in Sauton's medium without Tween80 and grown further at 37°C with shaking for 4 days. Cultures were harvested by centrifugation to obtain the cell pellet and the secreted fractions. The secreted fraction was filtered through 0.22-µm-pore-size filters to remove *M. tuberculosis* cells and concentrated 100x in Amicon filters with 3-kDa-molecular-weight-cutoff membranes (3,000 MWCO) (Millipore). To prepare the cell lysate, the cell pellet was washed once with PBS, resuspended in TBS buffer with Roche protease inhibitor cocktail tablets, disrupted by bead beating with 0.1mm zirconia beads, clarified by centrifugation and filtered through 0.22-µm-pore-size filters. Total protein concentration in all preparations was determined using the BCA assays with bovine serum albumin as the standard.

Immunoblotting

Indicated amounts of total proteins from the culture filtrate, total cell lysates and subcellular fractions were resolved in NuPAGE 4-12% bis-Tris gels (Invitrogen). Proteins were transferred to nitrocellulose membranes using the iBlot gel transfer system (Invitrogen). Membranes were blocked with 5% milk in TBS (150 mM NaCl, 20 mM Tris-HCl, pH 7.5 and nonfat milk powder) for 1h and then incubated with the required antibody diluted in TBST-1% BSA (TBS, 0.05% Tween-20, BSA) for 16h at 4°C. Membranes were washed with TBST 3 times before and after being incubated with the appropriate secondary antibody for 30 min at room temperature and subsequently developed using a chemiluminescent peroxidase substrate (Sigma-Aldrich). GroEL2 was used as a loading control for cell lysates and Ag85B, an ESX-1 independent secreted protein, as a loading control for culture filtrate.

Mass spectrometry-based secretome analysis

Culture filtrates were incubated 10 min in 100µl of 8 M urea in 0.1 M Tris-HCl pH 8 at room temperature. Each sample was digested by Filter Aided Sample Preparation (FASP) [54] with minor modifications. Dithiothreitol (DTT) was replaced by Tris(2-carboxyethyl)phosphine (TCEP) as reducing agent and Iodoacetamide by Chloracetamide as alkylating agent. A combined proteolytic digestion was performed using Endoproteinase Lys-C and Trypsin. Acidified peptides were desalted on C18 StageTips [55] and dried down by vacuum centrifugation. For LC MS/MS analysis, peptides were resuspended and separated by reversed-phase chromatography on a Dionex Ultimate 3000 RSLC nanoUPLC system in-line connected with an Orbitrap Q Exactive HF Mass-Spectrometer (Thermo Fischer Scientific). Database search was performed using MaxQuant 1.6.0.1 [56] against the TubercuListR27 database (http://tuberculist.epfl.ch/). Carbamidomethylation was set as fixed modification, whereas oxidation (M), phosphorylation (S,T,Y) and acetylation (Protein N-term) were considered as variable modifications. Label Free Quantification (MaxLFQ) was performed by MaxQuant using the standard settings [57]. Perseus [58] was used to highlight differentially quantified proteins. Reverse proteins, contaminants and proteins only identified by sites were filtered out. Biological replicates were grouped together and protein groups containing a minimum of two LFQ values in at least one group were conserved. Empty values were imputed with random numbers from a normal distribution. Significant hits were determined by a volcano plot-based strategy, combining t test p-values with ratio information [59]. Significance curves in the volcano plot corresponding to a SO value of 0.5 and 0.05

FDR were determined by a permutation-based method. Further graphical displays were generated using homemade programs written in R [60].

Cell fractionation

The cell fractionation protocol was based on previous work [36, 37]. *M. tuberculosis* Δ*eccE$_1$/eccE$_1$HA* mutant was grown in 100 ml of Sauton's medium without Tween-80 for 4 days with a starting OD_{600} 0.5. Bacteria were harvested by centrifugation and the supernatant concentrated 100 times with Vivaspin columns (3,000 Da MWCO) after 0.22 μm filtration to obtain the secreted fraction. The cell pellet was washed once with PBS and then treated with 0.25% Genapol-X080 for 30 min at room temperature with gentle shaking followed by centrifugation at 3,000 g for 10 min. Proteins present in the resulting supernatant were precipitated with trichloro-acetic acid (TCA) yielding the capsular fraction [61]. The remaining pellet was washed with PBS and subjected to sonication to break the cells. After centrifugation at 3,000 g for 10 min to eliminate unbroken cells, the supernatant was centrifuged at 20,000 rpm for 30 min. The resulting pellet, which corresponds to the cell wall fraction, was heat inactivated for 1h at 100°C and the supernatant filtered through a 0.22 μm filter and centrifuged at 45,000 rpm for 1h in an ultracentrifuge. The supernatant contained the cytosolic fraction, while the pellet was enriched with membrane proteins.

Fluorescence microscopy

mNeon expressing bacteria were grown in 7H9 broth to log phase (OD_{600} 0.4-0.8). 4 μl of bacterial suspension was mounted on a microscope slide with 1.5% agarose pads and directly examined with an Olympus IX81 microscope under a 100x objective. Images were analysed using ImageJ and normalised for brightness, contrast and resolution.

AKNOWLEDGMENTS

We thank A. Benjak for the analysis of high-throughput sequencing data, C. Avanzi for library preparation, the Proteomics Core Facility at EPFL for mass spectrometry experiments, the Lausanne Genomic

Technologies Facility at the University of Lausanne for high-throughput sequencing analyses and YW Chang for providing the mNeon protein and valuable advice. The research leading to these results has received funding from the Swiss National Science Foundation under grant 31003A-162641 to STC.

2.6 BIBLIOGRAPHY

1. Stoop EJM, Bitter W, van der Sar AM. Tubercle bacilli rely on a type VII army for pathogenicity. Trends Microbiol. 2012;20:477–84. doi:10.1016/j.tim.2012.07.001.

2. Cole ST, Brosch R, Parkhill J, Garnier T, Churcher C, Harris D, et al. Deciphering the biology of Mycobacterium tuberculosis from the complete genome sequence. Nature. 1998;393:537–44. doi:10.1038/31159.

3. Bitter W, Houben ENG, Bottai D, Brodin P, Brown EJ, Cox JS, et al. Systematic genetic nomenclature for type VII secretion systems. PLoS Pathog. 2009;5:e1000507. doi:10.1371/journal.ppat.1000507.

4. Simeone R, Bottai D, Brosch R. ESX/type VII secretion systems and their role in host-pathogen interaction. Curr Opin Microbiol. 2009;12:4–10. doi:10.1016/j.mib.2008.11.003.

5. Ates LS, Houben ENG, Bitter W. Type VII secretion: A highly versatile secretion system. Microbiol Spectr. 2016;4. doi:10.1128/microbiolspec.VMBF-0011-2015.

6. Simeone R, Bobard A, Lippmann J, Bitter W, Majlessi L, Brosch R, et al. Phagosomal rupture by Mycobacterium tuberculosis results in toxicity and host cell death. PLoS Pathog. 2012;8:e1002507. doi:10.1371/journal.ppat.1002507.

7. Simeone R, Sayes F, Song O, Gröschel MI, Brodin P, Brosch R, et al. Cytosolic access of Mycobacterium tuberculosis: critical impact of phagosomal acidification control and demonstration of occurrence in vivo. PLoS Pathog. 2015;11:e1004650. doi:10.1371/journal.ppat.1004650.

8. Conrad WH, Osman MM, Shanahan JK, Chu F, Takaki KK, Cameron J, et al. Mycobacterial ESX-1 secretion system mediates host cell lysis through bacterium contact-dependent gross membrane disruptions. Proc Natl Acad Sci USA. 2017;114:1371–6. doi:10.1073/pnas.1620133114.

9. Houben D, Demangel C, van Ingen J, Perez J, Baldeón L, Abdallah AM, et al. ESX-1-mediated translocation to the cytosol controls virulence of mycobacteria. Cell Microbiol. 2012;14:1287–98. doi:10.1111/j.1462-5822.2012.01799.x.

10. Stanley SA, Raghavan S, Hwang WW, Cox JS. Acute infection and macrophage subversion by Mycobacterium tuberculosis require a specialized secretion system. Proc Natl Acad Sci USA. 2003;100:13001–6. doi:10.1073/pnas.2235593100.

11. Brodin P, Majlessi L, Marsollier L, de Jonge MI, Bottai D, Demangel C, et al. Dissection of ESAT-6 system 1 of Mycobacterium tuberculosis and impact on immunogenicity and virulence. Infect Immun. 2006;74:88–98. doi:10.1128/IAI.74.1.88-98.2006.

12. Pym AS, Brodin P, Brosch R, Huerre M, Cole ST. Loss of RD1 contributed to the attenuation of the live tuberculosis vaccines Mycobacterium bovis BCG and Mycobacterium microti. Mol Microbiol. 2002;46:709–17. doi:10.1046/j.1365-2958.2002.03237.x.

13. Fortune SM, Jaeger A, Sarracino DA, Chase MR, Sassetti CM, Sherman DR, et al. Mutually dependent

secretion of proteins required for mycobacterial virulence. Proc Natl Acad Sci USA. 2005;102:10676–81. doi:10.1073/pnas.0504922102.

14. MacGurn JA, Raghavan S, Stanley SA, Cox JS. A non-RD1 gene cluster is required for Snm secretion in Mycobacterium tuberculosis. Mol Microbiol. 2005;57:1653–63. doi:10.1111/j.1365-2958.2005.04800.x.

15. Wards BJ, de Lisle GW, Collins DM. An esat6 knockout mutant of Mycobacterium bovis produced by homologous recombination will contribute to the development of a live tuberculosis vaccine. Tuber Lung Dis. 2000;80:185–9. doi:10.1054/tuld.2000.0244.

16. Renshaw PS, Panagiotidou P, Whelan A, Gordon SV, Hewinson RG, Williamson RA, et al. Conclusive evidence that the major T-cell antigens of the Mycobacterium tuberculosis complex ESAT-6 and CFP-10 form a tight, 1:1 complex and characterization of the structural properties of ESAT-6, CFP-10, and the ESAT-6*CFP-10 complex. Implications for pathogenesis and virulence. J Biol Chem. 2002;277:21598–603. doi:10.1074/jbc.M201625200.

17. Champion PAD, Champion MM, Manzanillo P, Cox JS. ESX-1 secreted virulence factors are recognized by multiple cytosolic AAA ATPases in pathogenic mycobacteria. Mol Microbiol. 2009;73:950–62. doi:10.1111/j.1365-2958.2009.06821.x.

18. Chen JM, Zhang M, Rybniker J, Boy-Röttger S, Dhar N, Pojer F, et al. Mycobacterium tuberculosis EspB binds phospholipids and mediates EsxA-independent virulence. Mol Microbiol. 2013;89:1154–66. doi:10.1111/mmi.12336.

19. Guinn KM, Hickey MJ, Mathur SK, Zakel KL, Grotzke JE, Lewinsohn DM, et al. Individual RD1-region genes are required for export of ESAT-6/CFP-10 and for virulence of Mycobacterium tuberculosis. Mol Microbiol. 2004;51:359–70. doi:10.1046/j.1365-2958.2003.03844.x.

20. Xu J, Laine O, Masciocchi M, Manoranjan J, Smith J, Du SJ, et al. A unique Mycobacterium ESX-1 protein co-secretes with CFP-10/ESAT-6 and is necessary for inhibiting phagosome maturation. Mol Microbiol. 2007;66:787–800. doi:10.1111/j.1365-2958.2007.05959.x.

21. Chen JM, Boy-Röttger S, Dhar N, Sweeney N, Buxton RS, Pojer F, et al. EspD is critical for the virulence-mediating ESX-1 secretion system in Mycobacterium tuberculosis. J Bacteriol. 2012;194:884–93. doi:10.1128/JB.06417-11.

22. Ohol YM, Goetz DH, Chan K, Shiloh MU, Craik CS, Cox JS. Mycobacterium tuberculosis MycP1 protease plays a dual role in regulation of ESX-1 secretion and virulence. Cell Host Microbe. 2010;7:210–20. doi:10.1016/j.chom.2010.02.006.

23. Bottai D, Di Luca M, Majlessi L, Frigui W, Simeone R, Sayes F, et al. Disruption of the ESX-5 system of Mycobacterium tuberculosis causes loss of PPE protein secretion, reduction of cell wall integrity and strong attenuation. Mol Microbiol. 2012;83:1195–209. doi:10.1111/j.1365-2958.2012.08001.x.

24. Houben ENG, Bestebroer J, Ummels R, Wilson L, Piersma SR, Jiménez CR, et al. Composition of the type VII secretion system membrane complex. Mol Microbiol. 2012;86:472–84. doi:10.1111/j.1365-2958.2012.08206.x.

25. Siegrist MS, Steigedal M, Ahmad R, Mehra A, Dragset MS, Schuster BM, et al. Mycobacterial Esx-3 requires multiple components for iron acquisition. MBio. 2014;5:e01073-14. doi:10.1128/mBio.01073-14.

26. van Winden VJC, Ummels R, Piersma SR, Jiménez CR, Korotkov KV, Bitter W, et al. Mycosins Are Required for the Stabilization of the ESX-1 and ESX-5 Type VII Secretion Membrane Complexes. MBio. 2016;7. doi:10.1128/mBio.01471-16.

27. Hsu T, Hingley-Wilson SM, Chen B, Chen M, Dai AZ, Morin PM, et al. The primary mechanism of attenuation of bacillus Calmette-Guerin is a loss of secreted lytic function required for invasion of lung interstitial tissue. Proc Natl Acad Sci USA. 2003;100:12420–5. doi:10.1073/pnas.1635213100.

28. Converse SE, Cox JS. A protein secretion pathway critical for Mycobacterium tuberculosis virulence is conserved and functional in Mycobacterium smegmatis. J Bacteriol. 2005;187:1238–45. doi:10.1128/JB.187.4.1238-1245.2005.

29. Beckham KSH, Ciccarelli L, Bunduc CM, Mertens HDT, Ummels R, Lugmayr W, et al. Structure of the mycobacterial ESX-5 type VII secretion system membrane complex by single-particle analysis. Nat Microbiol. 2017;2:17047. doi:10.1038/nmicrobiol.2017.47.

30. Roback P, Beard J, Baumann D, Gille C, Henry K, Krohn S, et al. A predicted operon map for Mycobacterium tuberculosis. Nucleic Acids Res. 2007;35:5085–95. doi:10.1093/nar/gkm518.

31. DeJesus MA, Gerrick ER, Xu W, Park SW, Long JE, Boutte CC, et al. Comprehensive Essentiality Analysis of the Mycobacterium tuberculosis Genome via Saturating Transposon Mutagenesis. MBio. 2017;8. doi:10.1128/mBio.02133-16.

32. Laencina L, Dubois V, Le Moigne V, Viljoen A, Majlessi L, Pritchard J, et al. Identification of genes required for Mycobacterium abscessus growth in vivo with a prominent role of the ESX-4 locus. Proc Natl Acad Sci USA. 2018;115:E1002–11. doi:10.1073/pnas.1713195115.

33. Carlsson F, Joshi SA, Rangell L, Brown EJ. Polar localization of virulence-related Esx-1 secretion in mycobacteria. PLoS Pathog. 2009;5:e1000285. doi:10.1371/journal.ppat.1000285.

34. Wirth SE, Krywy JA, Aldridge BB, Fortune SM, Fernandez-Suarez M, Gray TA, et al. Polar assembly and scaffolding proteins of the virulence-associated ESX-1 secretory apparatus in mycobacteria. Mol Microbiol. 2012;83:654–64. doi:10.1111/j.1365-2958.2011.07958.x.

35. Palomino J-C, Martin A, Camacho M, Guerra H, Swings J, Portaels F. Resazurin microtiter assay plate: simple and inexpensive method for detection of drug resistance in Mycobacterium tuberculosis. Antimicrob Agents Chemother. 2002;46:2720–2.

36. Lou Y, Rybniker J, Sala C, Cole ST. EspC forms a filamentous structure in the cell envelope of Mycobacterium tuberculosis and impacts ESX-1 secretion. Mol Microbiol. 2017;103:26–38. doi:10.1111/mmi.13575.

37. Odermatt NT, Sala C, Benjak A, Kolly GS, Vocat A, Lupien A, et al. Rv3852 (H-NS) of Mycobacterium tuberculosis Is Not Involved in Nucleoid Compaction and Virulence Regulation. J Bacteriol. 2017;199. doi:10.1128/JB.00129-17.

38. Shaner NC, Lambert GG, Chammas A, Ni Y, Cranfill PJ, Baird MA, et al. A bright monomeric green fluorescent protein derived from Branchiostoma lanceolatum. Nat Methods. 2013;10:407–9. doi:10.1038/nmeth.2413.

39. Hostettler L, Grundy L, Käser-Pébernard S, Wicky C, Schafer WR, Glauser DA. The Bright Fluorescent Protein mNeonGreen Facilitates Protein Expression Analysis In Vivo. G3 (Bethesda). 2017;7:607–15. doi:10.1534/g3.116.038133.

40. Wilton R, Ahrendt AJ, Shinde S, Sholto-Douglas DJ, Johnson JL, Brennan MB, et al. A New Suite of Plasmid Vectors for Fluorescence-Based Imaging of Root Colonizing Pseudomonads. Front Plant Sci. 2017;8:2242. doi:10.3389/fpls.2017.02242.

41. Lewis KN, Liao R, Guinn KM, Hickey MJ, Smith S, Behr MA, et al. Deletion of RD1 from Mycobacterium tuberculosis mimics bacille Calmette-Guérin attenuation. J Infect Dis. 2003;187:117–23. doi:10.1086/345862.

42. TMHMM Server, v. 2.0. http://www.cbs.dtu.dk/services/TMHMM/. Accessed 8 Aug 2018.

43. Kang C-M, Nyayapathy S, Lee J-Y, Suh J-W, Husson RN. Wag31, a homologue of the cell division protein DivIVA, regulates growth, morphology and polar cell wall synthesis in mycobacteria. Microbiology (Reading, Engl). 2008;154 Pt 3:725–35. doi:10.1099/mic.0.2007/014076-0.

44. Carel C, Nukdee K, Cantaloube S, Bonne M, Diagne CT, Laval F, et al. Mycobacterium tuberculosis proteins involved in mycolic acid synthesis and transport localize dynamically to the old growing pole and septum. PLoS One. 2014;9:e97148. doi:10.1371/journal.pone.0097148.

45. Gomez JE, Bishai WR. whmD is an essential mycobacterial gene required for proper septation and cell division. Proc Natl Acad Sci USA. 2000;97:8554–9. doi:10.1073/pnas.140225297.

46. Avanzi C, Del-Pozo J, Benjak A, Stevenson K, Simpson VR, Busso P, et al. Red squirrels in the British Isles are infected with leprosy bacilli. Science. 2016;354:744–7. doi:10.1126/science.aah3783.

47. Bolger AM, Lohse M, Usadel B. Trimmomatic: a flexible trimmer for Illumina sequence data. Bioinformatics. 2014;30:2114–20. doi:10.1093/bioinformatics/btu170.

48. Langmead B, Salzberg SL. Fast gapped-read alignment with Bowtie 2. Nat Methods. 2012;9:357–9. doi:10.1038/nmeth.1923.

49. Kolly GS, Boldrin F, Sala C, Dhar N, Hartkoorn RC, Ventura M, et al. Assessing the essentiality of the decaprenyl-phospho-d-arabinofuranose pathway in Mycobacterium tuberculosis using conditional mutants. Mol Microbiol. 2014;92:194–211. doi:10.1111/mmi.12546.

50. Uplekar S, Rougemont J, Cole ST, Sala C. High-resolution transcriptome and genome-wide dynamics of RNA polymerase and NusA in Mycobacterium tuberculosis. Nucleic Acids Res. 2013;41:961–77. doi:10.1093/nar/gks1260.

51. Liao Y, Smyth GK, Shi W. The Subread aligner: fast, accurate and scalable read mapping by seed-and-vote. Nucleic Acids Res. 2013;41:e108. doi:10.1093/nar/gkt214.

52. Love MI, Huber W, Anders S. Moderated estimation of fold change and dispersion for RNA-seq data with DESeq2. Genome Biol. 2014;15:550. doi:10.1186/s13059-014-0550-8.

53. Lambert RJ, Pearson J. Susceptibility testing: accurate and reproducible minimum inhibitory concentration (MIC) and non-inhibitory concentration (NIC) values. J Appl Microbiol. 2000;88:784–90.

54. Wiśniewski JR, Zougman A, Nagaraj N, Mann M. Universal sample preparation method for proteome analysis. Nat Methods. 2009;6:359–62. doi:10.1038/nmeth.1322.

55. Rappsilber J, Mann M, Ishihama Y. Protocol for micro-purification, enrichment, pre-fractionation and storage of peptides for proteomics using StageTips. Nat Protoc. 2007;2:1896–906. doi:10.1038/nprot.2007.261.

56. Cox J, Mann M. MaxQuant enables high peptide identification rates, individualized p.p.b.-range mass accuracies and proteome-wide protein quantification. Nat Biotechnol. 2008;26:1367–72. doi:10.1038/nbt.1511.

57. Cox J, Hein MY, Luber CA, Paron I, Nagaraj N, Mann M. Accurate proteome-wide label-free quantification by delayed normalization and maximal peptide ratio extraction, termed MaxLFQ. Mol Cell Proteomics. 2014;13:2513–26. doi:10.1074/mcp.M113.031591.

58. Tyanova S, Temu T, Sinitcyn P, Carlson A, Hein MY, Geiger T, et al. The Perseus computational platform for comprehensive analysis of (prote)omics data. Nat Methods. 2016;13:731–40. doi:10.1038/nmeth.3901.

59. Hubner NC, Bird AW, Cox J, Splettstoesser B, Bandilla P, Poser I, et al. Quantitative proteomics combined with BAC TransgeneOmics reveals in vivo protein interactions. J Cell Biol. 2010;189:739–54. doi:10.1083/jcb.200911091.

60. R: a language and environment for statistical computing. https://www.gbif.org/tool/81287/r-a-language-and-environment-for-statistical-computing. Accessed 28 Aug 2018.

61. Sani M, Houben ENG, Geurtsen J, Pierson J, de Punder K, van Zon M, et al. Direct visualization by cryo-

EM of the mycobacterial capsular layer: a labile structure containing ESX-1-secreted proteins. PLoS Pathog. 2010;6:e1000794. doi:10.1371/journal.ppat.1000794.

2.7 FIGURES

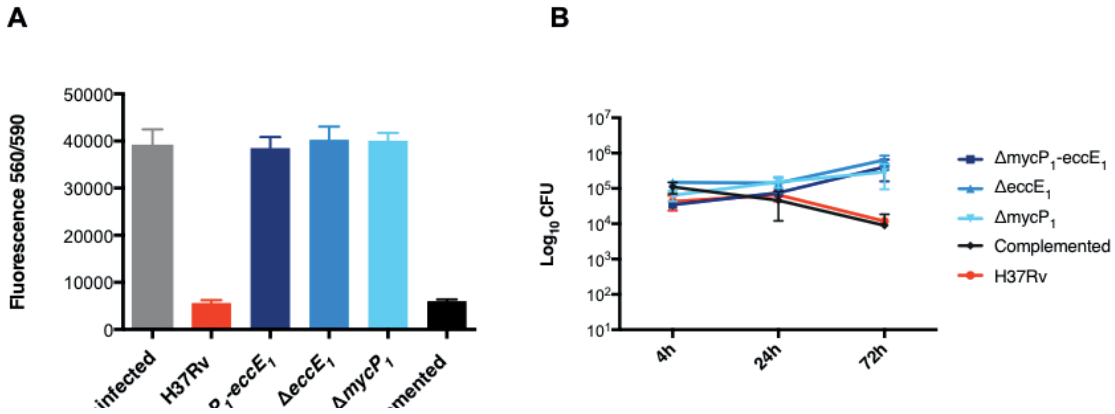

Figure 1. EccE1 is required to induce cell death but not for macrophage infection or intracellular survival. **A**. Cell viability of THP-1 human macrophages at 72h post-infection. Uninfected cells were used as a control for macrophage survival and the H37Rv wild type strain as a positive control for *M. tuberculosis*-mediated cell-death. The Δ*eccE1*, Δ*mycP1-eccE1* and Δ*mycP1* mutants did not affect survival of THP-1 macrophages in contrast to the complemented strain.
B. Intracellular bacterial burden at different time points post-infection. The similar number of bacteria at 4h post-infection indicates that the Δ*eccE1*, Δ*mycP1* and Δ*mycP1-eccE1* mutants infect macrophages with the same efficiency as the wild type strain. At 72h post-infection, the decreased number of intracellular bacteria in the wild type and the complemented strains correlates with its ability to lyse macrophages. The stable CFU numbers observed for Δ*eccE1*, Δ*mycP1* and Δ*mycP1-eccE1* over the course of the experiment suggest that these mutants can survive inside THP-1 cells.

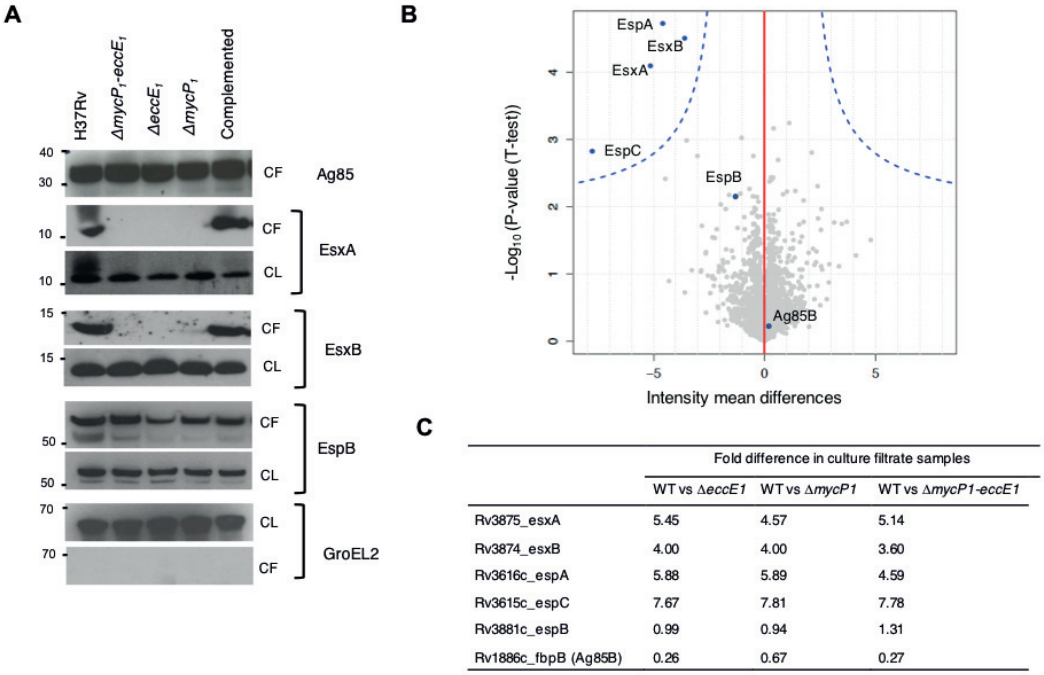

C

	Fold difference in culture filtrate samples		
	WT vs *ΔeccE1*	WT vs *ΔmycP1*	WT vs *ΔmycP1-eccE1*
Rv3875_esxA	5.45	4.57	5.14
Rv3874_esxB	4.00	4.00	3.60
Rv3616c_espA	5.88	5.89	4.59
Rv3615c_espC	7.67	7.81	7.78
Rv3881c_espB	0.99	0.94	1.31
Rv1886c_fbpB (Ag85B)	0.26	0.67	0.27

Figure 2. EccE$_1$ is required for ESX-1-dependent secretion.
A. Immunoblots of culture filtrates (CF, 15 µg per well) and whole cell lysates (CL, 10 µg per well). Detection of Ag85B was used as a loading control in the CF and GroEL2 as a loading control in the CL. Secretion of EsxA and EsxB but not EspB is disrupted in the Δ*eccE*$_1$, Δ*mycP*$_1$*-eccE*$_1$, and Δ*mycP*$_1$ mutants.
B. Proteomic analysis of the secreted fraction showing the difference of the Δ*mycP*$_1$*-eccE*$_1$ mutant versus the wild type strain. The abundance of EsxA, EsxB, EspA and EspC is highly affected in the double mutant Δ*mycP*$_1$*-eccE*$_1$ compared to the WT strain. It also demonstrates that EsxA, EsxB, EspA and EspC are the only significantly deregulated proteins. The blue dotted line represents the significant curve determined by combining T-test values with ratio information and it delineates the differentially quantified proteins. Three independent replicates per strain were used for the analysis.
C. Fold difference (Log2) of secreted proteins present in the WT versus the mutants. EsxA, EsxB, EspA and EspC are detected in significantly lower amounts in the culture filtrate of the mutants compared to the WT.

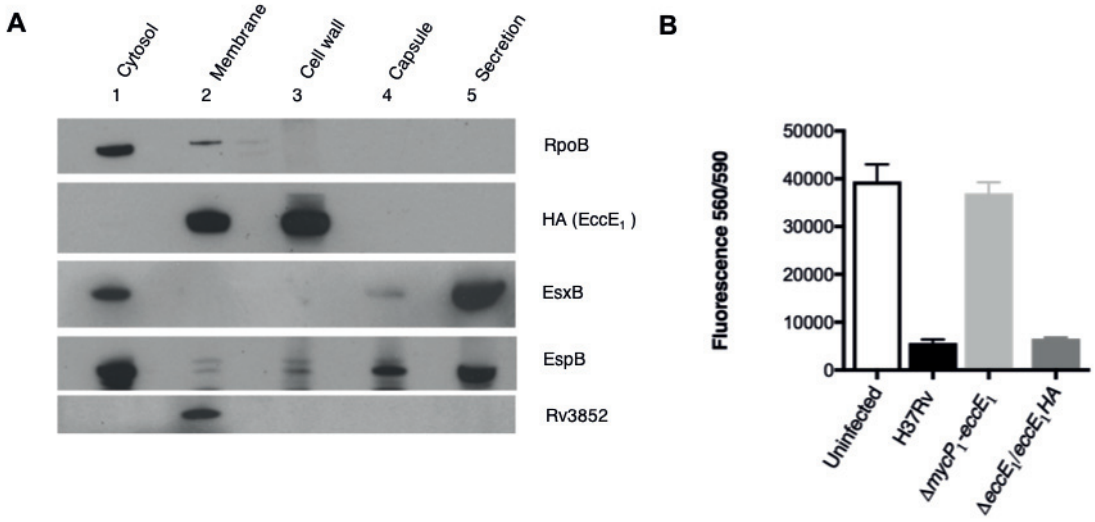

Figure 3. EccE$_1$ localizes to the membrane and cell wall fractions of *M. tuberculosis*.
A. Subcellular fractionation of the Δ*eccE$_1$/eccE$_1$HA* mutant followed by immunoblotting of each fraction (20 μg per well). Detection of RpoB represented a control for lysis, EsxB and EspB were controls for secretion and Rv3852 for the membrane fraction. Anti-HA antibodies localised EccE$_1$.
B. THP-1 macrophage survival at 72h post-infection. Δ*eccE$_1$/eccE$_1$HA* mutant can induce cell-death *ex vivo* indicating the presence of a functional ESX-1 system and therefore that the HA tag at the C-terminus part of the protein did not interfere with EccE$_1$ function. Uninfected cells were used as a control for macrophage survival, the H37Rv WT strain and the Δ*mycP$_1$-eccE$_1$* mutant served as positive and negative controls, respectively, for *M. tuberculosis*-mediated cell-death.

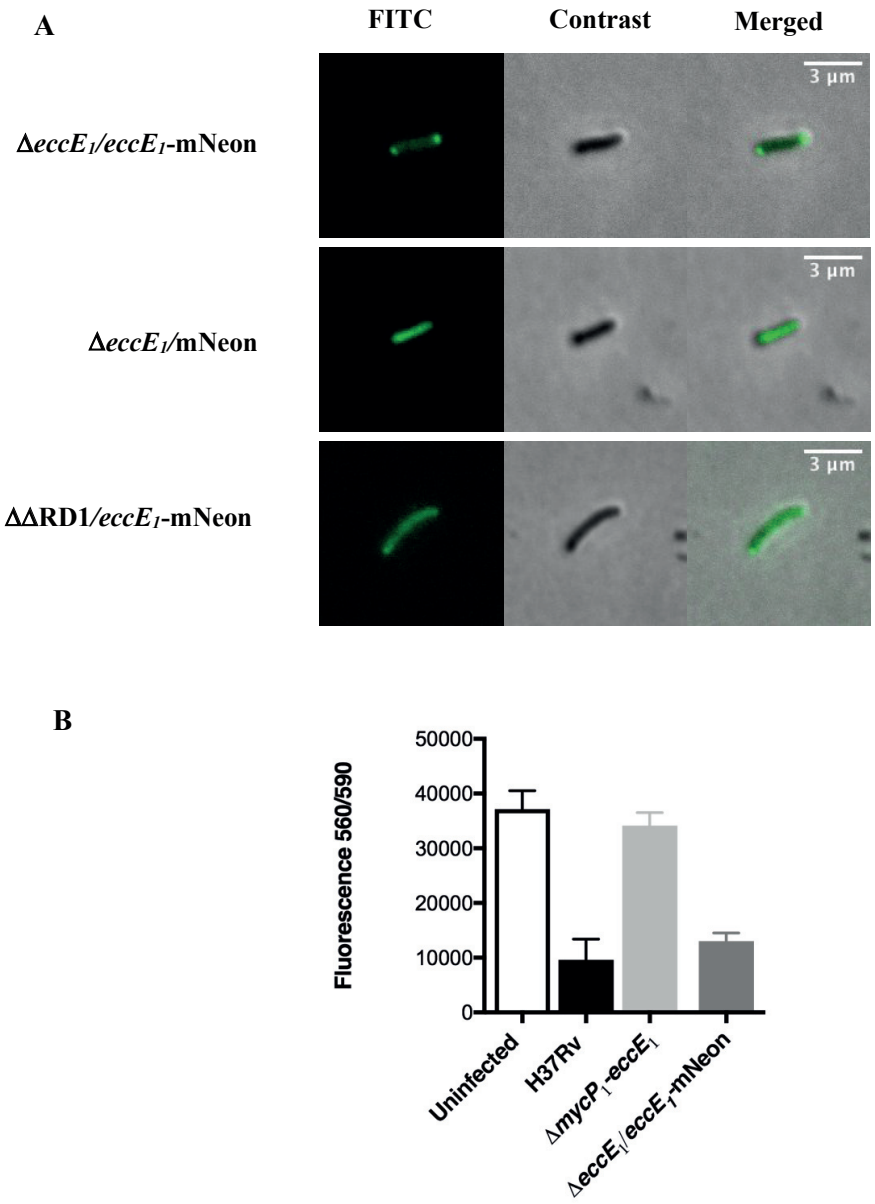

Figure 4. EccE$_1$-mNeon and the functional ESX-1 system localize to the poles of *M. tuberculosis*.
A. EccE$_1$-mNeon expressing cells (Δ*eccE$_1$*/*eccE$_1$*-mNeon) display a fluorescent signal at the poles of the bacilli. When mNeon is expressed without EccE$_1$ (Δ*eccE$_1$*/mNeon), the fluorescent signal distributes all over the bacterium. Expressing EccE$_1$-mNeon in the ΔΔRD1 mutant, which lacks many of the ESX-1 genes, did not result in polar localization, showing that EccE$_1$ requires other ESX-1 protein to localize at the poles.
B. THP-1 survival at 48h post-infection. The Δ*eccE$_1$*/*eccE$_1$*-mNeon mutant can induce cell-death ex vivo suggesting the presence of functional ESX-1 systems and therefore indicating that the addition of mNeon did not interfere with EccE$_1$ function. Uninfected cells were used as a control for macrophage survival, the H37Rv WT strain and the Δ*mycP$_1$-eccE$_1$* mutant were used as positive and negative controls respectively for M. tuberculosis-mediated cell-death.

2.8 SUPPLEMENTARY MATERIAL

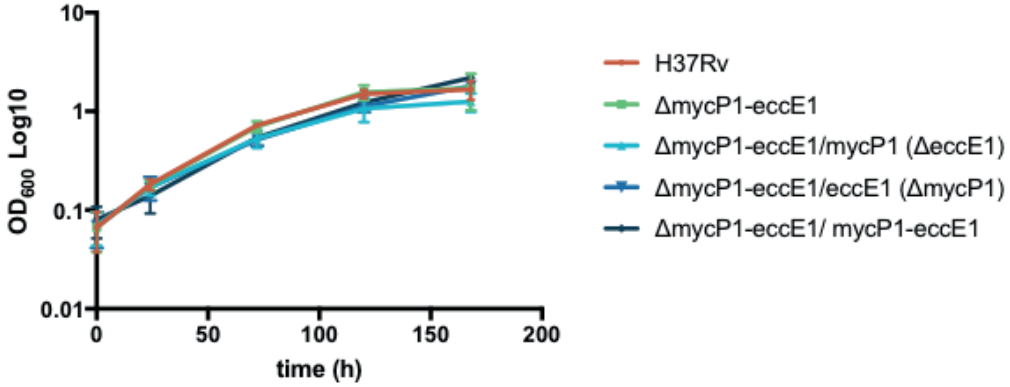

Figure S 1. **EccE$_1$ is not required for *in vitro* growth.**
Growth curves on synthetic medium (7H9 + ADC). The mutants and the wild type strain display similar growth rates.

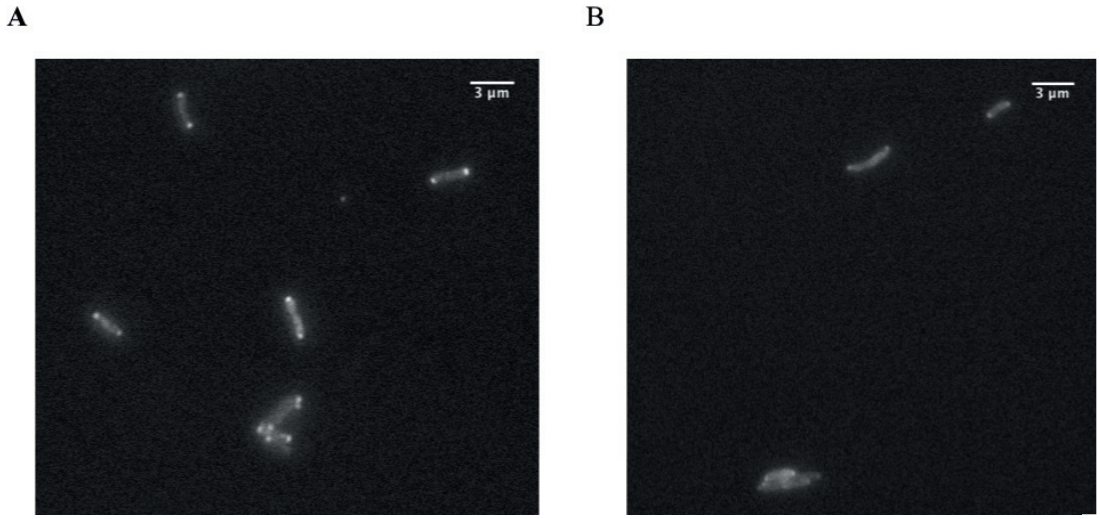

Figure S 2. **EccE$_1$-mNeon *M. tuberculosis* showed bi-polar foci in all bacilli.**
A. Δ*eccE$_1$*/*eccE$_1$*mNeon cells. Representative image of three independent cultures demonstrating that 100% of cells expressing EccE$_1$-mNeon displayed a bi-foci fluorescent pattern.
B. ΔΔRD1/*eccE$_1$*mNeon cells. Representative image of three independent cultures proving that EccE$_1$-mNeon needs other ESX-1 protein to form a stable complex at the poles of the bacilli.

Table S 1. Relative *mycP1* and *eccE1* expression levels by RNA-sequencing.

Gene name	Δ*mycP1-eccE1* vs H37Rv		complemented vs H37Rv	
	Fold Change	**padj**	**Fold Change**	**padj**
mycP1	NA*	NA	1.8166	1.12E-09
eccE1	NA*	NA	2.5552	1.76E-81

Padj: adjusted p-value. NA: not applicable (*no transcripts in this region).

Table S 2. EccE1 is not required for susceptibility to antibiotics targeting the cell wall.

	Amoxicillin	**Ampicillin**	**Cefadroxil**	**Cefdinir**	**Vancomycin**	**Rifampicin**
H37Rv (μg/ml)	6.38_a	8.32_a	2.06	0.83	0.35_a	0.00084_a
Δ*mycP1-eccE1* (μg/ml)	7.64_a	8.95_a	2.14	0.80	0.47_a	0.00086_a
Δ*eccE1* (μg/ml)	7.23	6.60	2.21	1.07	0.41	0.00066
Δ*mycP1* (μg/ml)	7.42	4.97	2.89	0.85	0.51	0.00066

Average MIC values (μg/ml) obtained from at least two independent experiments. The Δ*eccE1*, Δ*mycP1* Δ*mycP1-eccE1* and the H37Rv wild type strain responded similarly to cell wall targeting antibiotics. ($_a$) three independent experiments.

Table S 3. Plasmids used in this study

Plasmid name	Description	Reference
pJG1100	Suicide vector for mutant construction, Hyg^R, Kan^R, *sacB*.	[45]
pGA44	Integrative vector at L5 attB site, carrying the TET-PIP OFF expression system, StrR.	[49]
pGA80	pMV261-derived vector, carrying the L5 *int* gene for expression in trans, lacking *oriM*, KanR.	[49]
pMZ53	pGA44-derived vector carrying *mycP1HA* under the PTR promoter, integrative, Str^R.	In this study
pMZ45	pGA44-derived vector carrying *eccE1HA* under the PTR promoter, integrative, Str^R.	In this study
pPS10	pGA44-derived vector carrying *mycP1-eccE1* under the PTR promoter, integrative, Str^R.	In this study
pPS11	pGA44-derived vector carrying *mycP1-eccE1HA* under the PTR promoter, integrative, Str^R.	In this study
pPS12	pGA44-derived vector carrying *mycP1-eccE1mNeon* under the PTR promoter, integrative, Str^R.	In this study
pPS13	pGA44-derived vector carrying *mNeon* under the PTR promoter, integrative, Str^R.	In this study

Table S 4. Oligonucleotides used in this study

Primer name	**Restriction site**	**Sequence 5'→ 3'**	**Information**
MZ-198-F	PacI	AGT CAG TTA ATT AAC AGG TAA GAC AAC CAC CGC TG	To clone UP region of *mycP1-eccE1* in pJG1100
MZ-199-R	AvrII	AGT CAG CCT AGG CGC CAC CGT GAT CAG AAA GAT	To clone UP region of *mycP1-eccE1* in pJG1100
MZ-200-F	AvrII	AGT CAG CCT AGG GAA AGC CGC TAC CAG ATG GC	To clone DOWN region of *mycP1-eccE1* in pJG1100
MZ-201-R	AscI	AGT CAG GGC GCG CCG TAC ACC GGG AGA ATT TGG TC	To clone DOWN region of *mycP1-eccE1* in pJG1100
MZ-165-F	AvrII	AGT CAG CCT AGG GTG CAC CGT ATC TTT CTG ATC ACG GTG GCG CTG GC	To clone *mycP1* in pGA44
MZ-166-R	AscI	AGT CAG GGC GCG CCT TAG GCG TAG TCC GGC ACG TCG TAC GGG TAT CGG CGG CTC AGC GCC CGT C	To clone *mycP1* in pGA44
MZ-173-F	AvrII	AGT CAG CCT AGG ATG AGA AAT CCT TTA GGG CTG CGG TTC AGC	To clone *eccE1* in pGA44
MZ-174-R	AscI	AGT CAG GGC GCG CCT TAG GCG TAG TCC GGC ACG TCG TAC GGG TAC TTC GGC AGC GCC ATC TGG T	To clone *eccE1* in pGA44
PS-118-R	PacI	CTATTTAATTAACTACTTCGGCAGCGCCAT CTGGTAGCGGC	To clone *mycP1-eccE1* in pGA44
PS-124-R	PacI	CTATTTAATTAACTAAGCGTAATCTGGAA CATCGTATGGGTACTTCGGCAGCGCCATC TG	To clone *mycP1-eccE1HA* in pGA44
PS-119-F	AvrII	ACTACCTAGGCACCGTATCTTTCTGATCAC GGTGGCGC	To clone *mycP1-eccE1, mycP1-eccE1HA, mycP1-eccEmNeon* in pGA44
PS-147-R		CACCATTCCCGAACCTCCCGAACCTCCCTT CGGCAGCGCCATCTGG	To clone *mycP1-eccE*mNeon in pGA44
PS-148-F		CCG AAG GGA GGT TCG GGA GGT TCGGGAATGGTGAGCAAGGGCGAGG	To clone *mycP1-eccE*mNeon in pGA44
PS-149-R	PacI	CTATTTAATTAATTACTTGTACAGCTCGTC	To clone mNeon in pGA44
PS-153-F	AvrII	ATGCCTAGGATGGTGAGCAAGGGCGAGG AG	To clone mNeon in pGA44

Table S 5. Strains used in this study

Strain name	**Description/genotype**	**Plasmid**
Δ*mycP1-eccE1*	Deletion of *mycP1-eccE1* region	
Δ*eccE1*	Δ*mycP1- eccE1*/ *mycP1*	pMZ53
Δ*mycP1*	Δ*mycP1- eccE1*/ *eccE1*	pMZ45
Complemented	Δ*mycP1- eccE1*/ *mycP1-eccE1*	pPS10
Δ*eccE*1/*eccE1-HA*	Δ*mycP1- eccE1*/ *mycP1-eccE1HA*	pPS11
*Δ*eccE1*/*eccE1*-mNeon	Δ*mycP1- eccE1*/ *mycP1-eccE1*mNeon	pPS12
mNeon alone	Δ*mycP1- eccE1*/mNeon	pPS13
ΔΔRD1/*eccE1*-mNeon	ΔΔRD1/*mycP1-eccE1*mNeon	pPS12

Chapter 3

EspL is essential for virulence and stabilizes EspE, EspF and EspH levels in *Mycobacterium tuberculosis*

Claudia Sala[1*], Nina T. Odermatt[1,2†], Paloma Soler[1†], Muhammet F. Gülen[1], Sofia Von Schultz[1], Andrej Benjak[1], Stewart T. Cole[1,3]*

[1] Global Health Institute, Ecole Polytechnique Fédérale de Lausanne, Lausanne, Switzerland.
[2] Current address: Max Planck Institute for Terrestrial Microbiology, Marburg, Germany.
[3] Current address: Institut Pasteur, Paris, France.

[†] These authors contributed equally to this work.

Manuscript in preparation (2018)

3.1 ABSTRACT

The ESX-1, type VII, secretion system represents the major virulence determinant of *Mycobacterium tuberculosis*, one of the most successful intracellular pathogens. Here, by combining genetic and high-throughput approaches, we show that EspL, a protein of 115 amino acids, is essential for mediating ESX-1-dependent virulence and for stabilization of EspE, EspF and EspH protein levels. Indeed, an *espL* knock-out mutant was unable to replicate intracellularly, secrete ESX-1 substrates or stimulate innate cytokine production. Moreover, proteomic studies detected greatly reduced amounts of EspE, EspF and EspH in the *espL* mutant as compared to the wild type strain, suggesting a role for EspL as a chaperone. The latter conclusion was further supported by discovering that EspL interacts with EspD, which was previously demonstrated to stabilize the ESX-1 substrates and effector proteins, EspA and EspC. Loss of EspL also leads to downregulation in *M. tuberculosis* of WhiB6, a redox-sensitive transcriptional activator of ESX-1 genes. Overall, our data highlight the importance of a so-far overlooked, though conserved, component of the ESX-1 secretion system and begin to delineate the role played by EspE, EspF and EspH in virulence and host-pathogen interaction.

3.2 INTRODUCTION

Mycobacterium tuberculosis, the etiological agent of human tuberculosis, is arguably the world's most successful human pathogen. It is estimated that one third of the world's population is latently infected by the bacterium [1], which can survive in a dormant state inside specialized cellular structures in the lung parenchyma called granulomas [2,3]. As a consequence of immunodeficiency or co-morbidities, like HIV or diabetes [4,5], latent *M. tuberculosis* can reactivate and establish an acute infectious process which leads to the disease. Host-pathogen interaction and disease progression are mediated by various virulence factors encoded by the bacterial genome, the most important of them being the ESX-1 or type VII secretion system [6].

ESX loci are characterized by genes encoding small secreted proteins with a conserved tryptophan-x-glycine (WXG) motif and by transmembrane ATPases belonging to the FtsK-SpoIIIE-like family [7,8]. Five ESX systems, implicated in different functions, exist in *M. tuberculosis* [9]. The ESX-1 cluster comprises approximately twenty genes and encodes a specialized secretion apparatus, which releases effectors into the extracellular milieu. The relevance of the ESX-1 genes in mycobacterial physiology was recognized when attenuation of the vaccine strain *M. bovis* BCG and of the vole bacillus *M. microti* was associated with their partial deletion [10–14]. Since then, the role played by ESX-1 in cytosolic recognition and stimulation of innate immunity [15–17], phagosomal rupture and bacterial escape [18,19], intercellular spread and systemic disease [20,21] has been the object of numerous studies. Recently, the ESX-1 secretion system has also been considered as a potential drug target for the development of anti-virulence drugs [22].

Considerable progress has been made in understanding how the system works and is regulated. Electron microscopy-based studies showed that the *M. xenopi* ESX-5 core membrane complex is composed of four proteins ($EccB_5$, the ATPase $EccC_5$, the putative channel $EccD_5$, and $EccE_5$) which assemble into an oligomer with a six-fold symmetry [23]. However, it is still unknown how the secreted substrates can cross the mycobacterial external membrane, or mycomembrane, although the involvement of EspC, encoded by the distal *espA-espC-espD* locus, has been hypothesized in *M. tuberculosis* [24]. The current model for ESX-1 activity proposes heterodimeric and co-dependent complexes as the secreted substrates, i.e. EsxA/EsxB and EspA/EspC [25,26]. These are targeted to the inner membrane apparatus by a bipartite secretory signal

composed of the WXG motif on the first member of the dimer and of a tyrosine-x-x-x-aspartic acid (YxxxD) motif on the second [26,27]. ESX-1 function undergoes transcriptional regulation, exerted by EspR [28], Lsr2 [29], CRP [30], mIHF (manuscript accepted) and MprA [31] on the *espA-espC-espD* locus. Additional, post-transcriptional, control of secretion activity is carried out by the serine protease MycP1 through proteolytic cleavage of another ESX-1 substrate, EspB [32].

Here, we investigate the role of a previously overlooked ESX-1 component, EspL, in *M. tuberculosis*. We demonstrate that it is essential for mycobacterial replication inside macrophages, for eliciting innate cytokine production and for stabilizing the protein levels of the additional ESX-1 members EspE, EspF and EspH.

3.3 RESULTS

Construction of an *espL* deletion mutant

In order to evaluate the role of EspL in *M. tuberculosis* virulence and ESX-1-dependent secretion activity, construction of an unmarked deletion mutant was planned. The transcriptional profile of the H37Rv genomic region that includes *espL* was carefully considered to avoid polarity on the downstream gene *espK*. Studies by Cortes and colleagues [33] demonstrated the presence of a polycistronic RNA that covers *mycP1*, *eccE1*, *espB* and *espL*, but not *espK*, which is transcribed independently (S1A Fig). Additionally, sequence inspection revealed that the GTG translational start codon of *espL* overlaps the stop codon of the preceding gene *espB*. The pJG1100-derived suicide vector [34] was then constructed according to this pre-existing information and the *espL* coding sequence (CDS) was deleted from the chromosome by allelic exchange, from coordinate 4,360,199 to coordinate 4,360,543, thereby leaving the *espB* stop codon intact (S1B Fig). The resulting strain, named Δ*espL*, was validated by colony PCR (data not shown), immunoblot (Fig 1A) and whole genome sequencing. The latter technology identified one single nucleotide polymorphism (SNP) in gene *rv1403* (353T>C), which caused substitution of Val118 with Ala, and one SNP in *ethA* (A to G transition at position 368) which resulted in replacement of His123 with Arg. No other differences were noted upon comparison with the genome sequence of the parental strain, except for the intended deletion. Δ*espL* was transformed with the complementing plasmid pGA44-*espL*, which carries the *espL* gene under the control of the PTR promoter, or with the empty vector pGA44 as a control [35]. Immunoblot experiments proved that expression of EspL

was restored in the complemented strain Δ*espL*/pGA-*espL*, whereas no band was detected in the control Δ*espL*/pGA44 (Fig 1A). Consistent with these findings, qRT-PCR showed that the *espL* mRNA was expressed at a level similar to that of the wild type when the gene was provided *in trans* (Fig 1B). Transcriptional analysis was extended to include *espB*, *espK* and *esxA*. While *espB* and *esxA* mRNA levels were not altered significantly by the mutation introduced or by the ectopic expression of *espL*, the amount of *espK* transcript was 2.5-3-fold higher in the mutant strain (Fig 1B).

ΔespI is attenuated and does not stimulate innate immunity *ex vivo*

The Δ*espL* mutant did not show any major difference as compared to the wild type strain during *in vitro* growth in standard medium (S2A Fig). However, infection of THP-1 cells demonstrated severe reduction of the cytotoxicity of the mutant, which allowed cell survival to a similar extent as upon infection with the ΔΔRD1 strain, which lacks the extended RD1 region [36] (Fig 2A). Importantly, expression of *espL* by pGA44 complemented the phenotype to wild type levels (Fig 2A). These findings were further confirmed by colony forming unit (CFU) enumeration. While all of the strains were equally phagocytosed by THP-1 cells (S2B Fig), a major increase in the number of intracellular bacteria over one week was reported when H37Rv and the complemented strains, but not Δ*espL*, were used for infection (Fig 2B).

The crucial role played by the ESX-1 secretion system in inducing expression of cytokines of the innate immunity pathways was previously illustrated. In particular, EsxA secretion was found to be responsible for activating the cytosolic surveillance pathway based on cGAS-dependent sensing of DNA and the inflammasome [15–17]. Here, markedly reduced production of the pro-inflammatory cytokine IL-1β (Fig 2C), as well as decreased expression of type I interferon gene *IFNB1* (Fig 2D), interferon-stimulated gene *ISG15* (Fig 2E), and interleukin gene *IL6* (Fig 2F), were noted after THP-1 infection by the Δ*espL* strain. On the contrary, H37Rv and the complemented strain Δ*espL*/pGA-*espL* elicited production of cytokines belonging to both the cGAS-STING-type I Interferon (IFN) and inflammasome axes. Overall, these data indicate that EspL is a key player in *M. tuberculosis* virulence, interaction with the immune system and, likely, in ESX-1 secretion, as explained below.

Secretion of ESX-1 substrates is compromised in *ΔespL*

The secretion profile of the mutant was examined in parallel to that of the wild type strain H37Rv and of the complemented mutant strains. While the proteins were produced by all of the strains (Fig 3A), EsxA and EsxB were not detectable in the secreted fraction by immunoblot when EspL was missing, whereas EspA and EspD levels were greatly reduced (Fig 3B). As a consequence of the compromised secretion, accumulation of EsxA and EsxB occurred inside Δ*espL* cells (Fig 3A). Interestingly, EspB was found to be released into the culture supernatant in the absence of EspL (Fig 3B), confirming that its secretion is not dependent on EsxA, EsxB, EspA or EspD, as reported earlier [37]. Therefore, the severe attenuation of Δ*espL*, described above, correlates with lack of secretion of the major virulence factor EsxA.

Localization of EspL in sub-cellular fractions

To gain insight into EspL function, the localization of the protein in sub-cellular fractions was studied. Total extracts from strain H37Rv were separated into cytosolic, membrane and capsular proteins, in addition to culture filtrate preparations. Anti-EspL antibodies identified a protein, with the apparent molecular weight of EspL, mainly in the cytosol and, to a lesser extent, in the membrane (Fig 4). EspL was undetectable in the culture filtrate. Control antibodies against RpoB, Rv3852 and EsxB recognized their cognate antigens in the cytosolic/membrane, membrane only or cytosolic/secreted fractions, as expected [38]. EspL could thus exert its function in the cytosol or as a membrane-associated protein.

Deletion of *espL* causes reduced expression of *whiB6*

Since PFAM [39] and recent experimental work [40] predicted the presence of an YbaB-type DNA-binding domain [41–43] in EspL, we hypothesized that the protein may influence gene expression through binding to DNA. The transcriptome of the mutant strain was then analyzed and compared to that of the wild type by RNA-seq. Despite the low cut-off value (2-fold change), none of the *M. tuberculosis* genes was found to be deregulated in Δ*espL*, except for *whiB6*, whose expression level was decreased by 3-fold on average (S1 Table), and *espL* itself, which was not detected in the knock-out mutant. Genes belonging to the ESX-1 cluster, as well as genes which are part of other ESX loci (ESX-2 to ESX-5) were expressed at similar levels in the mutant as compared to the wild type. Curiously, genes that were reported to be included in the WhiB6 regulon

in the related species *Mycobacterium marinum* [44] were not found to be deregulated by RNA-seq in *M. tuberculosis* Δ*espL* (S1 Table). These findings were confirmed independently by qRT-PCR, which also proved that re-introduction of *espL* into the complemented strain was necessary and sufficient to restore *espL* and *whiB6* mRNA levels to normal (S3 Fig). Thus, EspL seems to control expression of *whiB6* either directly or indirectly.

Ectopic expression of *whiB6* in *ΔespL* increases ESX-1 gene expression levels but does not complement attenuation

Intrigued by the discoveries reported earlier, we examined the impact of constitutive expression of *whiB6* in the Δ*espL* mutant. Levels of *whiB6* mRNA were increased by approximately 4-fold in the Δ*espL* strain carrying pGA-*whiB6*, as compared to wild type. All of the tested genes (i.e. *espB*, *esxA*, *espE*, *espF*, *espH* and *espA*), which are part of different transcriptional units [33,45], were induced (Fig 5A), therefore indicating that WhiB6 works as an activator of ESX-1 genes in *M. tuberculosis*. However, despite the increased expression of virulence-related genes, Δ*espL*/pGA-*whiB6* displayed the same attenuation as Δ*espL*, Δ*espL*/pGA44 and ΔΔRD1 (Fig 5B). In other words, the lack of cytotoxicity caused by deletion of *espL* could not be bypassed by ectopic over-expression of *whiB6*. EspL is therefore essential for *M. tuberculosis* virulence.

EspL stabilizes the cytosolic levels of EspE, EspF and EspH

Inspired by the work of Stoop and colleagues [46], we thoroughly analyzed the proteome of the *espL* knock-out mutant and compared it to that of the wild type, of the complemented strain and of the mutant expressing *whiB6 in trans*. Results are reported in Fig 6, S2 Table and S3 Table. As expected, EspL was detected in the wild type and in the complemented strains only (Fig. 6A). On the other hand, WhiB6 levels could only be measured in the strain over-expressing *whiB6*, indicating that this transcriptional regulator is poorly expressed in wild type conditions (Fig. 6K). No significant difference was noted for EspB, EspA, EspC and EspD in the proteome of Δ*espL* (Fig 6J, 6G, 6H and 6I), whilst a small though statistically valid increase in EsxA and EsxB levels was reported (Fig 6B and 6C), thus corroborating the data obtained by immunoblot (Fig 3B). The most relevant variation in protein levels was noticed for EspE, EspF and EspH. Their abundance was greatly reduced in the mutant strain and complemented to

wild type levels in Δ*espL*/pGA-*espL* (Fig 6D, 6E and 6F). Proteomic data contrasted with RNA-seq and qRT-PCR results, which proved that *espE*, *espF* and *espH* mRNAs in the *espL* knock-out strain were unaltered compared to the wild type (S1 Table and S3 Fig).

EsxA, EsxB, EspB and EspE amounts increased when *whiB6* was provided ectopically (Fig 6B, 6C, 6J and 6D), thus reflecting the qRT-PCR assay in Fig 5A. However, EspF and EspH levels did not reach those of H37Rv upon WhiB6 expression in Δ*espL* (Fig 6E and 6F), in contrast to their transcripts which were induced by WhiB6 (Fig 5A). These results suggest that an additional, post-transcriptional control regulates the abundance of EspF, EspH and, most likely EspE, in *M. tuberculosis*. EspL contributes to this phenotype and the transcriptional increase caused by WhiB6 is not sufficient to bypass the destabilizing effect on the proteins provoked by the lack of EspL.

Further confirmation to these findings was obtained by constructing strains that constitutively expressed HA-tagged EspE in the H37Rv and Δ*espL* backgrounds. Complementation by *espL* and expression of *whiB6* were achieved by using the physiological *mycP1* promoter, which represents the natural promoter of *espL* according to Cortes and colleagues [33]. Expression of *espE*.HA was therefore independent from EspL and from WhiB6 as it was placed under control of the PTR promoter [35]. The wild type phenotype was restored in strain Δ*espL*/pGA-*espE*.HA + *espL*, as shown in S4A and S4B Fig, thereby confirming that expression of EspE.HA did not cause abnormal behavior. In line with what has been described before, expression of *whiB6* did not complement the lack of virulence in Δ*espL*/pGA-*espE*.HA + *whiB6* (S4B Fig) but did increase the transcriptional levels of *espE* and *esxA* (S4C Fig), the latter result mirrored by the detection of a strong signal for the EsxA protein in Fig 7. Transcription of *espE*.HA was measured by qRT-PCR and confirmed as constitutive, almost identical in all of the strains, independently of the presence or absence of EspL and WhiB6 (S4A and S4C Fig). However, immunoblot analysis demonstrated that EspE.HA amounts in Δ*espL*/pGA-*espE*.HA were dramatically reduced (Fig 7), despite the presence of the *espE*.HA transcript (S4A Fig). Conversely, Δ*espL*/pGA-*espE*.HA + *espL* (expression of *espL in trans*) produced levels of EspE.HA equal to those in H37Rv/pGA-*espE*.HA. Providing *whiB6* only (Δ*espL*/pGA-*espE*.HA + *whiB6*) did not restore the phenotype (Fig 7). Therefore, the effects mediated by EspL and WhiB6 were uncoupled here: WhiB6 was

proved to act at the transcriptional level, whereas EspL was demonstrated to exert its function post-transcriptionally, presumably on protein stability.

Taken together, these results highlight a new role for EspL in stabilizing EspE, EspF and EspH protein amounts.

EspL interacts with EspD

To identify EspL interacting partners, strains carrying HA-tagged EspL were made. Expression of N- or C-terminally tagged EspL in Δ*espL* was verified by immunoblot (S5A Fig) and the ability of the modified proteins to complement the attenuation profile was checked (S5B Fig). Total cell extracts of strains Δ*espL*/pGA-*espL*.HA and Δ*espL*/pGA-HA.*espL* were employed in immunoprecipitation experiments using anti-HA antibodies. Mass spectrometry analysis of the precipitated material demonstrated that EspD was significantly enriched in the pulled-down fractions of Δ*espL*/pGA-HA.*espL* and of Δ*espL*/pGA-*espL*.HA, together with HA.EspL and EspL.HA (S4 Table). Other proteins were detected but their abundance was not increased in the immunoprecipitated samples compared to the Input and to the untagged strains H37Rv and Δ*espL* (S4 Table). A second readout, i.e. immunoblot, was exploited to validate these data independently. As shown in Fig 8, both EspD and EspL levels were highly enriched upon anti-HA immunoprecipitation in both Δ*espL*/pGA-HA.*espL* and Δ*espL*/pGA-*espL*.HA as compared to the Input control and strain H37Rv. On the other hand, RpoB and GroEL2 levels were as expected. To conclude, EspL and EspD may interact directly or be part of a multiprotein complex inside *M. tuberculosis* cells.

3.4 DISCUSSION

The data presented here demonstrate the essentiality of EspL for ESX-1-dependent virulence and for stabilizing the intracellular levels of EspE, EspF and EspH in *M. tuberculosis*. ESX-1-dependent secretion in Δ*espL* was severely compromised, with undetectable levels of EsxA, EsxB, EspA and EspD in the culture filtrates. Conversely, secretion of EspB was not affected, confirming previous data generated by our group [37]. In line with the secretion profile, virulence and innate cytokine production were compromised when THP-1 cells were infected by the *espL* knock-out strain. In this regard, Δ*espL* behaves like the ESX-1-null mutants ΔRD1 [13]

and ΔΔRD1 [36], which fail to stimulate the innate immune response [15]. Whether these phenotypic traits are directly caused by lack of EspL or are mediated by EspE, EspF or EspH is currently unknown and additional research is required.

Although the mechanistic details of these functions remain unknown, a role for EspL as a chaperone protein can be proposed. Indeed, the presence of heterodimeric complexes, where one protein acts as a chaperone for the other, is not unusual in the ESX-1 system [24,47]. A direct effect of EspL on transcription of *espE*, *espF* and *espH* was ruled out by RNA-seq and further confirmed by qRT-PCR. On the other hand, proteomics identified EspE, EspF and EspH as the only proteins whose abundance was highly affected by *espL* deletion. Based on these findings, an interaction between EspL and EspE, EspF and EspH could be hypothesized. However, those proteins were not detected by mass-spectrometry and immunoblotting analysis of immunoprecipitated material from strains expressing EspL.HA or HA.EspL.

EspL-mediated stabilization of EspE, EspF and EspH levels might therefore occur by other means. Interestingly, compelling evidence was obtained for EspL interacting with EspD, which itself is known to act as a stabilizer [48], further suggesting the existence of a "chaperone complex" which contributes to regulating ESX-1 activity post-transcriptionally and/or post-translationally. Curiously, while EspD stabilizes EspA and EspC [48], EspL performs the same task on EspE, EspF and EspH, whose genes are paralogs of *espA-espC-espD* [9], although EspL and EspD are different in size and sequence.

Another interesting finding was the discovery of *whiB6* as the only deregulated gene in the Δ*espL* transcriptome. Despite reduced expression of *whiB6*, no difference in the mRNA levels of the genes belonging to the WhiB6 putative regulon [44] was observed. This can be ascribed to the culture conditions used in these experiments, as it was reported that WhiB6 senses reducing conditions in *M. marinum*, and regulates transcription accordingly, thanks to its Fe-S cluster [44]. Additionally, the 3-fold deregulation of *whiB6* may not be mirrored by deregulation of its own regulon. Nonetheless, when WhiB6 was provided *in trans*, expression of most of the ESX-1 substrates or components was increased. Thereby, WhiB6 controls transcription of the ESX-1 genetic locus in *M. tuberculosis* too.

A recent report described similar and even more pronounced deregulation of *whiB6* and of the WhiB6-dependent genes in *M. marinum* lacking *eccCb1* [49]. In that case, the existence of a negative feedback loop connecting the ESX-1 core complex in the membrane to ESX-1 gene expression was postulated [49]. This is consistent with our findings in *M. tuberculosis* as EspL localizes mainly in the cytosol but also in the membrane fraction (Fig 4). Another analogy with the *eccCb1* mutant in *M. marinum* lies in the EspE and EspF protein levels, which also seem to be subjected to post-transcriptional control [49]. Of note, we demonstrated that virulence cannot be restored in Δ*espL* by expression of WhiB6 *in trans*.

Altogether, our data indicate an important role for EspL in *M. tuberculosis* pathogenesis and encourage further investigations into the contributions of EspE, EspF and EspH to virulence and to ESX-1-dependent secretion. EspF was previously shown to reduce *M. tuberculosis* virulence in the mouse model when deleted [36], EspH was recently identified as a hypervirulence factor in *M. marinum* [50] but little is known about the role of EspE. Conservation of the genes for *espH*, *espD* and *espL*, in the greatly down-sized genome of *M. leprae* [51] suggests a conserved function and this justifies future investigation.

3.5 MATERIALS AND METHODS

Bacterial strains and culture conditions

Mycobacterium tuberculosis strains (described in S5 Table) were grown at 37°C in 7H9 medium (Difco) supplemented with 0.2% glycerol, 0.05% Tween 80 and 10% albumin-dextrose-catalase (ADC, Middlebrook) or on 7H10 plates supplemented with 0.5% glycerol and 10% oleic acid-albumin-dextrose-catalase (OADC, Middlebrook). Sauton's liquid medium was used for culture filtrate analysis. Streptomycin (20 μg/ml), kanamycin (20 μg/ml), hygromycin (50 μg/ml) or 2.5% sucrose were added when necessary. Experiments involving *M. tuberculosis* were performed in a Biosafety Level 3 (BSL3) laboratory, according to the national and international guidelines (Authorization number A070027/3). For cloning purposes, One Shot TOP10 chemically competent *Escherichia coli* (Invitrogen) were grown in Luria–Bertani (LB) broth or on LB agar with hygromycin (200 μg/ml), kanamycin (50 μg/ml) or spectinomycin (25 μg/ml).

Reagents, plasmid vectors and oligonucleotides

Chemical reagents were obtained from Sigma-Aldrich, unless otherwise stated. Restriction and modification enzymes were purchased from New England Biolabs. Plasmid vectors are described in S6 Table. Oligonucleotides were synthesized by Microsynth. Sequences are available upon request

Mutant construction

One kb up- and downstream regions of the *espL* gene were PCR-amplified, ligated in-frame with the AvrII site and cloned into the PacI and AscI sites of pJG1100 [34], resulting in the suicide vector pJG1100-espL-UP/DOWN. The complementing plasmid pGA44-espL was constructed by cloning the *espL* gene into vector pGA44 [35], under control of the PTR promoter. Deletion of the full-length *espL* gene was achieved by homologous recombination using plasmid pJG1100-espL-UP/DOWN. After transformation of *M. tuberculosis* H37Rv, the first recombination event was selected on 7H10 plates, supplemented with hygromycin and kanamycin. Colonies were screened by colony PCR. Two clones that had undergone homologous recombination were grown in liquid 7H9 medium with no antibiotics, in order to promote the second recombination event and plasmid excision. Selection of the recombinant clones was performed by plating the bacteria on 7H10 plates supplemented with sucrose. The resulting colonies were tested by PCR to confirm deletion of *espL* from its native locus and further validated by whole genome sequencing..

In vitro growth curves

M. tuberculosis strains were grown to mid-logarithmic phase and then diluted to an optical density at 600 nm (OD_{600}) of 0.05 in 7H9 medium. OD_{600} was recorded at different time points to obtain the growth curves.

Genomic DNA preparation and whole genome sequencing

M. tuberculosis genomic DNA was extracted as previously described [52]. Libraries were prepared using the Kapa LTP Library Prep kit (Kapa Biosystems) according to the manufacturer's recommendations. Cluster generation was performed using the Illumina TruSeq SR Cluster Kit v4 reagents and sequenced on the Illumina HiSeq 2500 using TruSeq SBS Kit v4 reagents. Sequencing data were demultiplexed using the bcl2fastq Conversion Software (v. 2.20, Illumina, San Diego, California, USA). Raw reads were adapter- and quality-

trimmed with Trimmomatic v0.33 [53]. The quality settings were "SLIDINGWINDOW:5:15 MINLEN:40". Preprocessed reads were mapped onto the *M. tuberculosis* H37Rv reference genome sequence (RefSeq NC_000962.3) with Bowtie2 v2.2.5 [54]. SNP calling was done using VarScan v2.3.9 [55]. To avoid false-positive SNP calls the following cutoffs were applied: minimum overall coverage of ten non-duplicated reads, minimum of five non-duplicated reads supporting the SNP, mapping quality score >8, base quality score >15, and a SNP frequency above 80%. All SNPs were manually checked by visualizing the corresponding read alignments. Sequencing data have been deposited to the Sequence Read Archive (SRA) under accession number SRP158673.

RNA preparation, reverse-transcription and quantitative polymerase chain reaction (RT-qPCR)

M. tuberculosis cultures were grown to OD_{600} of 0.3-0.4, harvested by centrifugation, pellets were resuspended in TRIzol Reagent (ThermoFisher) and stored at -80°C until further processing. Total RNA was extracted by bead-beating as previously described [35]. Integrity of RNA was checked by agarose gel electrophoresis, purity and amount of RNA were assessed using a Nanodrop instrument and Qubit Fluorometric Quantitation (ThermoFisher), respectively. SuperScript III First-Strand Synthesis System (Invitrogen) was used to generate randomly primed cDNA from 1 μg of RNA, according to the manufacturer's recommendations. qPCR reactions were performed on an ABI 7900HT instrument, using Power SybrGreen PCR Master Mix (Applied Biosystems), according to the manufacturer's instructions. The housekeeping gene *sigA* was used for normalization.

RNA-seq: library preparation, high-throughput sequencing and analysis

RNA was extracted from biological duplicates as described above. RNA-seq libraries were prepared from 1 μg of total RNA. The RNA samples were depleted of r-RNAs with the Illumina Ribo-Zero rRNA Removal Kit (Gram-Positive Bacteria) then used to generate sequencing libraries with the Illumina TruSeq Stranded mRNA reagents, omitting the polyA selection step (Illumina, San Diego, California, USA). Cluster generation was performed with the resulting libraries using the Illumina TruSeq SR Cluster Kit v4 reagents and sequenced on the Illumina HiSeq 2500 using TruSeq SBS Kit v4 reagents. Sequencing data were demultiplexed using the bcl2fastq Conversion Software (v. 2.20, Illumina, San Diego, California, USA).

Reads were processed and mapped to the reference genome sequence as described above. Counting reads over features was done with featureCounts [56] from the Subread package v1.4.6. Annotation was taken from TubercuList release R27 (https://mycobrowser.epfl.ch/releases). Differential gene expression analysis was done using DESeq2 [57]. RNA-seq data have been deposited to the Gene Expression Omnibus (GEO) repository under accession number GSE118994.

Mass spectrometry analysis of total protein extracts

M. tuberculosis cells, grown to mid-exponential phase in 15 ml cultures, were pelleted by centrifugation, washed once in PBS (Phosphate Buffered Saline) supplemented with 0.05% Tween 80 and the pellets stored at -80°C until further use. Total lysates were obtained by sonication in lysis buffer (100 mM Tris pH 8, 2% SDS, cOmplete mini EDTA free Roche) and boiled at 100°C for 1 h. Proteins were quantified by using the Pierce BCA Protein Assay kit and 30 µg were submitted for mass spectrometry analysis.

Each sample was digested by Filter Aided Sample Preparation (FASP) [58] with minor modifications. Dithiothreitol (DTT) was replaced by Tris(2-carboxyethyl)phosphine (TCEP) as reducing agent and Iodoacetamide by Chloracetamide as alkylating agent. A combined proteolytic digestion was performed using Endoproteinase Lys-C and Trypsin. Acidified peptides were desalted on C18 StageTips [59] and dried down by vacuum centrifugation. For LC MS/MS analysis, peptides were resuspended and separated by reversed-phase chromatography on a Dionex Ultimate 3000 RSLC nanoUPLC system in-line connected with an Orbitrap Fusion Lumos Mass-Spectrometer (Thermo Fischer Scientific). Database search was performed using MaxQuant 1.6.0.1 [60] against the TubercuListR27 database (http://tuberculist.epfl.ch/). Carbamidomethylation was set as fixed modification, whereas oxidation (M), phosphorylation (S,T,Y) and acetylation (Protein N-term) were considered as variable modifications. Label Free Quantification (MaxLFQ) was performed by MaxQuant using the standard settings [61]. Perseus [62] was used to highlight differentially quantified proteins. Reverse proteins, contaminants and proteins only identified by sites were filtered out. Biological replicates were grouped together and protein groups containing a minimum of two LFQ values in at least one group were conserved. Empty values were imputed with random numbers from a normal distribution. Significant hits were determined by a volcano plot-based strategy, combining t test p-values with ratio information [63]. Significance curves in the volcano plot corresponding to a SO value of 0.5 and 0.05

FDR were determined by a permutation-based method. Further graphical displays were generated using homemade programs written in R [64].

Immunoblot analysis of bacterial lysates and culture filtrates

M. tuberculosis cultures were grown in 7H9 to mid-logarithmic phase. The culture medium was then replaced by Sauton's supplemented with 0.05% Tween 80 and growth was continued for 3 d. Finally, bacteria were pelleted and resuspended in Sauton's medium without Tween 80 for collection of the culture filtrates. These were filtered through 0.22 μm Steriflip Millipore Express Plus Membranes (Millipore), concentrated 100x using Amicon Ultracel-3K centrifugal filters (Millipore), quantified by using the Qubit Fluorometric Quantitation device (ThermoFisher) and loaded on SDS-PAGE 12–15% NuPAGE gels (Invitrogen) for immunoblot analyses. Bacterial pellets were washed once in Tris-Buffered Saline (TBS, 20 mM Tris-HCl pH 7.5, 150 mM NaCl) and stored at -80°C until further processing. Cells were sonicated in TBS supplemented with a protease inhibitor tablet (cOmplete mini EDTA free, Roche) for 15 min and the protein solution was then sterilized by filtration through a 0.22 μm filter (Pall Life Sciences) to remove residual intact cells. Protein samples were quantified using Qubit. Equal amounts of protein preparations (10 μg for cell lysates, 15-20 μg for culture filtrates) were loaded on SDS-PAGE 12–15% NuPAGE gels (Invitrogen) and transferred onto PVDF membranes using a semidry electrophoresis transfer apparatus (Invitrogen). Membranes were incubated in TBS-Tween blocking buffer (25 mM Tris pH 7.5, 150 mM NaCl, 0.05 % Tween 20) with 5% w/v skimmed milk powder for 2h at 4°C prior to overnight incubation with primary antibody. Membranes were washed in TBS-Tween three times at room temperature, and then incubated with secondary antibody for 3 h before washing again. Signals were detected using Chemiluminescent Peroxidase Substrate 1 (Sigma-Aldrich).

Polyclonal anti-EspL, anti-EspB, anti-EspA [48], anti-EspD [48] antibodies were produced by Dr. Ida Rosenkrands (Statens Serum Institut, Copenhagen, Denmark). Monoclonal anti-RpoB antibodies were purchased from NeoClone, polyclonal anti-EsxB antibodies from Abcam, monoclonal anti-HA antibodies conjugated to Horseradish Peroxidase (HRP) from Cell Signaling. Polyclonal anti-Rv3852 antibodies were generated by Eurogentec [38]. The following reagents were obtained through BEI Resources, NIAID, NIH: monoclonal anti-Antigen 85, monoclonal anti-GroEL2 and polyclonal anti-EsxA antibodies.

Fractionation of total bacterial lysate

Cell fractions were obtained as described previously [38]. Briefly, M. tuberculosis was grown in Sauton's medium with 0.05% Tween 80 to mid-exponential phase, cells were collected by centrifugation, supernatants were filtered through 0.22 μm Steriflip Millipore Express Plus Membranes (Millipore) and concentrated 100x using Amicon Ultracel-3K centrifugal filters (Millipore) to obtain the culture filtrate fraction. The pellet was treated with 0.25 % Genapol-X080 for 30 min at room temperature, followed by centrifugation at 14,000 g for 10 min. The proteins in the resulting supernatant were precipitated with Trichloroacetic acid (TCA), yielding the capsular fraction. The remaining pellet was subjected to sonication to break the cells, sterilized by filtration through a 0.22 μm filter (Pall Life Sciences) followed by ultra-centrifugation at 45,000 rpm for 1h at 4°C. The supernatant contained the cytosolic fraction, while the pellet was enriched with membrane proteins. Analysis of the protein fractions was carried out by immunoblot as described above.

Co-immunoprecipitation experiments

M. tuberculosis cells in 30 ml cultures were pelleted by centrifugation, washed once in PBS (Phosphate Buffered Saline) supplemented with 0.05% Tween 80 and the pellets stored at -80°C until further use. Total lysates were obtained by sonication in TBS-T (25 mM Tris pH 7.5, 150 mM NaCl, 0.05% Tween 20), followed by filtration through 0.22 μm filters (Pall Life Sciences). Fifty microliters of Monoclonal Anti-HA Agarose Antibody beads (Sigma-Aldrich) were incubated with approximately 1 mg of bacterial extract in Spin-X centrifuge tubes (Costar) for 4 h at 4°C on an orbital shaker. The resin was washed four times in PBS and the immunoprecipitated material was eluted from the beads in PBS-SDS sample buffer (100 mM Tris HCl pH 6.8, 200 mM dithiothreitol, 4% SDS, 0.2% bromophenol blue, 20% glycerol) during a 5 min incubation at 95°C. Immunoprecipitated proteins were analyzed either by mass spectrometry as described [24] or by immunoblot. A mock (no antibody) control was run in parallel with agarose beads only.

Cell cultures and infection with *M. tuberculosis* strains

THP-1 cells were cultured in RPMI1640 (Life Technologies) supplemented with 10% (v/v) Fetal Calf Serum (Life Technologies) and 1% sodium pyruvate (Life Technologies). Cells were differentiated in 96- or 12-well plates by addition of 4 nM phorbol 12-myristate 13-acetate (PMA) for 24 h at 37°C in 5% CO2. Differentiated

cells were then infected with M. tuberculosis as follows. Bacteria were grown to exponential phase (OD600 between 0.4 and 0.8), washed once in 7H9 medium, resuspended in 7H9 to an OD600 of 1, equivalent to 3 x 108 bacteria/ml. The required volume of bacterial suspension was then added to RPMI1640 for infection of human THP-1 cells at the multiplicity of infection (MOI) reported in the text. Plates were sealed with gas-permeable sealing film and incubated at 37°C under 5% CO2. Intracellular bacteria were released by the infected cells by addition of 0.5% Triton-X. The suspension was serially diluted in 7H9 and plated on 7H10 plates. Colony forming units (CFU) were counted after incubation at 37°C for 4-5 weeks. PrestoBlue Assay (Thermofisher) to evaluate cell viability was performed according to the manufacturer's instructions. Fluorescence was measured using a Tecan Infinite M200 microplate reader.

ELISA assays

Cell culture supernatants from infections in 96-well plates were removed from infected cells 24 h post-infection. Supernatants were filtered through NANOSEP centrifugal devices (Pall Life Sciences) and assayed for human IL-1β (BD Biosciences) according to the manufacturer's instructions.

Quantitative polymerase chain reaction (qPCR) analysis of cytokine expression

RNA from infected cells in the 12-well format was extracted by using Qiagen RNeasy kit according to the manufacturer's instructions 24 h post-infection and reverse-transcribed using the RevertAid First Strand cDNA Synthesis kit (Fermentas). Quantitative PCR analysis was performed on an ABI 7900HT instrument. All gene expression data are presented as relative expression to GAPDH.

Statistical analysis

Statistical analyses were performed in GraphPad PRISM by one-way or two-way ANOVA followed by Tukey's multiple comparison test

Acknowledgements

The authors would like to acknowledge the Proteomics Core Facility at EPFL for mass spectrometry experiments, the Lausanne Genomic Technologies Facility at the University of Lausanne for high-throughput sequencing analyses, Philippe Busso for technical assistance, Dr. Ida Rosenkrands (Statens Serum Institut, Copenhagen, Denmark) for antibody production. We thank the Swiss National Science Foundation (grant number 31003A_162641) for financial support.

3.6 BIBLIOGRAPHY

1. WHO. Global Tuberculosis Report 2017. 2017.

2. Gengenbacher M, Kaufmann SHE. Mycobacterium tuberculosis: success through dormancy. FEMS Microbiol Rev. 2012;36: 514–532. doi:10.1111/j.1574-6976.2012.00331.x

3. Zumla A, Raviglione M, Hafner R, von Reyn CF. Tuberculosis. N Engl J Med. 2013;368: 745–755. doi:10.1056/NEJMra1200894

4. Stevenson CR, Forouhi NG, Roglic G, Williams BG, Lauer JA, Dye C, et al. Diabetes and tuberculosis: the impact of the diabetes epidemic on tuberculosis incidence. BMC Public Health. 2007;7: 234. doi:10.1186/1471-2458-7-234

5. Collins KR, Quiñones-Mateu ME, Toossi Z, Arts EJ. Impact of tuberculosis on HIV-1 replication, diversity, and disease progression. AIDS Rev. 2002;4: 165–176.

6. Gröschel MI, Sayes F, Simeone R, Majlessi L, Brosch R. ESX secretion systems: mycobacterial evolution to counter host immunity. Nat Rev Microbiol. 2016;14: 677–691. doi:10.1038/nrmicro.2016.131

7. Renshaw PS, Lightbody KL, Veverka V, Muskett FW, Kelly G, Frenkiel TA, et al. Structure and function of the complex formed by the tuberculosis virulence factors CFP-10 and ESAT-6. EMBO J. 2005;24: 2491–2498. doi:10.1038/sj.emboj.7600732

8. Pallen MJ. The ESAT-6/WXG100 superfamily -- and a new Gram-positive secretion system? Trends Microbiol. 2002;10: 209–212.

9. Cole ST, Brosch R, Parkhill J, Garnier T, Churcher C, Harris D, et al. Deciphering the biology of Mycobacterium tuberculosis from the complete genome sequence. Nature. 1998;393: 537–544. doi:10.1038/31159

10. Pym AS, Brodin P, Brosch R, Huerre M, Cole ST. Loss of RD1 contributed to the attenuation of the live tuberculosis vaccines Mycobacterium bovis BCG and Mycobacterium microti. Mol Microbiol. 2002;46: 709–717.

11. Mahairas GG, Sabo PJ, Hickey MJ, Singh DC, Stover CK. Molecular analysis of genetic differences between Mycobacterium bovis BCG and virulent M. bovis. J Bacteriol. 1996;178: 1274–1282.

12. Lewis KN, Liao R, Guinn KM, Hickey MJ, Smith S, Behr MA, et al. Deletion of RD1 from Mycobacterium tuberculosis mimics bacille Calmette-Guérin attenuation. J Infect Dis. 2003;187: 117–123. doi:10.1086/345862

13. Hsu T, Hingley-Wilson SM, Chen B, Chen M, Dai AZ, Morin PM, et al. The primary mechanism of attenuation of bacillus Calmette-Guerin is a loss of secreted lytic function required for invasion of lung interstitial tissue. Proc Natl Acad Sci U S A. 2003;100: 12420–12425. doi:10.1073/pnas.1635213100

14. Brodin P, Eiglmeier K, Marmiesse M, Billault A, Garnier T, Niemann S, et al. Bacterial artificial chromosome-based comparative genomic analysis identifies Mycobacterium microti as a natural ESAT-6 deletion mutant. Infect Immun. 2002;70: 5568–5578.

15. Wassermann R, Gulen MF, Sala C, Perin SG, Lou Y, Rybniker J, et al. Mycobacterium tuberculosis Differentially Activates cGAS- and Inflammasome-Dependent Intracellular Immune Responses through ESX-1. Cell Host Microbe. 2015;17: 799–810. doi:10.1016/j.chom.2015.05.003

16. Collins AC, Cai H, Li T, Franco LH, Li X-D, Nair VR, et al. Cyclic GMP-AMP Synthase Is an Innate Immune DNA Sensor for Mycobacterium tuberculosis. Cell Host Microbe. 2015;17: 820–828. doi:10.1016/j.chom.2015.05.005

17. Watson RO, Bell SL, MacDuff DA, Kimmey JM, Diner EJ, Olivas J, et al. The Cytosolic Sensor cGAS Detects Mycobacterium tuberculosis DNA to Induce Type I Interferons and Activate Autophagy. Cell Host Microbe. 2015;17: 811–819. doi:10.1016/j.chom.2015.05.004

18. Smith J, Manoranjan J, Pan M, Bohsali A, Xu J, Liu J, et al. Evidence for pore formation in host cell membranes by ESX-1-secreted ESAT-6 and its role in Mycobacterium marinum escape from the vacuole. Infect Immun. 2008;76: 5478–5487. doi:10.1128/IAI.00614-08

19. van der Wel N, Hava D, Houben D, Fluitsma D, van Zon M, Pierson J, et al. M. tuberculosis and M. leprae translocate from the phagolysosome to the cytosol in myeloid cells. Cell. 2007;129: 1287–1298. doi:10.1016/j.cell.2007.05.059

20. Simeone R, Bottai D, Brosch R. ESX/type VII secretion systems and their role in host-pathogen interaction. Curr Opin Microbiol. 2009;12: 4–10. doi:10.1016/j.mib.2008.11.003

21. van Leeuwen LM, Boot M, Kuijl C, Picavet DI, van Stempvoort G, van der Pol SMA, et al. Mycobacteria employ two different mechanisms to cross the blood-brain barrier. Cell Microbiol. 2018; e12858. doi:10.1111/cmi.12858

22. Rybniker J, Chen JM, Sala C, Hartkoorn RC, Vocat A, Benjak A, et al. Anticytolytic screen identifies inhibitors of mycobacterial virulence protein secretion. Cell Host Microbe. 2014;16: 538–548. doi:10.1016/j.chom.2014.09.008

23. Beckham KSH, Ciccarelli L, Bunduc CM, Mertens HDT, Ummels R, Lugmayr W, et al. Structure of the mycobacterial ESX-5 type VII secretion system membrane complex by single-particle analysis. Nat Microbiol. 2017;2: 17047. doi:10.1038/nmicrobiol.2017.47

24. Lou Y, Rybniker J, Sala C, Cole ST. EspC forms a filamentous structure in the cell envelope of *Mycobacterium tuberculosis* and impacts ESX-1 secretion: Filamentous structure formation by EspC. Mol Microbiol. 2017;103: 26–38. doi:10.1111/mmi.13575

25. Fortune SM, Jaeger A, Sarracino DA, Chase MR, Sassetti CM, Sherman DR, et al. Mutually dependent secretion of proteins required for mycobacterial virulence. Proc Natl Acad Sci U S A. 2005;102: 10676–10681. doi:10.1073/pnas.0504922102

26. Solomonson M, Setiaputra D, Makepeace KAT, Lameignere E, Petrotchenko EV, Conrady DG, et al. Structure of EspB from the ESX-1 type VII secretion system and insights into its export mechanism. Struct Lond Engl 1993. 2015;23: 571–583. doi:10.1016/j.str.2015.01.002

27. Daleke MH, Ummels R, Bawono P, Heringa J, Vandenbroucke-Grauls CMJE, Luirink J, et al. General secretion signal for the mycobacterial type VII secretion pathway. Proc Natl Acad Sci U S A. 2012;109: 11342–11347. doi:10.1073/pnas.1119453109

28. Blasco B, Chen JM, Hartkoorn R, Sala C, Uplekar S, Rougemont J, et al. Virulence Regulator EspR of Mycobacterium tuberculosis Is a Nucleoid-Associated Protein. PLOS Pathog. 2012;8: e1002621. doi:10.1371/journal.ppat.1002621

29. Gordon BRG, Li Y, Wang L, Sintsova A, van Bakel H, Tian S, et al. Lsr2 is a nucleoid-associated protein that targets AT-rich sequences and virulence genes in Mycobacterium tuberculosis. Proc Natl Acad Sci U S A. 2010;107: 5154–5159. doi:10.1073/pnas.0913551107

30. Rickman L, Scott C, Hunt DM, Hutchinson T, Menéndez MC, Whalan R, et al. A member of the cAMP receptor protein family of transcription regulators in Mycobacterium tuberculosis is required for virulence in mice and controls

transcription of the rpfA gene coding for a resuscitation promoting factor. Mol Microbiol. 2005;56: 1274–1286. doi:10.1111/j.1365-2958.2005.04609.x

31. Pang X, Samten B, Cao G, Wang X, Tvinnereim AR, Chen X-L, et al. MprAB regulates the espA operon in Mycobacterium tuberculosis and modulates ESX-1 function and host cytokine response. J Bacteriol. 2013;195: 66–75. doi:10.1128/JB.01067-12

32. Ohol YM, Goetz DH, Chan K, Shiloh MU, Craik CS, Cox JS. Mycobacterium tuberculosis MycP1 protease plays a dual role in regulation of ESX-1 secretion and virulence. Cell Host Microbe. 2010;7: 210–220. doi:10.1016/j.chom.2010.02.006

33. Cortes T, Schubert OT, Rose G, Arnvig KB, Comas I, Aebersold R, et al. Genome-wide Mapping of Transcriptional Start Sites Defines an Extensive Leaderless Transcriptome in Mycobacterium tuberculosis. Cell Rep. 2013;5: 1121–1131. doi:10.1016/j.celrep.2013.10.031

34. Gomez JE, Bishai WR. whmD is an essential mycobacterial gene required for proper septation and cell division. Proc Natl Acad Sci U S A. 2000;97: 8554–8559. doi:10.1073/pnas.140225297

35. Kolly GS, Boldrin F, Sala C, Dhar N, Hartkoorn RC, Ventura M, et al. Assessing the essentiality of the decaprenyl-phospho- D -arabinofuranose pathway in *M ycobacterium tuberculosis* using conditional mutants: Druggability of the *M. tuberculosis* DPA pathway. Mol Microbiol. 2014;92: 194–211. doi:10.1111/mmi.12546

36. Bottai D, Majlessi L, Simeone R, Frigui W, Laurent C, Lenormand P, et al. ESAT-6 secretion-independent impact of ESX-1 genes espF and espG1 on virulence of Mycobacterium tuberculosis. J Infect Dis. 2011;203: 1155–1164. doi:10.1093/infdis/jiq089

37. Chen JM, Zhang M, Rybniker J, Boy-Röttger S, Dhar N, Pojer F, et al. Mycobacterium tuberculosis EspB binds phospholipids and mediates EsxA-independent virulence. Mol Microbiol. 2013;89: 1154–1166. doi:10.1111/mmi.12336

38. Odermatt NT, Sala C, Benjak A, Kolly GS, Vocat A, Lupien A, et al. Rv3852 (H-NS) of Mycobacterium tuberculosis Is Not Involved in Nucleoid Compaction and Virulence Regulation. J Bacteriol. 2017;199. doi:10.1128/JB.00129-17

39. Finn RD, Coggill P, Eberhardt RY, Eddy SR, Mistry J, Mitchell AL, et al. The Pfam protein families database: towards a more sustainable future. Nucleic Acids Res. 2016;44: D279–D285. doi:10.1093/nar/gkv1344

40. Tian S, Chen H, Sun T, Wang H, Zhang X, Liu Y, et al. Expression, purification and characterization of Esx-1 secretion-associated protein EspL from Mycobacterium tuberculosis. Protein Expr Purif. 2016;128: 42–51. doi:10.1016/j.pep.2016.08.001

41. Cooley AE, Riley SP, Kral K, Miller MC, DeMoll E, Fried MG, et al. DNA-binding by Haemophilus influenzae and Escherichia coli YbaB, members of a widely-distributed bacterial protein family. BMC Microbiol. 2009;9: 137. doi:10.1186/1471-2180-9-137

42. Riley SP, Bykowski T, Cooley AE, Burns LH, Babb K, Brissette CA, et al. Borrelia burgdorferi EbfC defines a newly-identified, widespread family of bacterial DNA-binding proteins. Nucleic Acids Res. 2009;37: 1973–1983. doi:10.1093/nar/gkp027

43. Lim K, Tempczyk A, Parsons JF, Bonander N, Toedt J, Kelman Z, et al. Crystal structure of YbaB from Haemophilus influenzae (HI0442), a protein of unknown function coexpressed with the recombinational DNA repair protein RecR. Proteins. 2003;50: 375–379. doi:10.1002/prot.10297

44. Chen Z, Hu Y, Cumming BM, Lu P, Feng L, Deng J, et al. Mycobacterial WhiB6 Differentially Regulates ESX-1 and the Dos Regulon to Modulate Granuloma Formation and Virulence in Zebrafish. Cell Rep. 2016;16: 2512–2524. doi:10.1016/j.celrep.2016.07.080

45. Uplekar S, Rougemont J, Cole ST, Sala C. High-resolution transcriptome and genome-wide dynamics of RNA polymerase and NusA in Mycobacterium tuberculosis. Nucleic Acids Res. 2013;41: 961–977. doi:10.1093/nar/gks1260

46. Stoop EJM, Schipper T, Rosendahl Huber SK, Nezhinsky AE, Verbeek FJ, Gurcha SS, et al. Zebrafish embryo screen for mycobacterial genes involved in the initiation of granuloma formation reveals a newly identified ESX-1 component. Dis Model Mech. 2011;4: 526–536. doi:10.1242/dmm.006676

47. Renshaw PS, Panagiotidou P, Whelan A, Gordon SV, Hewinson RG, Williamson RA, et al. Conclusive Evidence That the Major T-cell Antigens of theMycobacterium tuberculosis Complex ESAT-6 and CFP-10 Form a Tight, 1:1 Complex and Characterization of the Structural Properties of ESAT-6, CFP-10, and the ESAT-6·CFP-10 Complex IMPLICATIONS FOR PATHOGENESIS AND VIRULENCE. J Biol Chem. 2002;277: 21598–21603. doi:10.1074/jbc.M201625200

48. Chen JM, Boy-Röttger S, Dhar N, Sweeney N, Buxton RS, Pojer F, et al. EspD is critical for the virulence-mediating ESX-1 secretion system in Mycobacterium tuberculosis. J Bacteriol. 2012;194: 884–893. doi:10.1128/JB.06417-11

49. Bosserman RE, Nguyen TT, Sanchez KG, Chirakos AE, Ferrell MJ, Thompson CR, et al. WhiB6 regulation of ESX-1 gene expression is controlled by a negative feedback loop in Mycobacterium marinum. Proc Natl Acad Sci U S A. 2017;114: E10772–E10781. doi:10.1073/pnas.1710167114

50. Phan TH, Leeuwen LM van, Kuijl C, Ummels R, Stempvoort G van, Rubio-Canalejas A, et al. EspH is a hypervirulence factor for Mycobacterium marinum and essential for the secretion of the ESX-1 substrates EspE and EspF. PLOS Pathog. 2018;14: e1007247. doi:10.1371/journal.ppat.1007247

51. Cole ST, Eiglmeier K, Parkhill J, James KD, Thomson NR, Wheeler PR, et al. Massive gene decay in the leprosy bacillus. Nature. 2001;409: 1007–1011. doi:10.1038/35059006

52. Pelicic V, Jackson M, Reyrat JM, Jacobs WR, Gicquel B, Guilhot C. Efficient allelic exchange and transposon mutagenesis in Mycobacterium tuberculosis. Proc Natl Acad Sci U S A. 1997;94: 10955–10960.

53. Bolger AM, Lohse M, Usadel B. Trimmomatic: a flexible trimmer for Illumina sequence data. Bioinforma Oxf Engl. 2014;30: 2114–2120. doi:10.1093/bioinformatics/btu170

54. Langmead B, Salzberg SL. Fast gapped-read alignment with Bowtie 2. Nat Methods. 2012;9: 357–359. doi:10.1038/nmeth.1923

55. Koboldt DC, Zhang Q, Larson DE, Shen D, McLellan MD, Lin L, et al. VarScan 2: somatic mutation and copy number alteration discovery in cancer by exome sequencing. Genome Res. 2012;22: 568–576. doi:10.1101/gr.129684.111

56. Liao Y, Smyth GK, Shi W. featureCounts: an efficient general purpose program for assigning sequence reads to genomic features. Bioinforma Oxf Engl. 2014;30: 923–930. doi:10.1093/bioinformatics/btt656

57. Love MI, Huber W, Anders S. Moderated estimation of fold change and dispersion for RNA-seq data with DESeq2. Genome Biol. 2014;15: 550. doi:10.1186/s13059-014-0550-8

58. Wiśniewski JR, Zougman A, Nagaraj N, Mann M. Universal sample preparation method for proteome analysis. Nat Methods. 2009;6: 359–362. doi:10.1038/nmeth.1322

59. Rappsilber J, Mann M, Ishihama Y. Protocol for micro-purification, enrichment, pre-fractionation and storage of peptides for proteomics using StageTips. Nat Protoc. 2007;2: 1896–1906. doi:10.1038/nprot.2007.261

60. Cox J, Mann M. MaxQuant enables high peptide identification rates, individualized p.p.b.-range mass accuracies and proteome-wide protein quantification. Nat Biotechnol. 2008;26: 1367–1372. doi:10.1038/nbt.1511

61. Cox J, Hein MY, Luber CA, Paron I, Nagaraj N, Mann M. Accurate proteome-wide label-free quantification by delayed normalization and maximal peptide ratio extraction, termed MaxLFQ. Mol Cell Proteomics MCP. 2014;13: 2513–2526. doi:10.1074/mcp.M113.031591

62. Tyanova S, Temu T, Sinitcyn P, Carlson A, Hein MY, Geiger T, et al. The Perseus computational platform for comprehensive analysis of (prote)omics data. Nat Methods. 2016;13: 731–740. doi:10.1038/nmeth.3901

63. Hubner NC, Bird AW, Cox J, Splettstoesser B, Bandilla P, Poser I, et al. Quantitative proteomics combined with BAC TransgeneOmics reveals in vivo protein interactions. J Cell Biol. 2010;189: 739–754. doi:10.1083/jcb.200911091

64. R Core Team RF for SC Vienna, Austria. R: A language and environment for statistical computing. 2017; Available: URL https://www.R-project.org/.

3.7 FIGURES AND TABLES

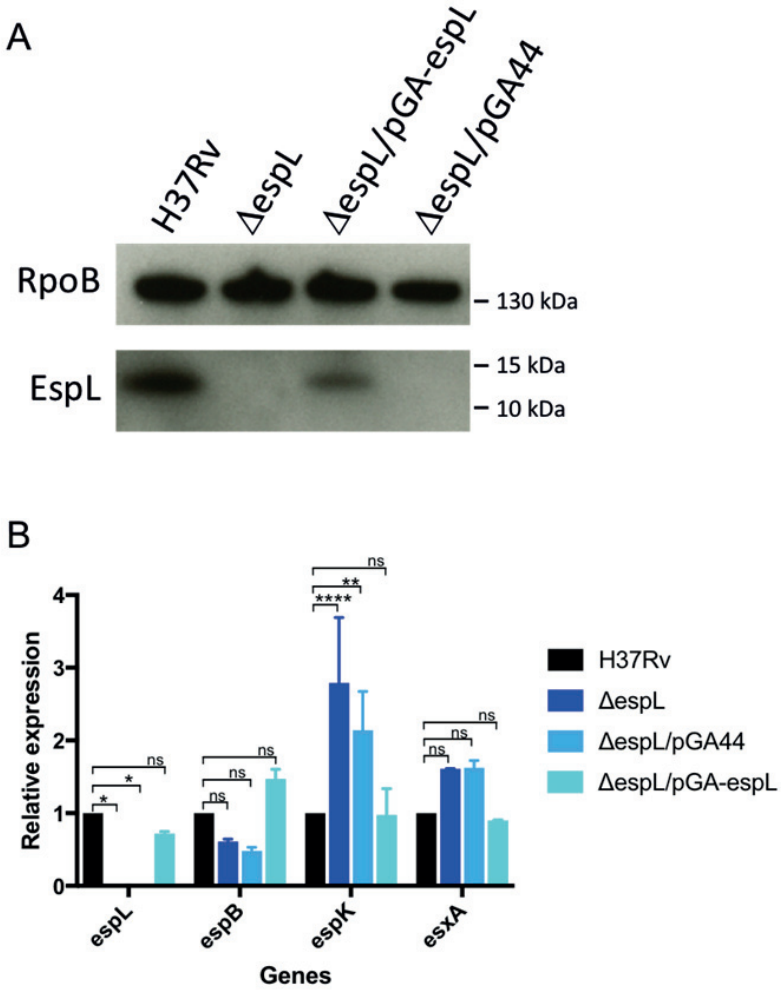

Figure 1. Validation of Δ*espL* mutant. A) Detection of EspL by immunoblot analysis of total protein extracts from *M. tuberculosis* H37Rv, Δ*espL* mutant and complemented strain. RpoB was used as a loading control. **B)** qRT-PCR analysis of *espL*, *espB*, *espK* and *esxA* gene expression levels in different strains. Data were obtained from two independent replicates, normalized to the housekeeping gene *sigA* and expressed as relative to H37Rv. *, $p < 0.05$. **, $p < 0.005$. ****, $p < 0.0001$. ns, not significant in two-way ANOVA followed by Tukey's multiple comparison test.

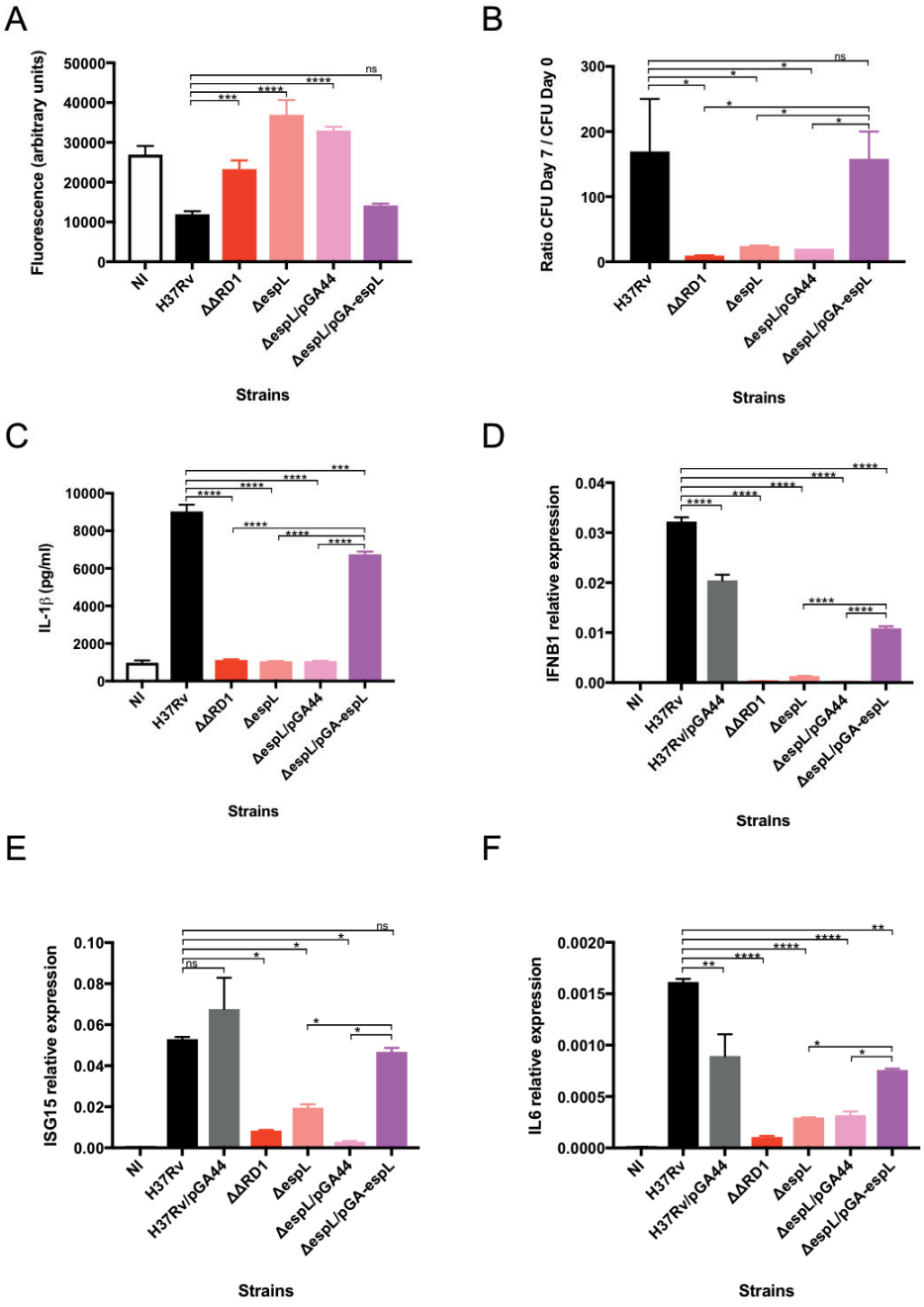

Figure 2. ***Ex vivo*** **phenotype of Δ*espL* mutant. A)** Virulence of Δ*espL* mutant compared to H37Rv and complemented strain in the THP-1 infection model. ΔΔRD1 carries a deletion of the extended ESX-1 locus. THP-1 cells were infected at multiplicity of infection (MOI) of 5. Fluorescence measurements directly correlate with THP-1 viability. Data were expressed as the mean and standard deviation (SD) of four independent replicates. **B)** Colony forming unit (CFU) evaluation of intracellular bacteria upon THP-1 infection. THP-1 cells were infected at multiplicity of infection (MOI) of 20:1 (cells:bacteria). Data were expressed as the mean and SD of two independent replicates. **C), D), E) and F)** Cytokine expression levels measured upon THP-1 infection with different bacterial strains. IL-1β was detected by ELISA assays. *IFNB*, *ISG15* and *IL6* were quantified by qRT-PCR. Data were expressed as the mean and SD of two independent replicates. NI: not infected control. *, $p < 0.05$. **, $p < 0.005$. ***, $p < 0.0005$. ****, $p < 0.0001$. ns, not significant in one-way ANOVA followed by Tukey's multiple comparison test.

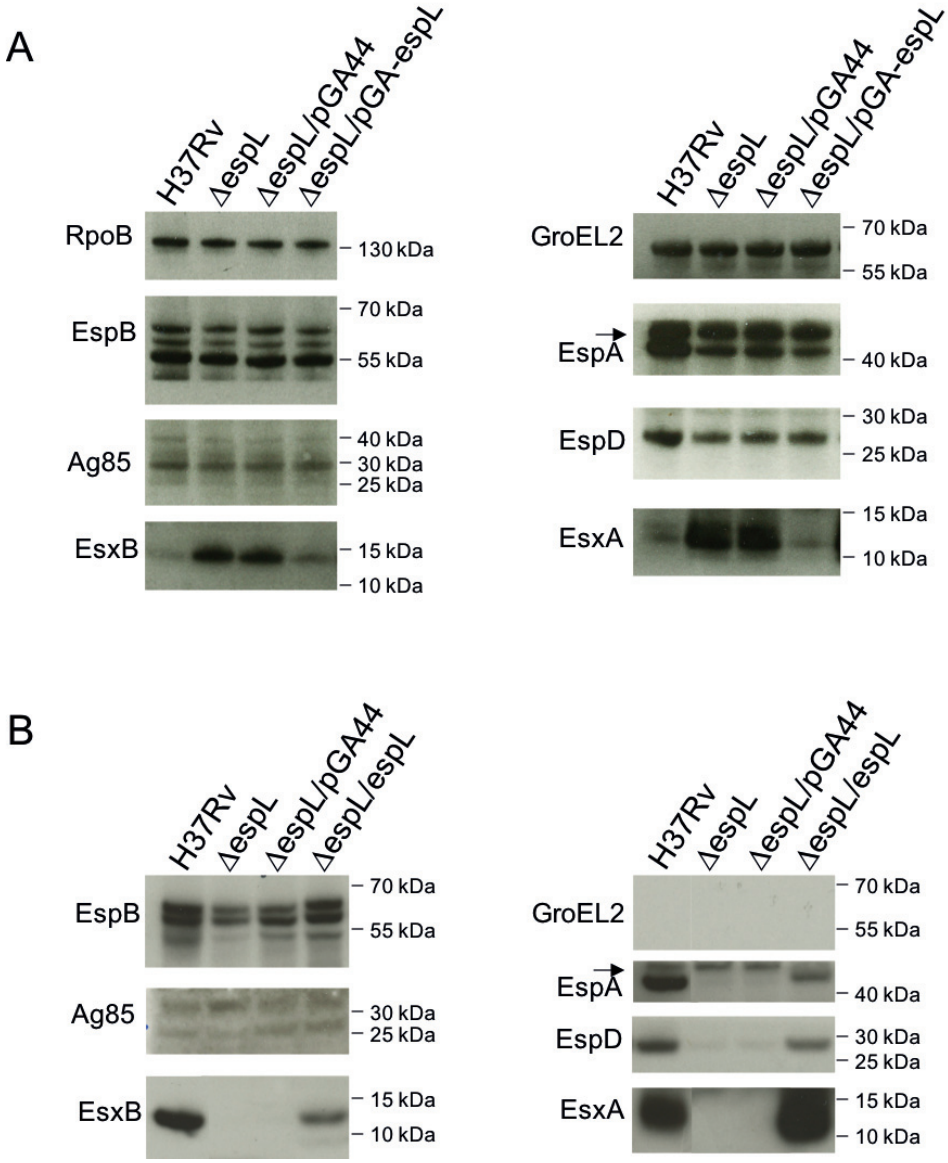

Figure 3. **Immunoblot analysis of Δ*espL* mutant. A)** Total cell lysates prepared from the indicated bacterial strains were analyzed by immunoblot. Membranes were probed for RpoB, which represented the loading control, EspB, Antigen 85 (Ag85), EsxB, GroEL2, EspA, EspD and EsxA. **B)** Culture filtrates were analyzed as described for the total cell lysates. Arrows indicate non-specific bands detected by the anti-EspB and anti-EspA antibodies. The experiment was repeated two times. One representative image is shown.

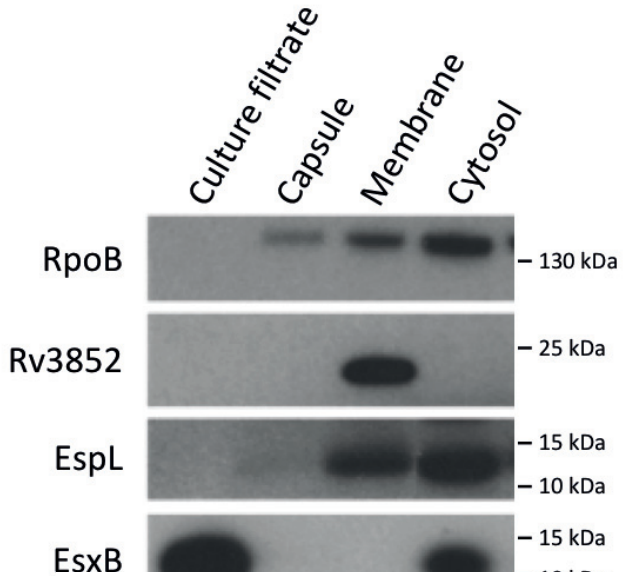

Figure 4. Localization of EspL in subcellular fractions. The culture filtrate, capsular, membrane and cytosolic fractions were analyzed by immunoblot. Membranes were probed for RpoB (cytosolic control), Rv3852 (membrane control), EsxB (culture filtrate control)

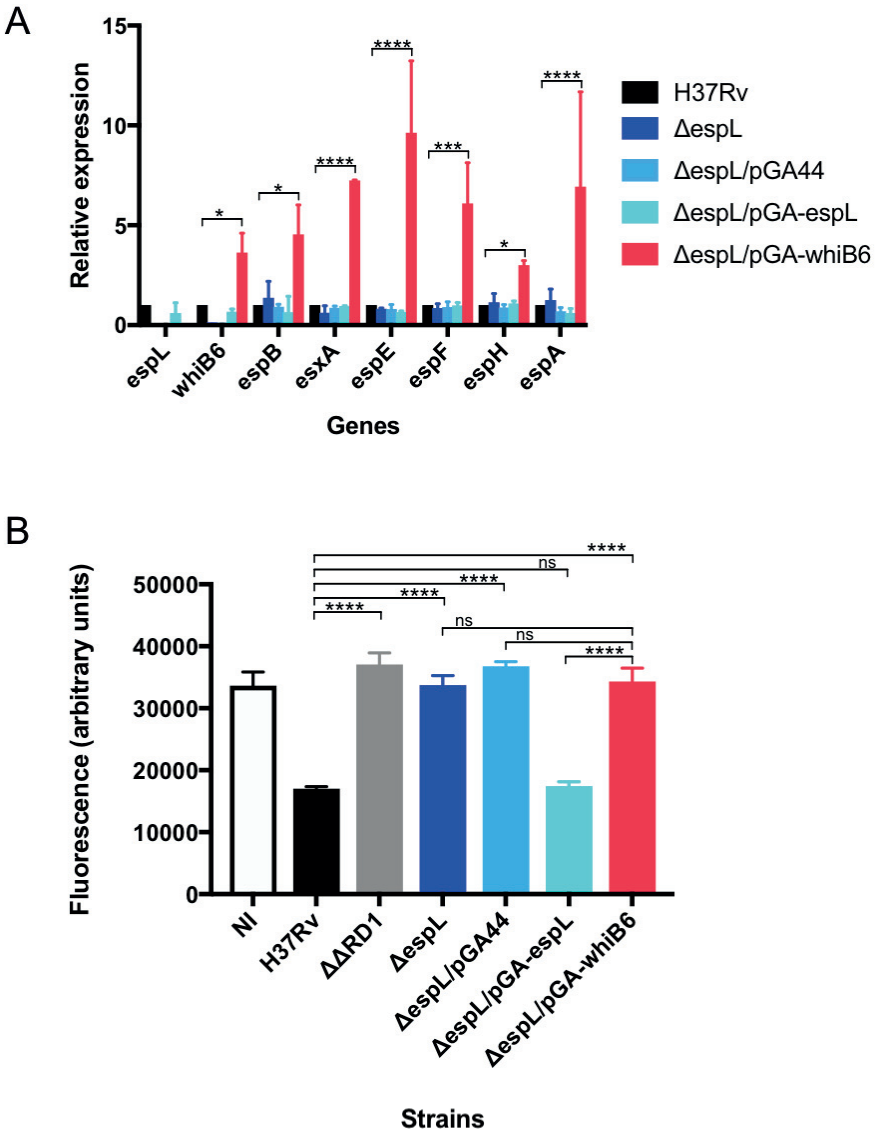

Figure 5. Phenotype obtained upon expression of *whiB6* in the *ΔespL* mutant. **A)** qRT-PCR analysis of the expression levels of the indicated genes in different strains. Data were obtained from two independent replicates, normalized to the housekeeping gene *sigA* and expressed as relative to H37Rv. *, $p < 0.05$. ***, $p < 0.0005$. ****, $p < 0.0001$ in two-way ANOVA followed by Tukey's multiple comparison test. **B)** Virulence of Δ*espL* mutant expressing *whiB6 in trans* compared to H37Rv, Δ*espL* and complemented strain in the THP-1 infection model. ΔΔRD1 carries a deletion of the extended ESX-1 locus. THP-1 cells were infected at multiplicity of infection (MOI) of 5. Fluorescence measurements directly correlate with THP-1 viability. Data were expressed as the mean and SD of four independent replicates. NI: not infected control. ****, $p < 0.0001$. ns, not significant in one-way ANOVA followed by Tukey's multiple comparison test.

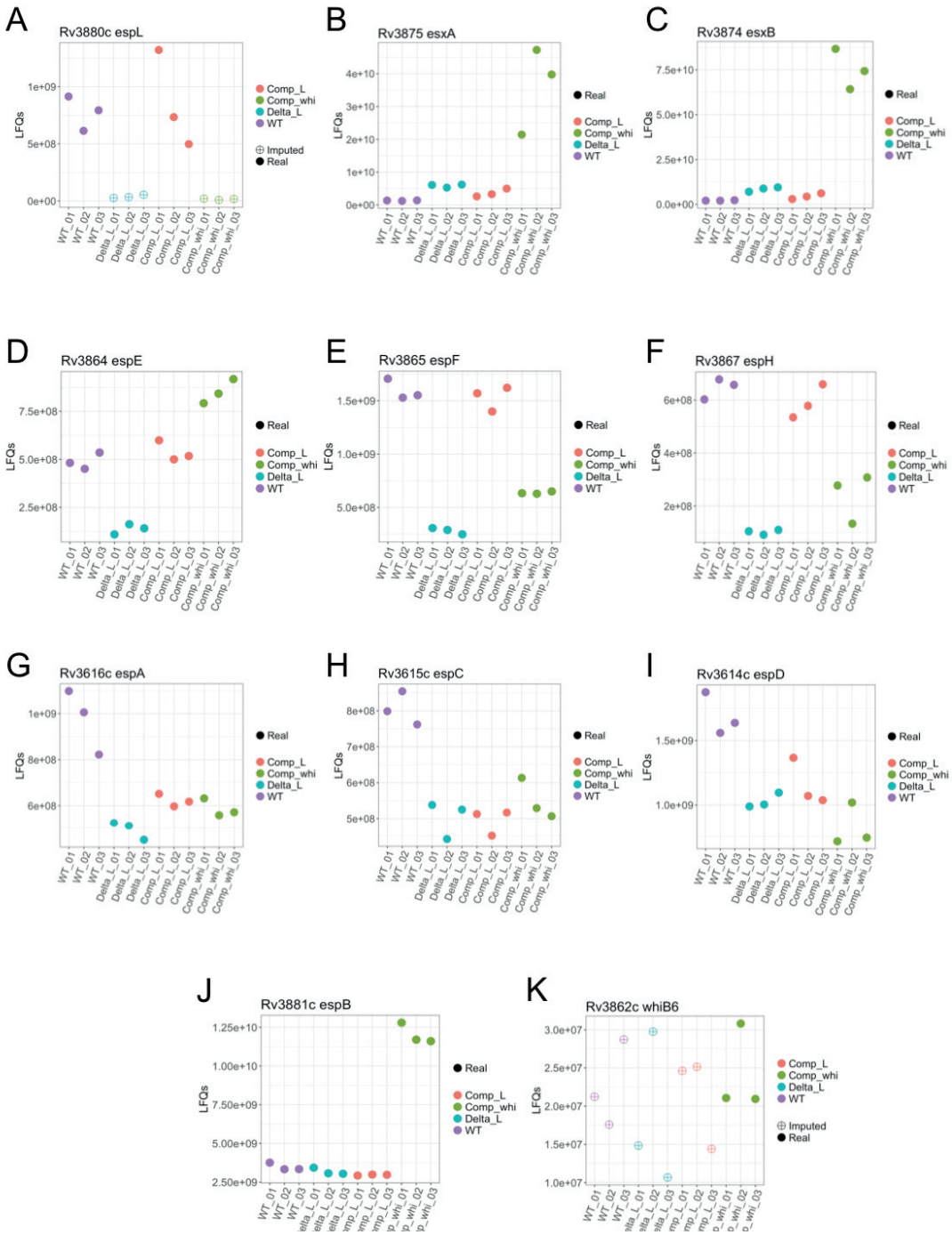

Figure 6. **Mass spectrometry analysis of protein abundance in the Δ*espL* mutant.** Total protein extracts were prepared in triplicate and subjected to Mass Spectrometry analysis. Each graph shows the abundance of the indicated protein in the three replicates in the various strains. WT: H37Rv. Delta_L: Δ*espL*. Comp_L: Δ*espL*/*espL* (complemented strain). Comp_whi: Δ*espL*/*whiB6* (strain expressing *whiB6 in trans*). Data are expressed as LFQs (Label Free Quantifications). Samples where EspL and WhiB6 could not be detected are labeled as "imputed".

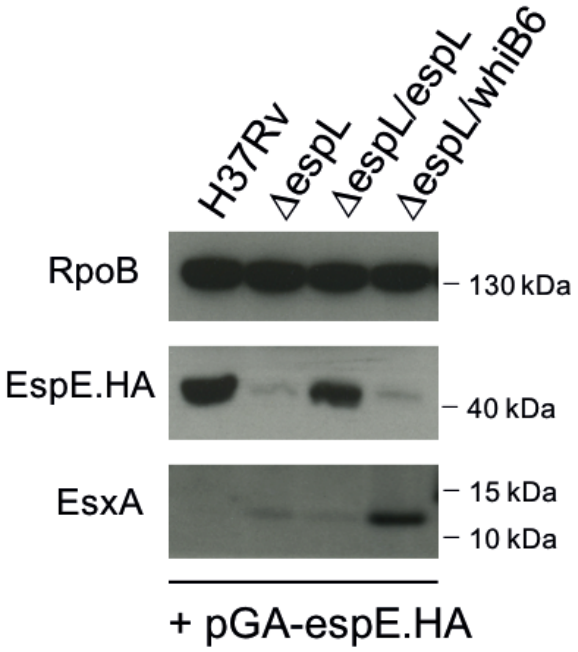

Figure 7. Validation of EspE levels in total cell lysates. Total cell lysates prepared from the indicated bacterial strains were analyzed by immunoblot. Note that all of the strains express HA-tagged EspE ectopically. EspE.HA was detected by immunodecoration with anti-HA antibodies. The experiment was repeated two times. One representative image is shown.

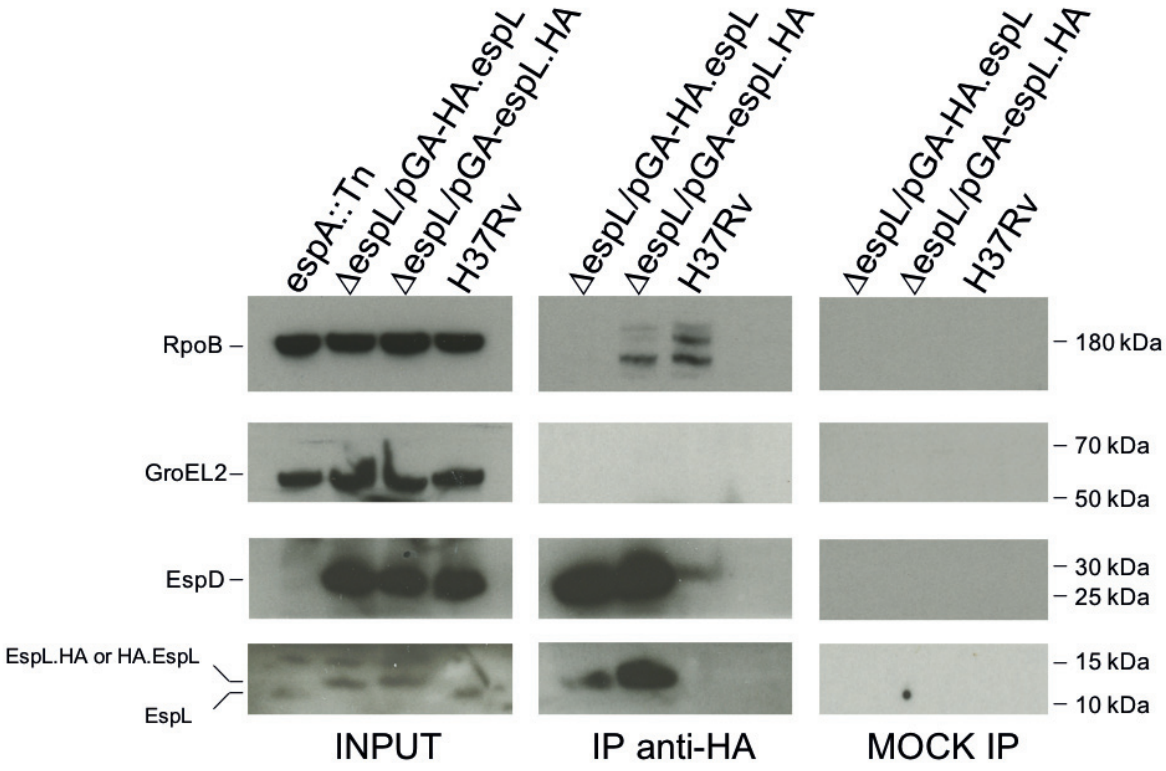

Figure 8. Interaction of EspL with EspD. Immunoprecipitation experiments on total protein extracts from the indicated strains were performed using anti-HA antibodies. Immunoprecipitated material was analyzed by immunoblot for detection of RpoB, GroEL2, EspL and EspD. The mock control was run in parallel without antibodies. The experiment was repeated three times. One representative image is shown.

3.8 SUPPORTING INFORMATION

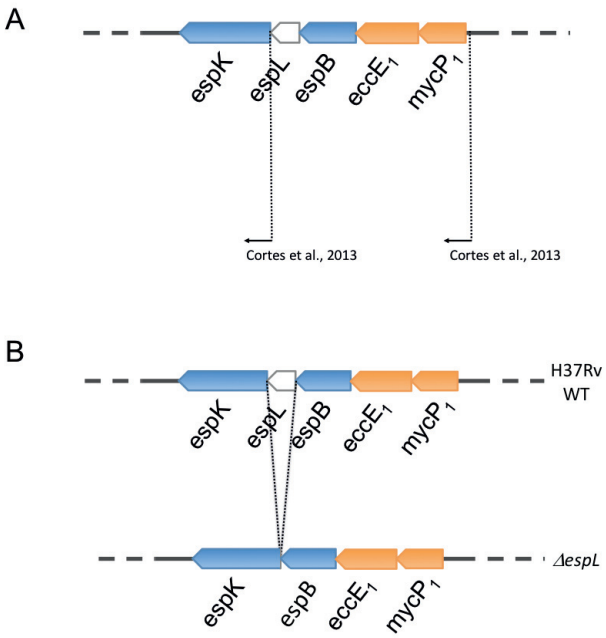

Figure S1. **Construction of Δ*espL* mutant. A)** Schematic representation of the H37Rv genomic region that encompasses the *espL* gene. The 5'-ends of the mRNAs detected by Cortes and colleagues [8] are indicate by bent arrows. **B)** Construction of the Δ*espL* mutant by allelic exchange. An unmarked deletion was introduced into the *espL* native locus

A

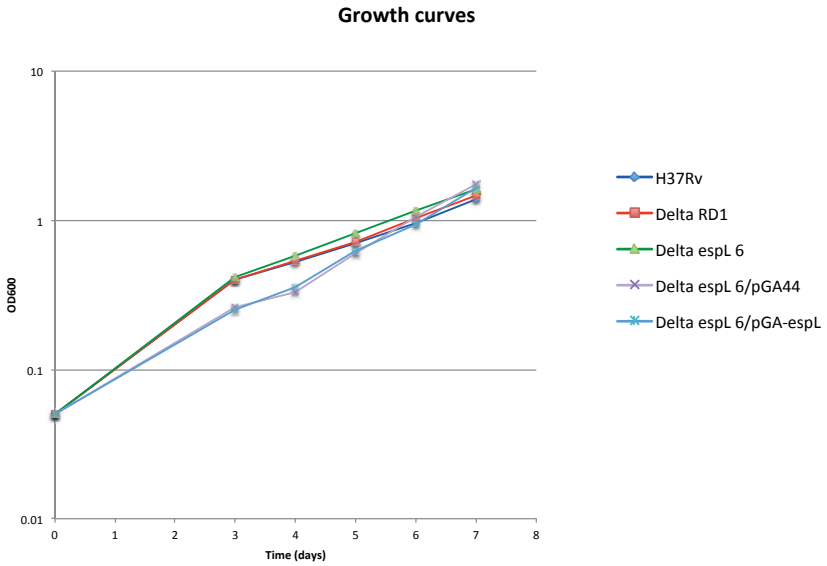

B

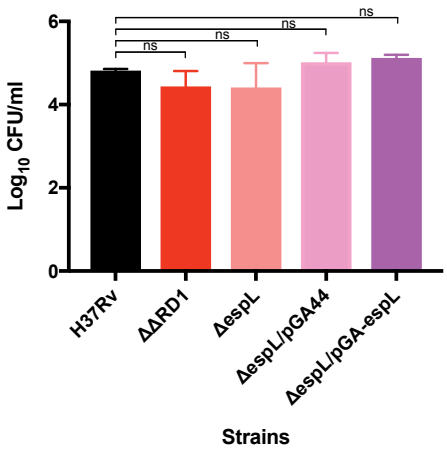

Figure S2. Phenotypic analysis of Δ*espL* mutant. A) Growth curves obtained by measuring the optical density at 600 nm of the different strains grown in 7H9 medium at 37°C with shaking. **B)** Uptake of various bacterial strains by THP-1 cells. The number of intracellular bacteria was evaluated by CFU 3 h post-infection. Data were expressed as the mean and SD of two independent replicates. ΔΔRD1 carries a deletion of the extended ESX-1 locus. ns, not significant in one-way ANOVA followed by Tukey's multiple comparison test.

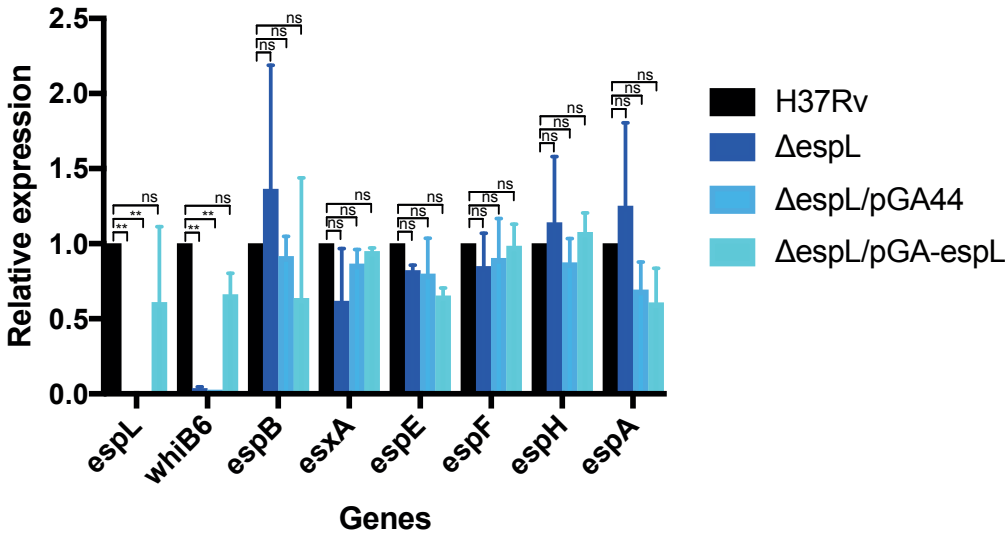

Figure S3. **Validation of RNA-seq results by qRT-PCR.** qRT-PCR analysis was performed on total RNA extracted from the indicated strains. Expression levels of the various genes were obtained from two independent replicates, normalized to the housekeeping gene *sigA* and expressed as relative to H37Rv. **, $p < 0.005$. ns, not significant in two-way ANOVA followed by Tukey's multiple comparison test.

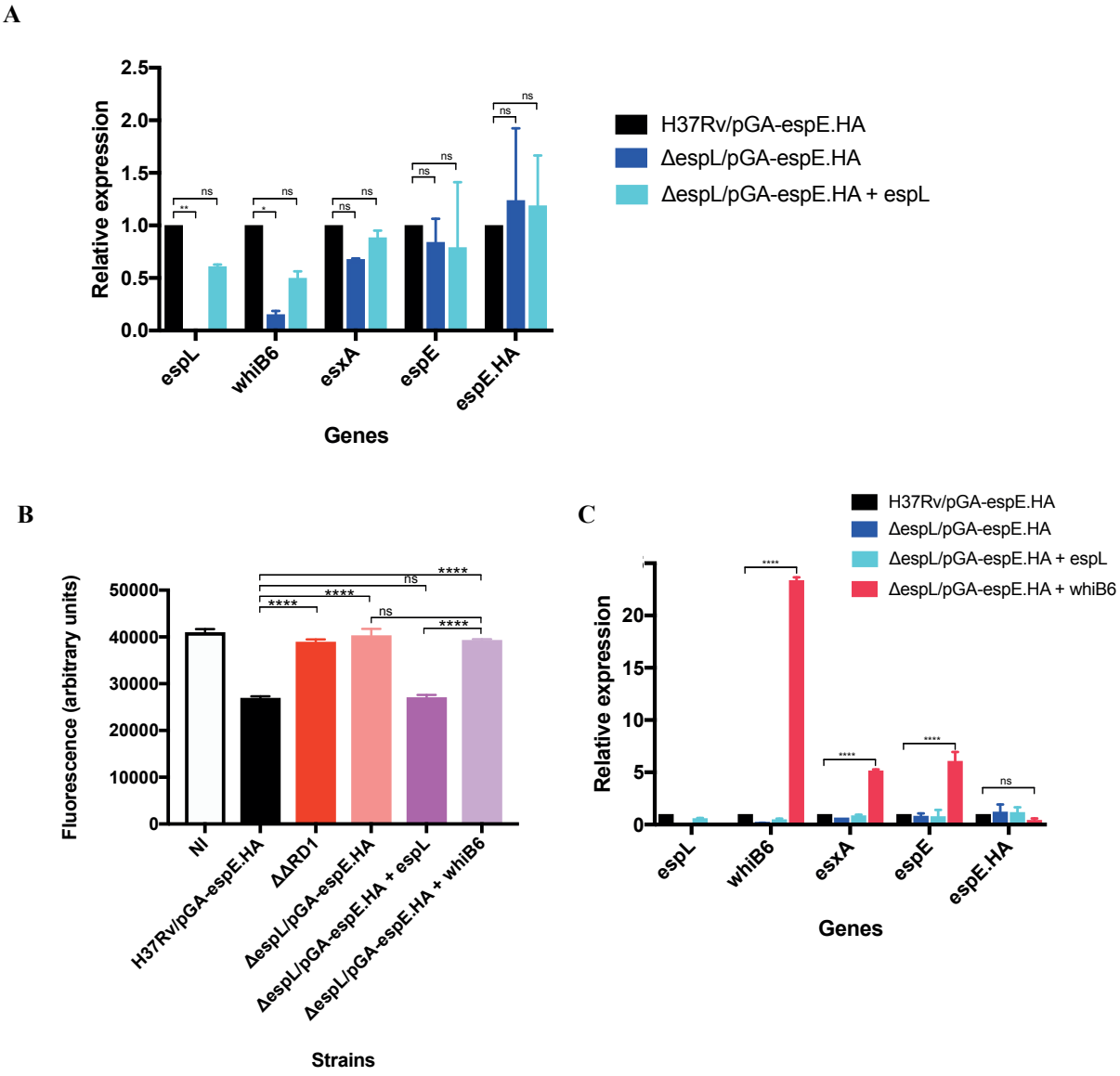

Figure S3. Expression of EspE.HA in H37Rv and in Δ*espL* mutant. A) qRT-PCR analysis of *espL*, *whiB6*, *esxA* and *espE* gene expression levels in different strains. Data were obtained from two independent replicates, normalized to the housekeeping gene *sigA* and expressed as relative to H37Rv. **, $p < 0.005$. ***, $p < 0.0005$. ns, not significant in two-way ANOVA followed by Tukey's multiple comparison test. **B)** Virulence of Δ*espL* mutant expressing *whiB6 in trans* compared to H37Rv, Δ*espL* and complemented strain in the THP-1 infection model. Note that all of the strains, except ΔΔRD1, express espE.HA. ΔΔRD1 carries a deletion of the extended ESX-1 locus. Fluorescence measurements directly correlate with THP-1 viability. Data were expressed as the mean and standard deviation (SD) of four independent replicates. NI: not infected control. ****, $p < 0.0001$. ns, not significant in one-way ANOVA followed by Tukey's multiple comparison test. **C)** qRT-PCR analysis of the expression levels of the indicated genes in different strains, upon ectopic expression of *whiB6*. Data were obtained from two independent replicates, normalized to the housekeeping gene *sigA* and expressed as relative to H37Rv. ****, $p < 0.0001$. ns, not significant in two-way ANOVA followed by Tukey's multiple comparison test.

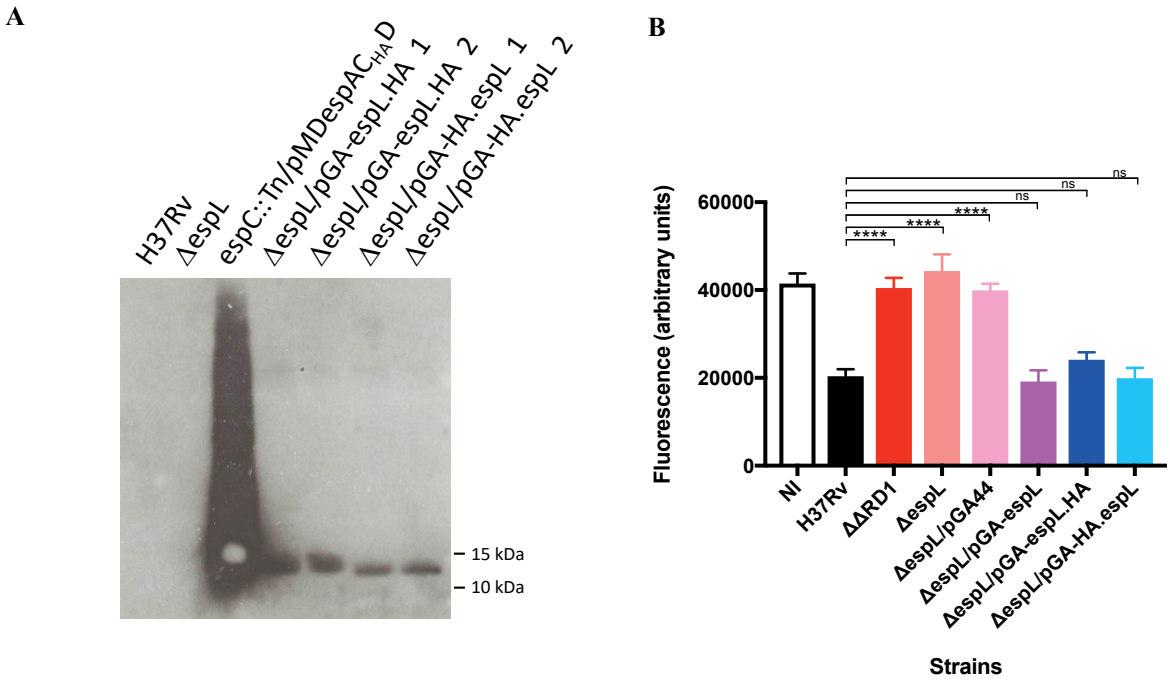

Figure S4. Validation of the expression of HA-tagged EspL and virulence analysis. A) Immunoblot showing expression of EspL.HA and HA.EspL in total protein extracts from two independent clones (1 and 2) obtained upon transformation of Δ*espL* with a plasmid encoding *espL*.HA or HA.*espL*, respectively. Protein extract from *espC::Tn*/pMD*espAC*$_{HA}$*D* [4] was used as a control. **B)** Virulence of Δ*espL* mutant complemented by *espL*.HA or by HA.*espL* compared to H37Rv, Δ*espL* and complemented strain in the THP-1 infection model. ΔΔRD1 carries a deletion of the extended ESX-1 locus. Fluorescence measurements directly correlate with THP-1 viability. Data were expressed as the mean and standard deviation (SD) of four independent replicates. NI: not infected control. ****, $p < 0.0001$. ns, not significant in one-way ANOVA followed by Tukey's multiple comparison test.

TABLES SUPPORTING INFORMATION

Table S1. Results of RNA-seq experiments (.xlsx) (available upon request).

Table S2. Results of Mass Spectrometry experiments (.xlsx) (available upon request).

Table S3. Results of mass spectrometry experiments. The Table reports the values obtained upon comparison of protein abundance in the indicated strains. Statistically significant differences are indicated by an asterisk (*). This Table represents an excerpt from S2 Table.H37Rv: wild type strain. Δ*espL*: *espL* knock-out mutant. Δ*espL/espL*: *espL* knock-out mutant complemented by *espL in trans*. Δ*espL/whiB6*: *espL* knock-out mutant expressing *whiB6 in trans*. nd: not determined. WhiB6 o.e.: WhiB6 overexpression.

Protein	Δ*espL* vs. H37Rv ratio	Δ*espL* vs. H37Rv p value and significance (*)	Δ*espL/espL* vs. Δ*espL* ratio	Δ*espL/espL* vs. Δ*espL* p value and significance (*)	Δ*espL/espL* vs. H37Rv ratio	Δ*espL/espL* vs. H37Rv p value and significance (*)	Δ*espL/whiB6* vs. Δ*espL* ratio	Δ*espL/whiB6* vs. Δ*espL* p value and significance (*)	Δ*espL/whiB6* vs. H37Rv ratio	Δ*espL/whiB6* vs. H37Rv p value and significance (*)
EspL	nd	nd	nd	nd	0.039	0.029	nd	nd	nd	nd
EsxA	2.131	4.636 *	-0.741	1.237	1.39	2.125	2.549	2.708 *	4.679	3.738 *
EsxB	1.957	3.804 *	-0.959	1.355	0.998	1.492	3.152	4.204 *	5.109	5.509 *
EspE	-1.848	3.277 *	1.986	3.368 *	0.138	0.569	2.647	3.924 *	0.799	2.961
EspF	-2.506	4.764 *	2.444	4.593 *	-0.062	0.308	1.184	3.677	-1.322	4.852 *
EspH	-2.673	5.039 *	2.541	4.553 *	-0.132	0.579	1.152	1.383	-1.521	1.778*
EspA	-0.974	2.626	0.335	1.882	-0.639	2.112	0.250	1.321	-0.724	2.230
EspC	-0.688	2.592	-0.021	0.065	-0.708	3.038	0.134	0.471	-0.554	2.346
EspD	-0.712	2.825	0.160	0.527	-0.552	1.687	-0.340	0.932	-1.052	2.349
EspB	-0.128	0.732	-0.100	0.808	-0.228	1.773	1.918	4.924 *	1.790	4.793 *
WhiB6	nd	nd	nd	nd	nd	nd	WhiB6 o.e.	WhiB6 o.e.	WhiB6 o.e.	WhiB6 o.e.

S4 Table.

Table S4. Table. Immunoprecipitation experiment analyzed by mass spectrometry. The Table reports peptide counts for the indicated proteins in the samples obtained upon immunoprecipitation (IP) with anti-HA antibodies. The total protein extract (Input) was used as a control. EspL.HA, HA.EspL and EspD are indicated in bold.MW: molecular weight. H37Rv: wild type strain. Δ*espL*: *espL* knock-out mutant. Δ*espL*/*espL*.HA: *espL* knock-out mutant complemented by HA-tagged *espL* (HA at C-terminus). Δ*espL*/HA.*espL*: *espL* knock-out mutant complemented by HA-tagged *espL* (HA at N-terminus).

Protein	MW (kDa)	Counts Input Δ*espL*/HA.*espL*	Counts IP H37Rv	Counts IP Δ*espL*	Counts IP Δ*espL*/*espL*.HA	Counts IP Δ*espL*/HA.*espL*
GroEL2	57	121	16	48	58	45
DnaK	67	19	8	8	13	11
EspL.HA or HA.EspL	**14**	**3**	**4**	**11**	**125**	**187**
RpoB	129	3	19	5	5	2
RpoC	147	4	4	0	18	2
SigA	58	3	27	11	16	14
Tuf	44	11	0	20	8	8
mIHF	21	10	0	9	3	0
GyrA	92	1	5	11	0	0
RplK	15	3	0	6	0	2
EspD	**20**	**0**	**5**	**0**	**11**	**35**
EsxB	11	5	0	0	5	0

Table S5. Bacterial strains used in this study.

Bacterial species	Strain name	Description or genotype	Reference
M. tuberculosis	H37Rv	Wild type strain	[1]
	H37Rv/pGA44	H37Rv transformed with empty vector pGA44. Plasmid integrated at L5 *attB* site.	This study
	H37Rv/pGA-*espE*.HA	H37Rv expressing HA-tagged EspE. Plasmid integrated at L5 *attB* site.	This study
	ΔΔRD1	H37Rv background. Deletion of extended ESX-1 locus.	[2]
	Δ*espL*	H37Rv background. Deletion of *espL*.	This study
	Δ*espL*/pGA44	*espL* knockout transformed with empty vector pGA44. Plasmid integrated at L5 *attB* site.	This study
	Δ*espL*/pGA-*espL*	*espL* knockout complemented by *espL* expressed *in trans*.	This study
	Δ*espL*/pGA-*whiB6*	*espL* knockout transformed with vector expressing *whiB6*.	This study
	Δ*espL*/pGA-*espL*.HA	*espL* knockout complemented by *espL*.HA expressed *in trans*.	This study
	Δ*espL*/pGA-HA.*espL*	*espL* knockout complemented by HA.*espL* expressed *in trans*.	This study
	Δ*espL*/pGA-*espE*.HA	*espL* knockout transformed with vector expressing *espE*.HA.	This study
	Δ*espL*/pGA-*espE*.HA+*pmycP1-espL*	*espL* knockout transformed with vector expressing *espE*.HA and complemented by *espL* expressed *in trans*.	This study
	Δ*espL*/pGA-*espE*.HA+*pmycP1-whiB6*	*espL* knockout transformed with vector expressing *espE*.HA and *whiB6*.	This study
	espA::Tn	Erdman background. Transposon insertion in *espA*.	[3]
	espC::Tn/pMD*espAC*$_{HA}$*D*	Erdman background. Transposon insertion in *espC*. Complemented by pMD31-derived vector carrying *espA-espC-espD*. EspC is HA-tagged.	[4]
E. coli	TOP10	F- *mcrA* Δ(*mrr-hsd*RMS-*mcr*BC) Φ80*lac*ZΔM15 Δ *lac*X74 *rec*A1 *ara*D139 Δ(*araleu*)7697 *gal*U *gal*K *rps*L (StrR) *end*A1 *nup*G	Invitrogen

Table S6. Plasmids used in this study.

Plasmid name	Description	Reference
pJG1100	Suicide vector for mutant construction, Hyg^R, Kan^R, *sacB*.	[5]
pGA44	Integrative vector at L5 *attB* site, PTR promoter, Str^R/$Spect^R$.	[6]
pGA80	pMV261-derived vector, carrying the L5 *int* gene for expression *in trans*, lacking oriM, Kan^R.	[6]
pJG1100-*espL*-UP/DOWN	Suicide vector for mutant construction derived from pJG1100, carrying 1 kbp upstream and downstream regions of *espL*.	This study
pGA44-*espL*	Vector for complementation of Δ*espL* mutant strain. Derived from pGA44, *espL* is expressed by the PTR promoter.	This study
pGA44-*whiB6*	Vector for expression of *whiB6*. Derived from pGA44, *whiB6* is expressed by the PTR promoter.	This study
pGA44-*espL*.HA	Vector for complementation of Δ*espL* mutant strain. Derived from pGA44, *espL*.HA (tag at C-terminus) is expressed by the PTR promoter.	This study
pGA44-HA.*espL*	Vector for complementation of Δ*espL* mutant strain. Derived from pGA44, HA.*espL* (tag at N-terminus) is expressed by the PTR promoter.	This study
pGA44-*espE*.HA	Vector for expression of *espE*.HA (tag at C-terminus). Derived from pGA44, *espE*.HA is expressed by the PTR promoter.	This study
pGA44-*espE*.HA+*pmycP1-espL*	Vector for expression of *espE*.HA (tag at C-terminus). Derived from pGA44, *espE*.HA is expressed by the PTR promoter. *espL* is expressed by the *mycP1* promoter.	This study
pGA44-*espE*.HA+*pmycP1-whiB6*	Vector for expression of *espE*.HA (tag at C-terminus). Derived from pGA44, *espE*.HA is expressed by the PTR promoter. *whiB6* is expressed by the *mycP1* promoter.	This study

BIBLIOGRAPHY SUPPORTING INFORMATION

1. Cole ST, Brosch R, Parkhill J, Garnier T, Churcher C, Harris D, et al. Deciphering the biology of Mycobacterium tuberculosis from the complete genome sequence. Nature. 1998;393: 537–544. doi:10.1038/31159

2. Bottai D, Majlessi L, Simeone R, Frigui W, Laurent C, Lenormand P, et al. ESAT-6 secretion-independent impact of ESX-1 genes espF and espG1 on virulence of Mycobacterium tuberculosis. J Infect Dis. 2011;203: 1155–1164. doi:10.1093/infdis/jiq089

3. Chen JM, Boy-Röttger S, Dhar N, Sweeney N, Buxton RS, Pojer F, et al. EspD is critical for the virulence-mediating ESX-1 secretion system in Mycobacterium tuberculosis. J Bacteriol. 2012;194: 884–893. doi:10.1128/JB.06417-11

4. Lou Y, Rybniker J, Sala C, Cole ST. EspC forms a filamentous structure in the cell envelope of M ycobacterium tuberculosis and impacts ESX-1 secretion: Filamentous structure formation by EspC. Mol Microbiol. 2017;103: 26–38. doi:10.1111/mmi.13575

5. Gomez JE, Bishai WR. whmD is an essential mycobacterial gene required for proper septation and cell division. Proc Natl Acad Sci U S A. 2000;97: 8554–8559. doi:10.1073/pnas.140225297

6. Kolly GS, Boldrin F, Sala C, Dhar N, Hartkoorn RC, Ventura M, et al. Assessing the essentiality of the decaprenyl-phospho- D -arabinofuranose pathway in M ycobacterium tuberculosis using conditional mutants: Druggability of the M. tuberculosis DPA pathway. Mol Microbiol. 2014;92: 194–211. doi:10.1111/mmi.12546

7. Bange FC, Collins FM, Jacobs WR. Survival of mice infected with Mycobacterium smegmatis containing large DNA fragments from Mycobacterium tuberculosis. Tuber Lung Dis Off J Int Union Tuberc Lung Dis. 1999;79: 171–180. doi:10.1054/tuld.1998.0201

8. Cortes T, Schubert OT, Rose G, Arnvig KB, Comas I, Aebersold R, et al. Genome-wide Mapping of Transcriptional Start Sites Defines an Extensive Leaderless Transcriptome in Mycobacterium tuberculosis. Cell Rep. 2013;5: 1121–1131. doi:10.1016/j.celrep.2013.10.031

1. Cole ST, Brosch R, Parkhill J, Garnier T, Churcher C, Harris D, et al. Deciphering the biology of Mycobacterium tuberculosis from the complete genome sequence. Nature. 1998;393: 537–544. doi:10.1038/31159

2. Bottai D, Majlessi L, Simeone R, Frigui W, Laurent C, Lenormand P, et al. ESAT-6 secretion-independent impact of ESX-1 genes espF and espG1 on virulence of Mycobacterium tuberculosis. J Infect Dis. 2011;203: 1155–1164. doi:10.1093/infdis/jiq089

3. Chen JM, Boy-Röttger S, Dhar N, Sweeney N, Buxton RS, Pojer F, et al. EspD is critical for the virulence-mediating ESX-1 secretion system in Mycobacterium tuberculosis. J Bacteriol. 2012;194: 884–893. doi:10.1128/JB.06417-11

4. Lou Y, Rybniker J, Sala C, Cole ST. EspC forms a filamentous structure in the cell envelope of M ycobacterium tuberculosis and impacts ESX-1 secretion: Filamentous structure formation by EspC. Mol Microbiol. 2017;103: 26–38. doi:10.1111/mmi.13575

5. Gomez JE, Bishai WR. whmD is an essential mycobacterial gene required for proper septation and cell division. Proc Natl Acad Sci U S A. 2000;97: 8554–8559. doi:10.1073/pnas.140225297

6. Kolly GS, Boldrin F, Sala C, Dhar N, Hartkoorn RC, Ventura M, et al. Assessing the essentiality of the decaprenyl-phospho- D -arabinofuranose pathway in M ycobacterium tuberculosis using conditional mutants: Druggability of the M. tuberculosis DPA pathway. Mol Microbiol. 2014;92: 194–211. doi:10.1111/mmi.12546

7. Bange FC, Collins FM, Jacobs WR. Survival of mice infected with Mycobacterium smegmatis containing large DNA fragments from Mycobacterium tuberculosis. Tuber Lung Dis Off J Int Union Tuberc Lung Dis. 1999;79: 171–180. doi:10.1054/tuld.1998.0201

8. Cortes T, Schubert OT, Rose G, Arnvig KB, Comas I, Aebersold R, et al. Genome-wide Mapping of Transcriptional Start Sites Defines an Extensive Leaderless Transcriptome in Mycobacterium tuberculosis. Cell Rep. 2013;5: 1121–1131. doi:10.1016/j.celrep.2013.10.031

Chapter 4

Investigation of the transcriptional regulator WhiB6 of *Mycobacterium tuberculosis*

Paloma Soler[1], Claudia Sala[1], Andrej Benjak[1], Stewart T. Cole[2]

[1] Global Health Institute, Ecole Polytechnique Fédérale de Lausanne, Lausanne, Switzerland.
[2] Current address: Institut Pasteur, Paris, France.

4.1 ABSTRACT

The specialised ESX-1 secretion system is regulated by multiple transcriptional regulators such the redox sensor WhiB6. A single nucleotide insertion in the promoter region of whiB6 downregulates its expression but also the expression of various ESX-1 genes. In consequence, the intracellular levels and secretion of EsxA are decreased. This single nucleotide insertion is exclusively found in the H37R strain derivatives, H37Rv and H37Ra. To gain a deeper knowledge about the role of WhiB6 in regulating the ESX-1 secretion system, we have generated a Δ*whiB6* mutant by recombineering in *M. tuberculosis*. The absence of WhiB6 markedly decreased the ability of the mutant to induce cell death, suggesting that WhiB6 is required for full virulence in *M. tuberculosis*.

4.2 INTRODUCTION

In Chapter 3, we demonstrated that deletion of the *espL* gene results in downregulation of *whiB6* expression and affects ESX-1 function. To further study this mechanism of regulation, we examined the impact of WhiB6 on ESX-1 activity.

As a facultative intracellular pathogen, *M. tuberculosis* needs to adapt to a variety of environmental stresses. To avoid intracellular killing and survive inside the host, *M. tuberculosis* secretes virulence factors through the specialized ESX-1 system. Some ESX-1 substrates are potent immunodominant antigens and their secretion needs to be tightly regulated to avoid detrimental effects on bacteria [1]. Although the regulation of the ESX-1 system is largely unknown, its secretion activity is controlled by a co-dependent export mechanism and also by several transcriptional factors [2]. For instance, the transcriptional regulator WhiB6, a member of the WhiB family of redox sensor proteins, can tightly regulate transcription of *esxA*, *esxB*, or *espE* [3]. On the *M. tuberculosis* chromosome, WhiB6 is localized upstream of the ESX-1 cluster and its expression is controlled by the master regulator PhoP [4]. Comparison of the genomes of *M. tuberculosis* laboratory strains with those of numerous clinical isolates revealed that the promoter region of *whiB6* carries a point mutation that is exclusively found in the H37R strain derivatives, H37Rv and H37Ra [5]. This polymorphism consists of the insertion of a single G 74 bp upstream of *whiB6* start codon, which overlaps the PhoP binding site. The extra base alters PhoP binding affinity and leads to downregulation of *whiB6* expression, which ultimately results in different EsxA levels in H37Rv as compared to other isolates. Importantly, when the H37Rv strain is complemented with an episomal copy of *whiB6* that does not carry the extra base in the promoter region, production and secretion of EsxA is restored to the levels of clinical strains [5].

The link between WhiB6 and ESX-1 was further studied in the fish pathogen *Mycobacterium marinum*. In this bacterium, disruption of *whiB6* resulted in lower mRNA levels of *esxA* and *esxB*, reduced ESX-1-protein secretion and decreased hemolytic activity compared to the WT strain [3]. Moreover, chromatin immunoprecipitation experiments (ChIP) demonstrated that WhiB6 binds to the promoter regions of *espA*, *espE*, $eccA_1$ and *whiB6*, providing evidence of autoregulation and direct transcriptional control of ESX-1 substrates and components [3]. WhiB6 has a redox-sensitive Fe-S cluster which is required to regulate ESX-1-related genes. When this Fe-S cluster is disrupted by continuous exposure to O_2, ESX-1 genes are

downregulated [3]. Thereby, this transcriptional regulator was hypothesized to sense redox change in the environment and mediate an appropriate transcriptional response to modulate ESX-1 secretion [3]. Recently, an additional model was proposed for *M. marinum* where expression of *whiB6* and, therefore, of some ESX-1 genes, is controlled by the presence of the ESX-1 membrane complex [6]. WhiB6 may also sense the presence of the secretory machinery and consequently regulate ESX-1 gene expression.

4.3 RESULTS

Mutant construction

To study the role of WhiB6 on ESX-1 secretion, we tried to generate *whiB6* mutants in *M. tuberculosis* by recombineering [7]. Inspired by the work of Solans and colleagues [5], we first planned to remove the point mutation that is naturally present in the *whiB6* promoter of H37Rv and absent in most of the other *M. tuberculosis* strains. This extra base leads to downregulation of *whiB6* expression and eventually lower EsxA levels [5]. To prove that the mutation in the promoter region is the primary cause of *whiB6* downregulation, we also sought to introduce the extra nucleotide in the *M. tuberculosis* Erdman strain. To obtain these modifications in the chromosome, we designed a pair of oligonucleotides (Table 1) and followed the recombineering procedure as described in Material and Methods. Despite several attempts, this approach was unsuccessful probably due to the highly stable hairpin structures found in these oligonucleotides (Table 1). These secondary structures may also occur in the promoter region of *whiB6* in both H37Rv and Erdman, thus making recombination complicated and infrequent. As an alternative strategy, we designed *whiB6* null mutants by introducing two stop codons at the beginning of the *whiB6* coding sequence (CDS). In this case, the oligonucleotide does not form stable hairpin structures (Table 1). One of the challenges faced in this approach was the selection of clones that underwent homologous recombination. Modifying *whiB6* does not result in an easily detectable phenotype such as drug resistance or morphological changes. Therefore, PCR screening followed by Sanger sequencing was used to identify positive recombinants. Of the 34 colonies screened, only one carried the desired mutations (efficiency of recombination 2.9%). This mutant was further validated by whole-genome sequencing which confirmed the presence of two stop codons at the beginning of *whiB6* CDS and the absence of additional mutations in the genome. The resulting mutant, named Δ*whiB6*, was

complemented with an integrative plasmid carrying *whiB6* bearing an HA tag coding sequence at the 3'-end. This complemented derivative has a copy of *whiB6* expressed under the control of a constitutive promoter. Transformation with the empty vector was also performed as a control.

WhiB6 is required for *M. tuberculosis*-mediated host cell lysis

M. tuberculosis requires a functional ESX-1 system to mediate host-cell death and survive inside the host [8]. To investigate the impact of WhiB6 on ESX-1 function, we analysed the ability of the mutant to induce cell lysis in cultured macrophages. THP-1 human cells were infected with the wild type (WT), the *ΔwhiB6* mutant and the complemented HA variant and, after three days, macrophage survival was evaluated. In the presence of the WT strain, THP-1 survival was drastically reduced compared to uninfected cells. However, when macrophages were infected with the *ΔwhiB6* mutant, the THP-1 survival level was substantially higher, indicating that this mutant has an impaired cytolytic activity. In contrast, when the *ΔwhiB6* mutant is complemented with *whiB6-HA*, cell survival was significantly compromised and close to that observed with the WT (Fig. 1). To exclude the possibility of a negative impact on macrophage survival due to the presence of the integrative plasmid, the Δ*whiB6* mutant transformed with an empty vector was also tested. This strain displayed a similar phenotype to the Δ*whiB6* mutant (Fig. 1) demonstrating that the plasmid used for complementation did not affect macrophage viability. Overall, these data suggest that *whiB6* is needed to mediate macrophage cell lysis and underline the critical role of this transcription factor in the virulence response of *M. tuberculosis ex vivo*.

4.4 DISCUSSION

ESX-1 secretion is controlled by several mechanisms including transcriptional regulation. To gain deeper knowledge into the role played by WhiB6, we generated a *ΔwhiB6* knockout mutant in *M. tuberculosis*. During the construction of the mutant, we realized that the promoter of *whiB6* is not an amenable region to introduce point mutations probably due to the presence of highly stable stem-loops. The presence of these structures might interfere with recombination events explaining why we could only obtain a chromosomal modification in the *whiB6* CDS.

ΔwhiB6 showed impaired ability to cause cell lysis compared to the WT or to the complemented strain. This attenuated phenotype was also observed with the mutant carrying the empty vector used for complementation. As *M. tuberculosis*-mediated cytolysis depends on a functional ESX-1 system, it is plausible that EsxA and other ESX-1-related proteins are not secreted in the absence of WhiB6. This assumption agrees with previous observations in *M. marinum* where reduced levels of ESX-1 secretion and hemolytic activity were observed when the *whiB6* gene was disrupted [3]. Interestingly, complementation of the mutant with a single copy of *whiB6* induced a stronger cytolytic response compared to the WT. This effect may be due to the constitutive expression of *whiB6* by the PTR promoter, which provides higher levels of mRNA compared to the H37Rv strain (results in Chapter 3). Consequently, it is likely that ESX-1 genes regulated by WhiB6 are upregulated as well as ESX-1 secretion activity. Although no experimental evidence on gene expression and protein secretion are provided here, a similar outcome was observed when H37Rv was transformed with a copy of *whiB6* from a clinical isolate [5]. In that case, *whiB6* was upregulated in H37Rv and bacteria produced and secreted larger amounts of EsxA [5]. The cytolytic phenotype displayed by the *whiB6-HA* complemented mutant also indicates that the addition of the HA tag at the C-terminal part of the protein did not interfere with WhiB6 activity. The presence of this tag in a functional mutant can be useful for future research aimed to study the binding region of WhiB6 by ChIP or protein interactions by immunoprecipitation.

A link between ESX-1 components and *whiB6* expression has been previously studied [6]. Depletion of EccCb1 in *M. marinum* was found to strongly downregulate *whiB6* expression. In the same direction, we also demonstrated that deletion of *espL* resulted in downregulation of *whiB6* (Chapter 3). These observations suggest that ESX-1 could be regulated by a feedback control mechanism where the presence of ESX-1 components in the bacterial membrane may regulate expression of ESX-1 related genes through WhiB6. In contrast to this hypothesis, deletion of the core components $eccE_1$ and $mycP_1$ did not impact *whiB6* expression or any ESX-1 genes (Chapter 2). As EccCb1 and EspL were shown to interact with and stabilise ESX-1 substrates [9], it is likely that WhiB6 may need to interact with specific ESX-1 proteins or even with the ESX-1 complex to mediate a transcriptional response and therefore regulate ESX-1 secretion.

4.5 MATERIALS AND METHODS

Bacterial cultures

M. tuberculosis was routinely grown in 7H9 broth (supplemented with 0.2% glycerol, 10% ADC, 0.05% Tween-80) or on 7H10 agar (supplemented with 0.5% glycerol and 10% OADC). *Escherichia coli* TOP10 or chemically-competent *E. coli* DH5α cells were used for cloning and plasmid propagation and were grown on LB broth or agar.

Mutant construction by recombineering

Generation of point mutations in *M. tuberculosis* H37Rv was done by a recombineering method [10, 11]. First, a 70-mer oligonucleotide corresponding to the lagging strand was designed with the mutation in the middle of the sequence (Table 1). Then, H37Rv transformed with pJV53, a plasmid that codes for a mycobacterial phage recombination system (Che9 RecET), was grown to log phase (OD_{600} of 0.8) in 7H9 medium containing kanamycin (20 μg/ml). Subsequently, the recombination system encoded by pJV53 was induced with 0.2% acetamide for 8h before addition of 0.2 M glycine. Bacteria were incubated for additional 16h and then collected to prepare competent cells. 500 ng of 70-bp single-stranded oligonucleotide containing the desired mutation was transformed by electroporation with plasmid pYUB412 (0.1μg) [12] which was used for counter-selection. After incubation for 3 days, transformants were selected on 7H10 agar plates containing hygromycin (50 μg/ml). PCR followed by Sanger sequencing were used to identify the presence of single-nucleotide polymorphisms (SNPs) in the chromosome.

DNA extraction and whole-genome sequencing

The *M. tuberculosis* Δ$mycP_1$-$eccE_1$ mutant was grown in 10 mL 7H9 broth to OD_{600} 0.8. Bacteria were harvested by centrifugation and DNA was extracted using the QIAmp UCP pathogen kit (Qiagen) as described previously [13]. DNA was quantified using the Qubit dsDNA HS Assay Kit and the Qubit 2.0 Fluorometer (Thermo Fisher Sc.). Ilumina libraries were prepared using the Kapa Hyper prep kit as described [13]. Briefly, 1 μg of extracted DNA was sonicated to obtain 400 bp long fragments with the S220 Covaris (Covaris) using the manufacturer's protocol and purified using 1.8X AMPure beads

(ThermoFisher Sc.) and eluted in 50 µL of Tris-HCl 10mM. Sequencing libraries were synthesised with the Kapa Hyper prep kit (Kapa Biosystems) according to the manufacturer's instructions and an adapter stock of 15 µM of PentAdaptersTM (PentaBase) was used to barcode the library. After the final amplification step, libraries were quantified using Qubit dsDNA BR Assay Kit (Thermo Fisher Sc) and the fragment size was assessed on a Fragment Analyzer (Advanced Analytical Technologies). Finally, libraries were multiplexed and sequenced as 100 base-long single-end reads on an Illumina HiSeq 2500 instrument. Reads were adapter- and quality-trimmed with Trimmomatic v0.33 [14] and mapped onto the *M. tuberculosis* H37Rv reference genome (RefSeq NC_000962.3) using Bowtie2 v2.2.5 [15].

Complemented derivative constructions

The integrative pGA44 vector [16] was used to construct the *whiB6-HA* complemented derivative. The *whiB6* CDS was PCR amplified from *M. tuberculosis* H37Rv genomic DNA using oligonucleotides PS-135 and PS-136 (Table 1). The PCR fragments were cloned in-frame under the control of the PTR promoter, into the AvrII and PacI sites. The plasmid was checked by Sanger sequencing and was transformed into competent *M. tuberculosis ΔwhiB6* cells together with pGA80 [16] which provided the L5 integrase. Transformants were selected on 7H10 agar containing streptomycin (20 µg/ml). The empty pGA44 vector was also transformed. The plasmids used in this study are listed in Table 2.

Macrophage survival

Human monocytic THP-1 cells were grown in RPMI medium supplemented with 10% FBS. Monocytes were prepared at a concentration of $2x10^6$ cells/ml and differentiated into macrophages using phorbol-12-myristate-13-acetate (PMA) at a final concentration of 4 nM. Subsequently, 10^5 cells/well (50 µl/well) were pipetted into a 96 well-plate, the plate was sealed with a gas-permeable film and incubated at 37°C with 5% CO_2 for 18h. Medium containing PMA was removed and replaced with 50 µl of new pre-warm RPMI medium. Bacteria were grown to OD_{600} 0.4-0.8, washed, resuspended in 7H9 broth to an OD_{600} of 1 (3×10^8 bacteria/ml) and diluted in RPMI medium at a concentration of 10^7 bacteria/ml. THP-1 cells were then infected at a multiplicity of infection (MOI) of 5 (50 µl/well of 10^7 bacteria/ml in RPMI) and incubated for three days at 37°C with 5% CO_2. Afterwards, 5 µl (1:20) of PrestoBlue cell viability reagent (Life Technologies) was added to each well,

the plate incubated for 30 min at 37°C and the fluorescence measured using a Tecan M200 instrument (excitation/emission wavelength of 560/590 nm). Fluorescence values of three biological replicates (for each strain tested) were analyzed in GraphPad Prism (version 5) and significant differences between the conditions determined using one-way ANOVA followed by Turkey's multiple comparison test.

4.6 FIGURES AND TABLES

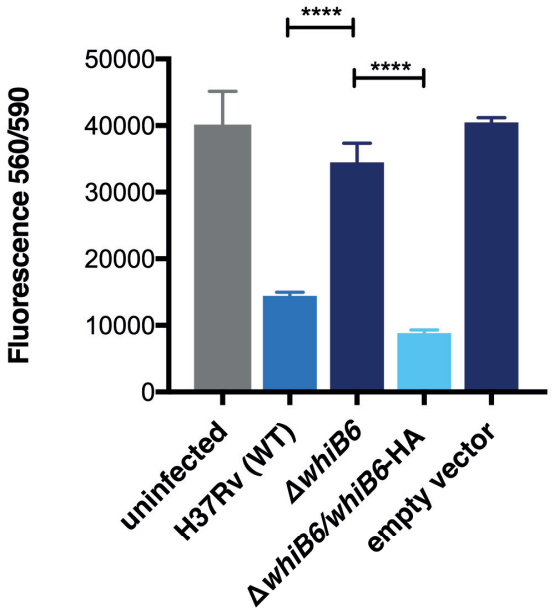

Figure 1. Δ*whiB6* displays an impaired cytolytic effect. Cell viability of THP-1 human macrophages at 72h post-infection. Uninfected cells were used as a control for macrophage survival and the H37Rv WT strain as a positive control for M. tuberculosis-mediated cell-death. **** p-value<0.0001

Table 1 Primers used in this study.

Primer name	Sequence 5'→ 3'	Hairpin ΔG (kcal.mole-1)[a]	Information
PS-39	ctatgccctggtactcggcggtgcgcgcactag**AC**tc ggagctcgccgaaccggagccgcagcaccgct	-5.92	To eliminate the extra base (G) present in the *whiB6* promoter of H37Rv strain.
PS-40	agcggtgctgcggctccggttcggcgagctccga**GT** ctagtgcgcgcaccgccgagtaccagggcatag	-6.23	To eliminate the extra base (G) present in the *whiB6* promoter of H37Rv strain.
PS-45	ctatgccctggtactcggcggtgcgcgcactaga**G**ct cggagctcgccgaaccggagccgcagcaccgct	-7.82	To introduce the extra base (G) in the *whiB6* promoter of Erdman strain.
PS-46	agcggtgctgcggctccggttcggcgagctccgag**C**t ctagtgcgcgcaccgccgagtacc agggcatag	-7.26	To introduce the extra base (G) in the *whiB6* promoter of Erdman strain.
PS-138	agcgttgcaggttgtagcctctgccgcgaaagc**T**tatc **A**cattaaccatagcgatgcaacagtttcctc	-1.9	To introduce two stop codons in the 2nd and 3rd codons of *whiB6* CDS.
PS-135	atatcctaggatgcgatacgctttcgcggcagaggctac aac	NA	To clone *whiB6-HA* into pGA44. AvrII restriction site.
PS-136	gcattaattaatcaagcgtaatctggaacatcgtatgggt atgccgattgggcagac	NA	To clone *whiB6-HA* into pGA44. PacI restriction site.

[a] Hairpin ΔG was calculated using OligoAnalyzer 3.1 [17].

Table 2 Plasmids used in this study

Plasmid name	Description	Reference
pJV53	Recombineering plasmid, replicative, expression of gp60 and gp61 by acetamide-inducible promoter. Kan^R	(van Kessel et al. 2008)
pGA44	Integrative vector at L5 attB site, carrying the TET-PIP OFF expression system, Str^R	(Kolly et al. 2014)
pGA80	pMV261-derived vector, carrying the L5 *int* gene for expression *in trans*, lacking oriM, Kan^R	(Kolly et al. 2014)
pPS14	pGA44-derived vector carrying *whiB6-HA* under the PTR promoter, integrative, Str^R	In this study
pYUB412	Integrative mycobacteria shuttle vector, L5 attB site, Hyg^R	(Bange et al. 1999)

4.7 BIBLIOGRAPHY

1. Lazarevic V, Nolt D, Flynn JL. Long-term control of Mycobacterium tuberculosis infection is mediated by dynamic immune responses. J Immunol. 2005;175:1107–17.

2. Gröschel MI, Sayes F, Simeone R, Majlessi L, Brosch R. ESX secretion systems: mycobacterial evolution to counter host immunity. Nat Rev Microbiol. 2016;14:677–91. doi:10.1038/nrmicro.2016.131.

3. Chen Z, Hu Y, Cumming BM, Lu P, Feng L, Deng J, et al. Mycobacterial WhiB6 Differentially Regulates ESX-1 and the Dos Regulon to Modulate Granuloma Formation and Virulence in Zebrafish. Cell Rep. 2016;16:2512–24. doi:10.1016/j.celrep.2016.07.080.

4. Solans L, Gonzalo-Asensio J, Sala C, Benjak A, Uplekar S, Rougemont J, et al. The PhoP-dependent ncRNA Mcr7 modulates the TAT secretion system in Mycobacterium tuberculosis. PLoS Pathog. 2014;10:e1004183. doi:10.1371/journal.ppat.1004183.

5. Solans L, Aguiló N, Samper S, Pawlik A, Frigui W, Martín C, et al. A specific polymorphism in Mycobacterium tuberculosis H37Rv causes differential ESAT-6 expression and identifies WhiB6 as a novel ESX-1 component. Infect Immun. 2014;82:3446–56. doi:10.1128/IAI.01824-14.

6. Bosserman RE, Nguyen TT, Sanchez KG, Chirakos AE, Ferrell MJ, Thompson CR, et al. WhiB6 regulation of ESX-1 gene expression is controlled by a negative feedback loop in Mycobacterium marinum. Proc Natl Acad Sci USA. 2017;114:E10772–81. doi:10.1073/pnas.1710167114.

7. van Kessel JC, Marinelli LJ, Hatfull GF. Recombineering mycobacteria and their phages. Nat Rev Microbiol. 2008;6:851–7. doi:10.1038/nrmicro2014.

8. Simeone R, Bobard A, Lippmann J, Bitter W, Majlessi L, Brosch R, et al. Phagosomal rupture by Mycobacterium tuberculosis results in toxicity and host cell death. PLoS Pathog. 2012;8:e1002507. doi:10.1371/journal.ppat.1002507.

9. Champion PAD, Stanley SA, Champion MM, Brown EJ, Cox JS. C-terminal signal sequence promotes virulence factor secretion in Mycobacterium tuberculosis. Science. 2006;313:1632–6. doi:10.1126/science.1131167.

10. van Kessel JC, Hatfull GF. Efficient point mutagenesis in mycobacteria using single-stranded DNA recombineering: characterization of antimycobacterial drug targets. Mol Microbiol. 2008;67:1094–107. doi:10.1111/j.1365-2958.2008.06109.x.

11. van Kessel JC, Hatfull GF. Recombineering in Mycobacterium tuberculosis. Nat Methods. 2007;4:147–52. doi:10.1038/nmeth996.

12. Bange FC, Collins FM, Jacobs WR. Survival of mice infected with Mycobacterium smegmatis containing large DNA fragments from Mycobacterium tuberculosis. Tuber Lung Dis. 1999;79:171–80. doi:10.1054/tuld.1998.0201.

13. Avanzi C, Del-Pozo J, Benjak A, Stevenson K, Simpson VR, Busso P, et al. Red squirrels in the British Isles are infected with leprosy bacilli. Science. 2016;354:744–7. doi:10.1126/science.aah3783.

14. Bolger AM, Lohse M, Usadel B. Trimmomatic: a flexible trimmer for Illumina sequence data. Bioinformatics. 2014;30:2114–20. doi:10.1093/bioinformatics/btu170.

15. Langmead B, Salzberg SL. Fast gapped-read alignment with Bowtie 2. Nat Methods. 2012;9:357–9. doi:10.1038/nmeth.1923.

16. Kolly GS, Boldrin F, Sala C, Dhar N, Hartkoorn RC, Ventura M, et al. Assessing the essentiality of the decaprenyl-phospho-d-arabinofuranose pathway in Mycobacterium tuberculosis using conditional mutants. Mol Microbiol. 2014;92:194–211. doi:10.1111/mmi.12546.

17. OligoAnalyzer 3.1 | IDT. https://eu.idtdna.com/calc/analyzer. Accessed 4 Aug 2018.

Chapter 5

Conclusions and perspectives

Since the discovery of the ESX-1 secretion system, considerable research effort has focused on elucidating its composition, function, regulation and structure. However, the molecular mechanism underlying the ESX-1 secretion process is still not fully understood. To further unravel its functioning, this thesis was dedicated to the study of various ESX-1 components within the framework of the Swiss National Science Foundation (SNF)-financed project entitled "Integrated investigation of the ESX-1 protein secretion system of *Mycobacterium tuberculosis*". The present work has provided new insights into the structural component $EccE_1$, the ESX-1-specific chaperone EspL and the transcriptional regulator WhiB6.

$EccE_1$ assembles at polar regions

We confirmed that $EccE_1$ is a membrane- and cell wall-associated protein required for secretion of ESX-1 substrates and induction of host cell lysis. Based on our results, $EccE_1$ seems to be exclusively involved in ESX-1-dependent activity as the deletion of *eccE1* from the chromosome did not impact other bacterial functions such as gene expression, susceptibility to antibiotics, *in vitro* growth or secretion by other ESX systems.

In Chapter 2 we presented a strategy to localise $EccE_1$ by using mNeon, a fluorescent protein that can be visualised without overexpression. This approach allowed us to work with a fully virulent, complemented mutant that does not express the WT copy of $EccE_1$ but the fusion protein $EccE_1$-mNeon instead. As a consequence, all functional ESX-1 complexes assembled in the bacterium should contain $EccE_1$-mNeon.

Our findings indicate that $EccE_1$ is located at the cell poles of *M. tuberculosis* when a functional ESX-1 system is present but not when the *esx-1* locus is deleted, as in ΔΔRD1. This observation suggests that $EccE_1$ requires other ESX-1 proteins to assemble in a stable complex in polar regions. As $EccE_5$ was shown to be part of the membrane complex of the ESX-5 secretion system [1, 2], it is very likely that the foci observed at the poles not only correspond to $EccE_1$ but also to the whole ESX-1 apparatus. More evidence is required to validate the polar localisation of ESX-1 by detecting other components. For instance, $MycP_1$ or $EccD_1$ can also be tagged using the same strategy as presented in this study. In the case of $MycP_1$, the Δ*mycP1-eccE1* mutant and the complementation approach generated in our lab can be used for such a purpose. Eventually, co-localization of various ESX-1 components by combining different fluorescent proteins may result in a powerful tool.

ESX-1 proteins have been identified at the poles in *M. marinum* and *M. smegmatis* [3, 4]. In many bacteria, polar proteins are involved in a variety of functions, including pathogenesis and secretion [5]. Interestingly, the type IV secretion systems were also found to assemble at polar regions in *Agrobacterium tumefaciens* [6]. A question which arises is why ESX-1 proteins preferentially localise at the cell poles. A possible explanation is that segregation to opposite ends ensures equal inheritance between daughter cells. Considering that polar regions are specific and limited areas in the bacterium, directing proteins to cell poles could also serve as a strategy to locally increase the concentration of different subunits. In this context, membrane curvature or lipids that mainly accumulate at curved membranes may also play an essential role in ESX-1 localisation [5]. Misfolded proteins and protein aggregates often accumulate at the poles. Therefore, special care is required when working with non-native or fusion proteins as artefactual localization can arise upon overexpression or fusion to some fluorescent tag [7].

Isolating the membrane apparatus of the ESX-1 complex in *M. tuberculosis* is also an important step towards the elucidation of its structure. To this end, a pull-down experiment using Strep-tag labeling can be performed as described for *M. marinum* (van Winden et al. 2016; Beckham et al. 2017). Indeed, a virulent $EccE_1$-Strep complemented mutant has been already generated in our laboratory following the same strategy as described for the $EccE_1$-HA derivative in Chapter 2. This Strep-tagged mutant may not only be used to identify $EccE_1$ partners and the ESX-1 membrane complex but also to purify $EccE_1$ directly from *M. tuberculosis* and perform structural studies using high-resolution imaging, such as Cryo-electron microscopy.

EspL

In Chapter 3, we demonstrated that EspL is mainly a cytosolic and partly membrane-associated protein, essential for stabilising EspE, EspF and EspH. In addition, EspL was shown to be important for the secretion of EsxA, EsxB, EspA and EspD, although EspL itself was not detected in the culture filtrates. Lack of *espL* resulted in intracellular growth defect, loss of cytotoxicity and marked reduction of innate cytokine production *ex vivo*. Interestingly, EspL interacts with EspD and controls *whiB6* expression by an unknown mechanism.

The essentiality of EspL for stabilising and secreting ESX-1-related proteins suggests that it could act as a chaperone of the ESX-1 apparatus with a dual role: stabilising and targeting substrates to the secretion

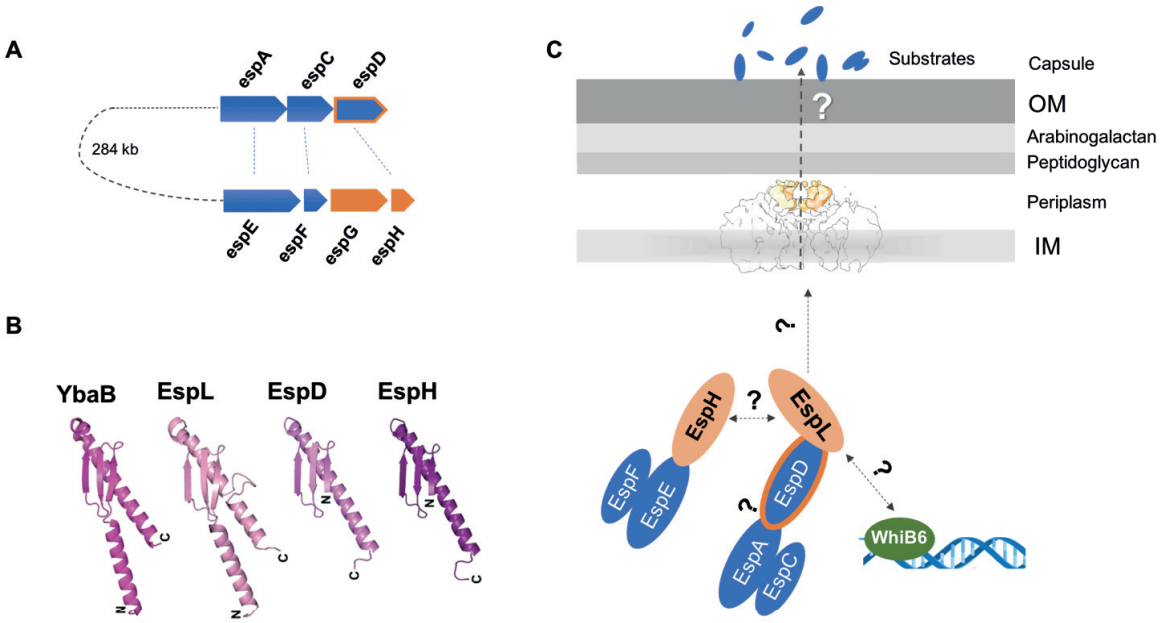

Figure 1. Model of EspL interactions. **A)** *espA, espC* and *espD* are paralogues of *espE, espF* and *espH,* respectively. **B)** Taken from [8]**.** EspH, EspD and EspL are predicted to have structural similarities with YbaB, a DNA binding protein. **C)** EspL interacts with EspD, which in turn stabilizes EspA and EspC levels [9]. Since the sequence and structure of EspD and EspH are similar, it is plausible that EspL may also interact with EspH. This interaction may explain the requirement of EspL to stabilize EspE, EspF and EspH levels in the cytosol. Thus, EspL may recognize ESX-1 substrates to stabilise and direct them to the secretion machinery. EspL may also directly or indirectly control the expression of the transcriptional regulator WhiB6. **OM**: outer membrane; **IN**: inner membrane.

machinery. In the absence of *espL*, intracellular levels of EspD, EspA and EspC are not affected whereas their secretion is severely compromised. As EspL was also found to be a membrane-associated protein, it is plausible that EspL may be involved in recruiting substrates to the ESX-1 apparatus through interaction with EspD. This hypothesis could be tested by additional studies of the EspD point mutants previously generated by our group [9]. Immunoprecipitation experiments as well as mass spectrometry may reveal which amino acid residues are important for interaction with EspL and/or with other ESX-1 components.

To understand the role of EspL in *M. tuberculosis* virulence, it is essential to investigate the contributions of EspE, EspF and EspH. EspF was previously shown to reduce *M. tuberculosis* virulence in the mouse model of tuberculosis when deleted [10]. Recently, EspH was investigated in *M. marinum* and reported to interact with and to stabilise EspE. Deletion of *espH* was shown to block EspE and EspF secretion and increase virulence in zebrafish larvae but not in cultured macrophages [11]. Interestingly, the effects of the *espH* deletion on other substrates such as EsxA, EsxB and EspB were minor, suggesting that there is no dependency for secretion between EspE/EspF and other Esp proteins [11]. An *M. tuberculosis espE* deletion mutant has been generated

in our laboratory (data not presented here) and will be analyzed for its ability to secrete ESX-1 substrates and cause toxicity in the macrophage.

Altogether, EspL seems to be important not only for EspE, EspF and EspH stability but also for secretion of other ESX-1 substrates. Therefore, it may be part of a post-translational regulatory mechanism involving complex protein-protein interactions.

WhiB6 regulator

The transcriptional regulator WhiB6 was found to positively regulate genes within the *esx-1* locus and the distal *espACD* operon. WhiB6 was also reported here to be important for *M. tuberculosis* virulence as its loss resulted in severe reduction of cytotoxicity *ex vivo*.

To further define the role played by WhiB6 in *M. tuberculosis* virulence, it is essential to check the secretion profile as well as the intracellular protein levels of the knock-out mutant, as we did in Chapters 2 and 3. These experiments will identify deregulated proteins and discover if lack of WhiB6 also impacts the function of other ESX systems.

Analyzing the global transcriptional profile of the *whiB6*-deficient strain by RNA-sequencing (RNA-seq) and mapping the binding sites of WhiB6 by Chromatin Immunoprecipitation-sequencing (ChIP-seq) will provide a global picture of the genes directly and indirectly regulated by WhiB6. The complemented mutant expressing WhiB6-HA presented in this study can be used in ChIP-seq experiments as antibodies against HA are commercially available and highly specific. This mutant can also represent an excellent negative control in pull-down experiments which aim to detect WhiB6 interactors.

ESX-1 model

In this study, we consistently found a strong correlation between ESX-1 functionality and cytotoxicity. Furthermore, we observed that ESX-1 activity is not required for uptake or intracellular survival of *M. tuberculosis* in THP-1 human macrophages.

Disruption of the structural component $EccE_1$ and of the chaperone EspL severely compromised secretion of EsxA, EsxB, EspA and EspC. In contrast, secretion of EspB was not affected by deletion of either the $EccE_1$

or EspL components, implying a different mechanism of translocation or a role for EspB which goes beyond that of a secreted substrate.

Secretion across the cell envelope by specialized secretion systems can occur either by a one-step or a two-step mechanism (Chapter 1). Based on the subcellular fractionation data presented in Chapter 2, we think that ESX-1 secretion probably occurs in a one-step process. The ESX-1 substrate EsxB was mainly found in the cytosol and in the secreted fractions but not in the cell wall. If ESX-1 secretion is a two-step process, the substrates should be exported into the periplasmic space before being translocated across the outer membrane, and thus, EsxB should also be found in the cell wall fraction. The size of the ESX-5 membrane channel observed by negative stain electron microscopy indicates that the complex is embedded exclusively in the inner membrane and it does not span the mycomembrane [1]. Therefore, additional components are required to transport substrates across the outer membrane. Two candidates that may be involved in this process are EspC and EspB. EspC was proposed as a needle protein, as it polymerises upon secretion and forms filaments on the surface of *M. tuberculosis* although it does not appear to localize to the poles of the cells [12]. EspB is also an interesting candidate because it can form oligomers and donut-shaped particles [13, 14] and was located in the cell membrane and cell wall fractions in the present study (Figure 3, Chapter 2). These observations are compatible with EspB assembling in a multimeric complex in the cell envelope. To explore this possibility, EspB and its interactors could be immunoprecipitated from the cell wall fraction of a strain expressing a tagged version of EspB. Such a strain, carrying the Strep tag on EspB, has been constructed by other members of our group and will be used to this purpose. Isolating EspB from *M. tuberculosis* and visualising its structure by electron microscopy could give us a more precise idea of its natural conformation and function.

ESX-1 visualisation

Despite twenty years of research, type VII secretion systems are among the most poorly described secretion systems in bacteria. A better understanding of this apparatus requires the visualisation of the nanomachine in its natural setting to provide a broad view of its architecture and assembly process. Recently, the molecular architecture of the ESX-5 membrane complex was determined at 13 Å resolution by electron microscopy [1]. This study offers a valuable but yet partial understanding of the type VII structural organisation. Using correlation Light Electron Microscopy coupled with Cryo Focus Ion Beam milling (CryoFIB) and Cryo-

Electron Tomography (CryoET) will offer the possibility to visualise the machinery in a life-like state inside intact cells at the macromolecular resolution. CryoFIB is used to prepare very thin samples (~200 nm) suitable for recording high-quality tomograms with CryoET. From subtomogram averaging, a sub-nanometric 3D volume could be solved. Both technologies were successfully employed to visualise bacterial complexes such as the type IV and VI secretion systems [15, 16]. The fluorescent $EccE_1$-mNeon strain presented in Chapter 2 can be exploited to establish the coordinates along the x,y,z axes of the assembled and active ESX-1 complex needed for preparing the cryo-sections before imaging.

Finally, combining these advanced techniques with time-lapse microscopy will provide a more comprehensive picture model of the functional mechanisms underlying ESX secretion.

5.1 BIBLIOGRAPHY

1. Beckham KSH, Ciccarelli L, Bunduc CM, Mertens HDT, Ummels R, Lugmayr W, et al. Structure of the mycobacterial ESX-5 type VII secretion system membrane complex by single-particle analysis. Nat Microbiol. 2017;2:17047. doi:10.1038/nmicrobiol.2017.47.

2. Houben ENG, Bestebroer J, Ummels R, Wilson L, Piersma SR, Jiménez CR, et al. Composition of the type VII secretion system membrane complex. Mol Microbiol. 2012;86:472–84. doi:10.1111/j.1365-2958.2012.08206.x.

3. Carlsson F, Joshi SA, Rangell L, Brown EJ. Polar localization of virulence-related Esx-1 secretion in mycobacteria. PLoS Pathog. 2009;5:e1000285. doi:10.1371/journal.ppat.1000285.

4. Wirth SE, Krywy JA, Aldridge BB, Fortune SM, Fernandez-Suarez M, Gray TA, et al. Polar assembly and scaffolding proteins of the virulence-associated ESX-1 secretory apparatus in mycobacteria. Mol Microbiol. 2012;83:654–64. doi:10.1111/j.1365-2958.2011.07958.x.

5. Surovtsev IV, Jacobs-Wagner C. Subcellular organization: A critical feature of bacterial cell replication. Cell. 2018;172:1271–93. doi:10.1016/j.cell.2018.01.014.

6. Judd PK, Kumar RB, Das A. Spatial location and requirements for the assembly of the Agrobacterium tumefaciens type IV secretion apparatus. Proc Natl Acad Sci USA. 2005;102:11498–503. doi:10.1073/pnas.0505290102.

7. Laloux G, Jacobs-Wagner C. How do bacteria localize proteins to the cell pole? J Cell Sci. 2014;127 Pt 1:11–9. doi:10.1242/jcs.138628.

8. Phan TH, Houben ENG. Bacterial secretion chaperones: the mycobacterial type VII case. FEMS Microbiol Lett. 2018;365. doi:10.1093/femsle/fny197.

9. Chen JM, Boy-Röttger S, Dhar N, Sweeney N, Buxton RS, Pojer F, et al. EspD is critical for the virulence-mediating ESX-1 secretion system in Mycobacterium tuberculosis. J Bacteriol. 2012;194:884–93. doi:10.1128/JB.06417-11.

10. Bottai D, Majlessi L, Simeone R, Frigui W, Laurent C, Lenormand P, et al. ESAT-6 secretion-independent impact of ESX-1 genes espF and espG1 on virulence of Mycobacterium tuberculosis. J Infect Dis. 2011;203:1155–64. doi:10.1093/infdis/jiq089.

11. Phan TH, van Leeuwen LM, Kuijl C, Ummels R, van Stempvoort G, Rubio-Canalejas A, et al. EspH is a hypervirulence factor for Mycobacterium marinum and essential for the secretion of the ESX-1 substrates EspE and EspF. PLoS Pathog. 2018;14:e1007247. doi:10.1371/journal.ppat.1007247.

12. Lou Y, Rybniker J, Sala C, Cole ST. EspC forms a filamentous structure in the cell envelope of Mycobacterium tuberculosis and impacts ESX-1 secretion. Mol Microbiol. 2017;103:26–38. doi:10.1111/mmi.13575.

13. Korotkova N, Piton J, Wagner JM, Boy-Röttger S, Japaridze A, Evans TJ, et al. Structure of EspB, a secreted substrate of the ESX-1 secretion system of Mycobacterium tuberculosis. J Struct Biol. 2015;191:236–44. doi:10.1016/j.jsb.2015.06.003.

14. Solomonson M, Setiaputra D, Makepeace KAT, Lameignere E, Petrotchenko EV, Conrady DG, et al. Structure of EspB from the ESX-1 type VII secretion system and insights into its export mechanism. Structure. 2015;23:571–83. doi:10.1016/j.str.2015.01.002.

15. Böck D, Medeiros JM, Tsao H-F, Penz T, Weiss GL, Aistleitner K, et al. In situ architecture, function, and evolution of a contractile injection system. Science. 2017;357:713–7. doi:10.1126/science.aan7904.

16. Medeiros JM, Böck D, Pilhofer M. Imaging bacteria inside their host by cryo-focused ion beam milling and electron cryotomography. Curr Opin Microbiol. 2018;43:62–8. doi:10.1016/j.mib.2017.12.006.

Acknowledgements

I would like to express my deepest gratitude to those who helped me and gave me advice and guidance through these four years of PhD. I feel most fortunate to have been part of the excellent UPCOL team! Thanks to all fellow lab members, present and former, to be exceptional professionals and amazing colleagues. Especially, I would like to thank Prof. Stewart Cole for giving me the opportunity to do my PhD in such a dynamic and stimulating environment. I really appreciate his dedication as well as the freedom he gave me to explore my own interests. I also would like to extend my special gratitude to Jérémie and Claudia for their supervision, guidance and training, for the inspiring discussions, and for the many hours they spent helping me. Thanks to Jan for introduce me into the mycobacteria world and the ESX-1 project; Andreanne for fruitful discussions, numberless advice and friendship; Andrej for all the bioinformatic analysis and for taking us to crazy hikes and cross-country skiing; Charlotte for her energy and enthusiasm that boosted me in many critical situations; Rapha for always being willing to help and accompany me with his friendship and daily care; Sofia, Caroline, Nina and Ye for sharing countless tips, protocols and hours in the lab; Philippe, Stefanie, Anthony, Cecile and Suzanne for their support and for ensuring the smooth running of the lab. I am also thankful to the EPFL community, especially to the Global Health Institute and particularly the neighbouring McKinney, Lemaitre and Blokesch labs. Thanks to the lunch team and the burrito-plating team for the friendship, for looking out for each other and for the numerous unforgettable moments. I also greatly appreciate Prof. Roland Brosch, Prof. Wilbert Bitter, Dr Neeraj Dhar and Prof. Joachim Lingner for taking the time to correct this thesis and participate as jury members of the committee.

Last, but certainly not the least, I would like to extend my gratitude to my dear family, my parents Manolo and Ana as well as my brothers Manuel and Rafa, for their love and unconditional support. Muchas gracias familia por todos vuestros cuidados y apoyo, así como por los valores que me habéis transmitido, los cuales han sido fundamentales para llegar hasta aquí y continuarán guiándome en cualquier desafío que emprenda. Gracias también a Ángela y Mari Carmen por vuestro cariño y vuestras llamadas que me han acompañado siempre. And of course, thanks to Pablo, my love, to be by my side every day, for your support and encouragement during the long working hours, the weekends in P3 and for helping me in the writing of this thesis. Your patience and love have certainly made this job much smoother and rewarding.

PALOMA SOLER-ARNEDO

PhD candidate

MICROBIOLOGIST

Expertise in *Mycobacterium tuberculosis* virulence and pathogenesis with a background in cellular and molecular biology.

Bacteriology
Molecular biology
Genetic engineering
Immunoblotting
Cell culture
Basic microscopy
Drug susceptibility
Protein production and purification
BSL-3
Office package
Student supervision

Native B2-C1 B2

CONTACT

Address
Grand-rue 73-75, 1110
Morges
Phone
+41 789322714
Email
Soler.paloma@gmail.com

EDUCATION

Swiss Federal Institute of Technology
(EPFL, Lausanne)
2014 - Oct.2018

PhD in Molecular Life Science

Laboratory of microbial pathogenesis – Prof. Stewart T. Cole

Functional characterization of the virulence determinant ESX-1 from *Mycobacterium tuberculosis*

Multidisciplinary approach: Bacterial-molecular genetics, transcriptomics, proteomics, immuno-biochemistry, *ex vivo* models of infection, reporter strains, fluorescence microscopy and drug susceptibility. BSL 2 and BSL 3- laboratories.

Courses: Pharmacological chemistry, pharmaceutical biotechnology, my thesis in 180 seconds, academical writing.

Pierre and Marie Curie University
(UPMC, Paris)
2013-2014

Master in Molecular and cellular biology

Advanced enzymology (Montréal university and UPMC), biology of aging, immunology, cell signalling.

Complutense University
(UCM, Madrid)
2007-2013

Science Bachelor's degree (Licenciatura en Biología)

Biochemistry, genetics, cell biology, immunology, enzymology, molecular pathology, microbiology.
Erasmus exchange (1 year) at Pierre and Marie Curie University, France.

EXPERIENCE

Teaching Assistant
Lausanne, Switzerland
2014-2018

Swiss Federal Institute of Technology

Practical and theorical courses on molecular and cellular biology.

Master Internship
Lyon, France
2014

École Normale Supérieure de Lyon

Understanding the genetic of aging using *C. elegans* as a model – Prof. Hugo Aguilaniu

Master Internship
Paris, France
2012

Hôpital Pitié-Salpêtrière, INSERN-CNRS

Production of antibodies against *P. falciparum* to evaluate parasite's infection – Prof. Dominique Mazier

Bachelor Internship
Boston, USA
2010

Harvard Medical School, Brigham and Women's Hospital Pathology

Elucidating the role of p50/p105 in inflammatory bowel disease – Prof. Bruce H. Horwitz

CONFERENCES

EMBO Conference Tuberculosis 2016 - Institut Pasteur, Paris.September 19-23, 2016.
Poster: Investigating the role of $MycP_1$ and $EccE_1$ in *Mycobacterium tuberculosis* virulence.